Prospects for DM-induced gamma-rays from galaxy clusters

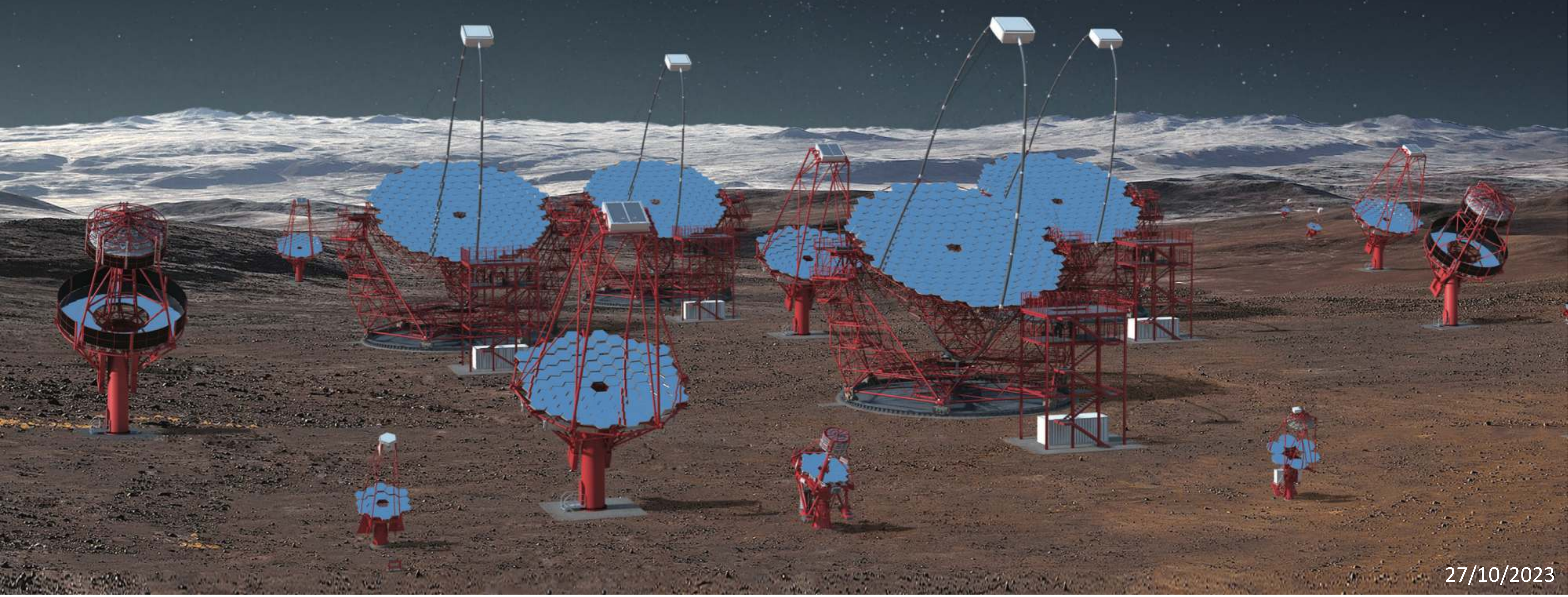

27/10/2023

Judit Pérez-Romero

Work as part of the CTA Consortium and the *Fermi*-LAT Collaboration

judit.perez@ung.si

20th MultiDark Workshop, Gandía

cherenkov telescope array

MultiDark
Multimessenger Approach for Dark Matter Detection

UNIVERZA V NOVI GORICI
SCIENTIA VINCES 1995

Center for Astrophysics and Cosmology

DARK MATTER IN CDM COSMOLOGY

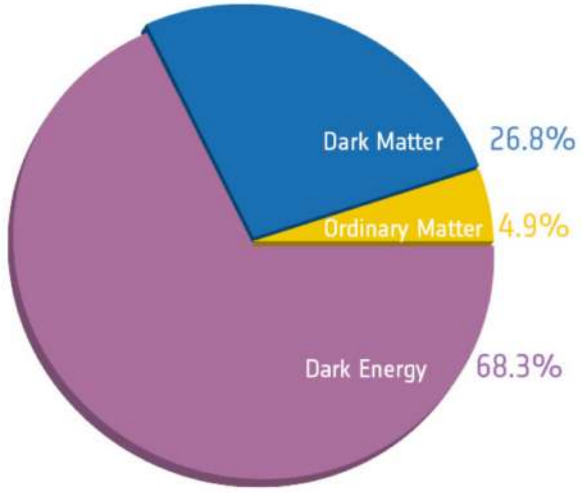

Observational Dark Matter evidences

Component of

ΛCDM Cosmology

- Structure formation driven by DM
- Bottom-up scenario: smaller structures form first

→ DM distribution in Halos and Subhalos

- Different DM candidates:

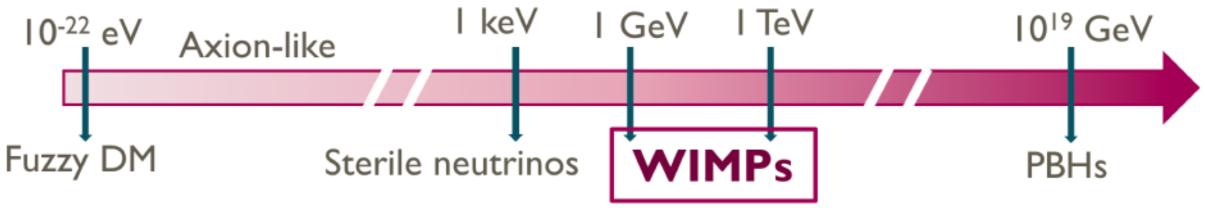

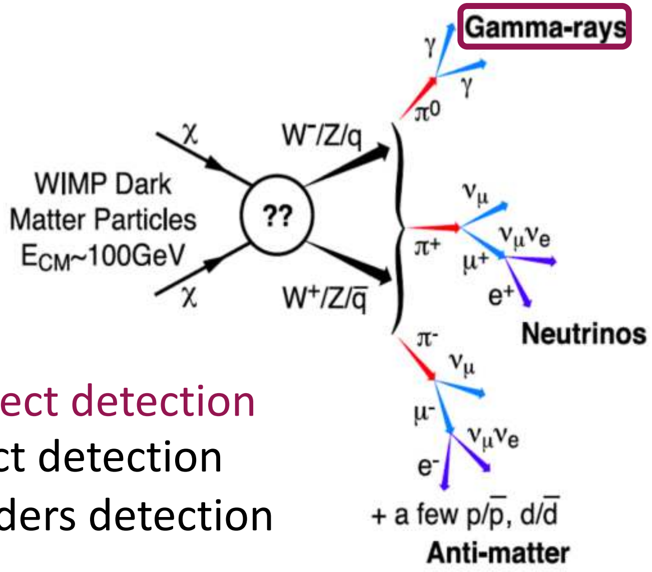

This γ-ray emission allows to perform Indirect DM Searches with current telescopes

- The search for the WIMP
  - Annihilation/Decay → Indirect detection
  - Collision → Direct detection
  - Production → Colliders detection

GAMMA-RAY DM SEARCHES

- Optimal conditions for indirect DM searches:
  - High DM density ($\phi_{DM} \propto \rho_{DM}^2$ for annihilation, $\phi_{DM} \propto \rho_{DM}$ for decay)
  - Massive nearby objects ($\phi_{DM} \propto M/d_{Earth}^2$)
  - Low astrophysical background

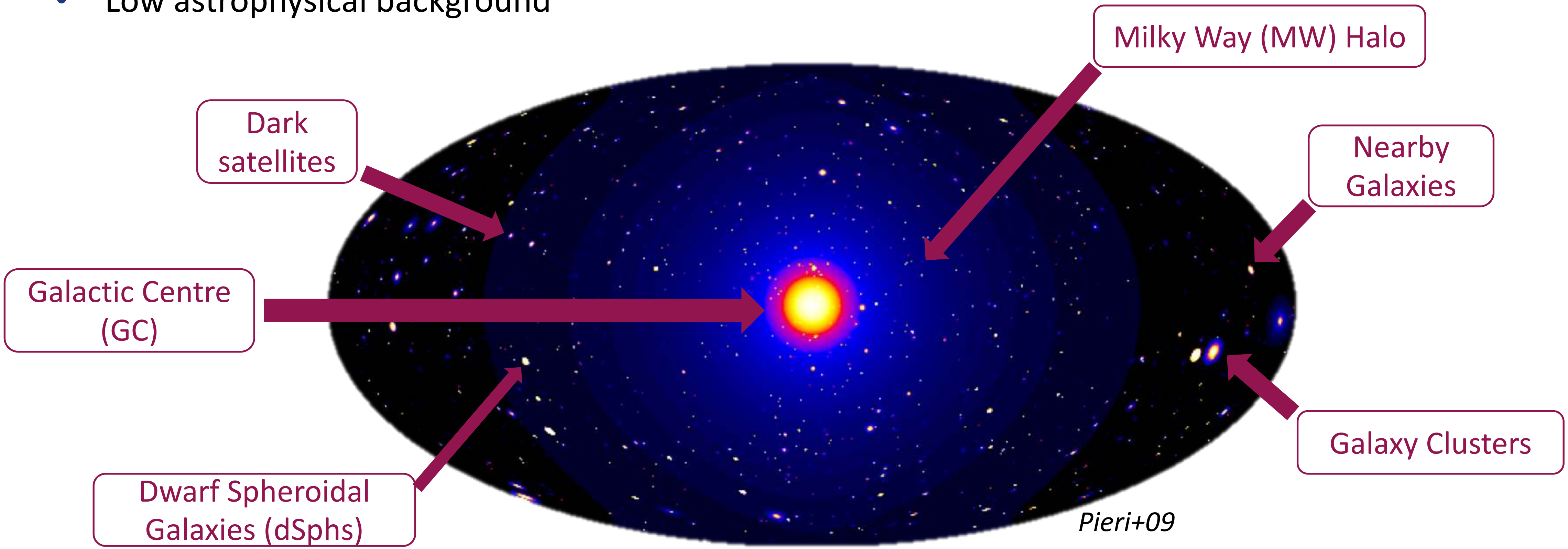

GAMMA-RAY DM SEARCHES IN CLUSTERS

- Largest gravitationally bound structures formed by gravitational collapse
- Masses of order ~10^{14}-10^{15} $M_\odot$
- Components:
  - Baryonic Matter
  - Dark Matter (~80%)
- Several in local Universe

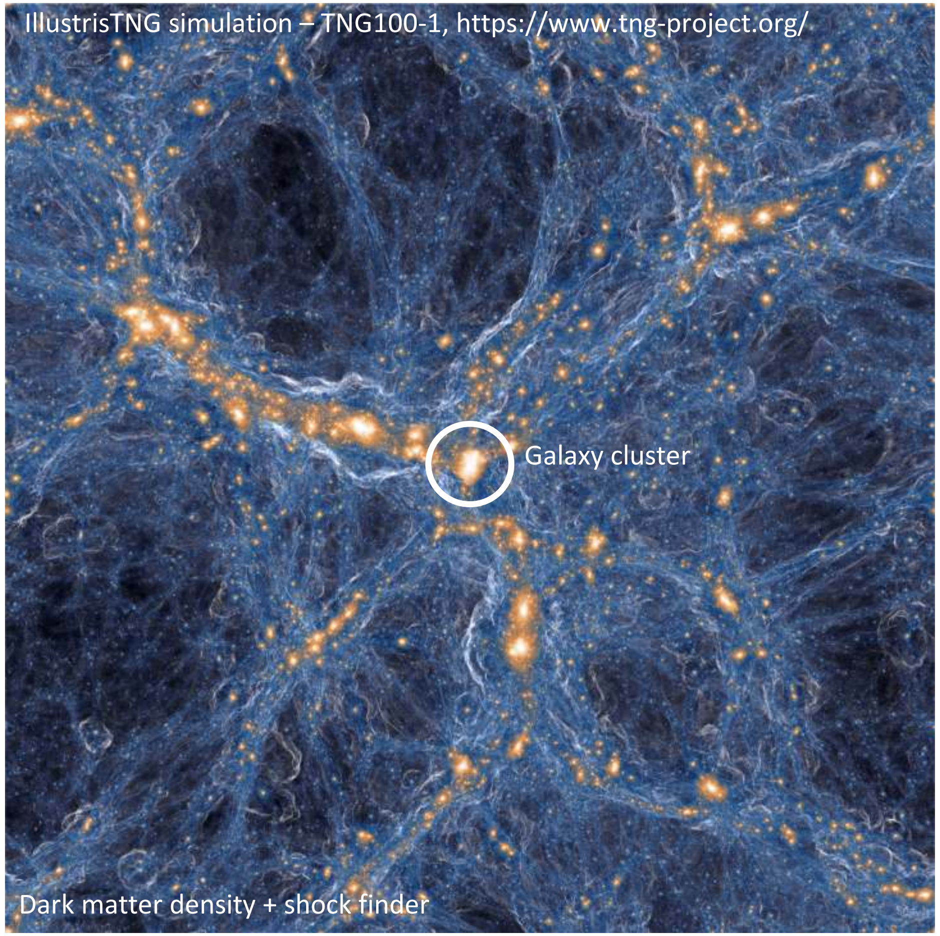

GAMMA-RAY DM SEARCHES IN CLUSTERS

- Largest gravitationally bound structures formed by gravitational collapse
- Masses of order ~10^{14}-10^{15} $M_\odot$ ← Very massive objects
- Components:
  - Baryonic Matter
  - Dark Matter (~80%) ← High DM density
- Several in local Universe ← Closeby

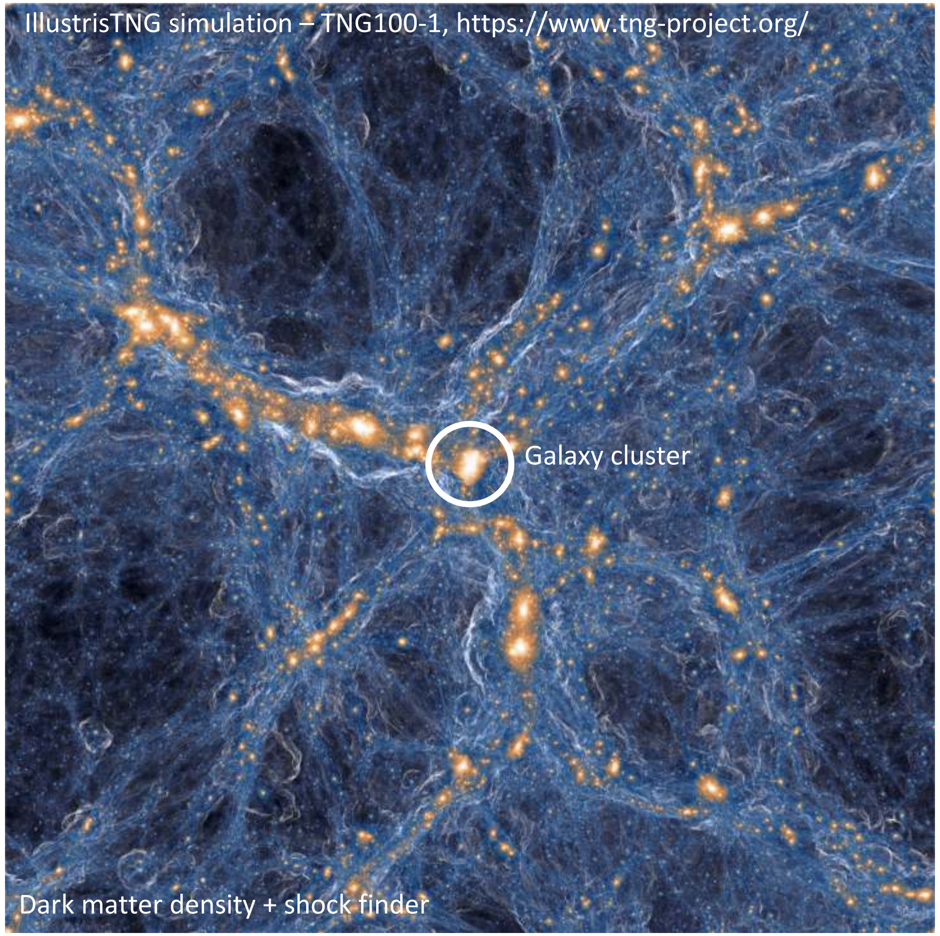

GAMMA-RAY DM SEARCHES IN CLUSTERS

- Largest gravitationally bound structures formed by gravitational collapse
- Masses of order ~10^{14}-10^{15} $M_\odot$ ← Very massive objects
- Components:
  - Baryonic Matter
  - Dark Matter (~80%) ← High DM density
- Several in local Universe ← Closeby

Decay
- Best possible targets to consider → $\phi_{DM} \propto \rho_{DM}$

Annihilation
- Competitive to other prime targets

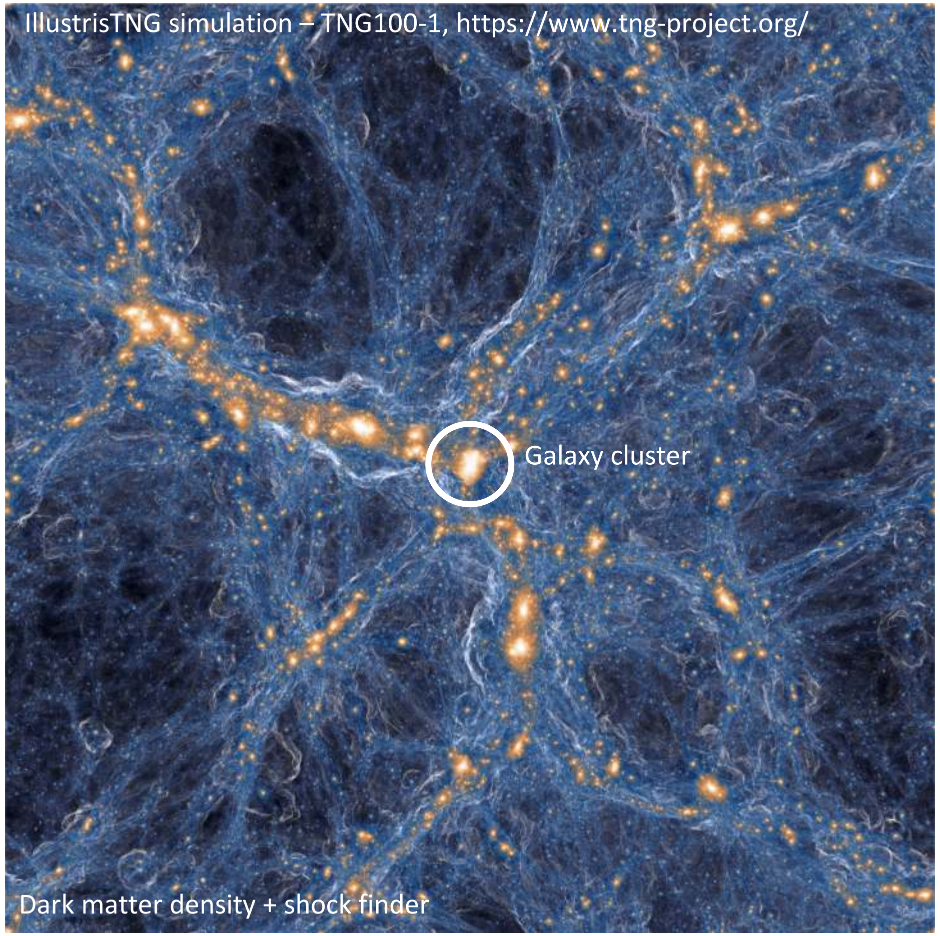

GAMMA-RAY DM SEARCHES IN CLUSTERS

- Largest gravitationally bound structures formed by gravitational collapse
- Masses of order ~10^{14}-10^{15} $M_\odot$ ← Very massive objects ✓
- Components:
  - Baryonic Matter
  - Dark Matter (~80%) ← High DM density ✓
- Several in local Universe ← Closeby ✓

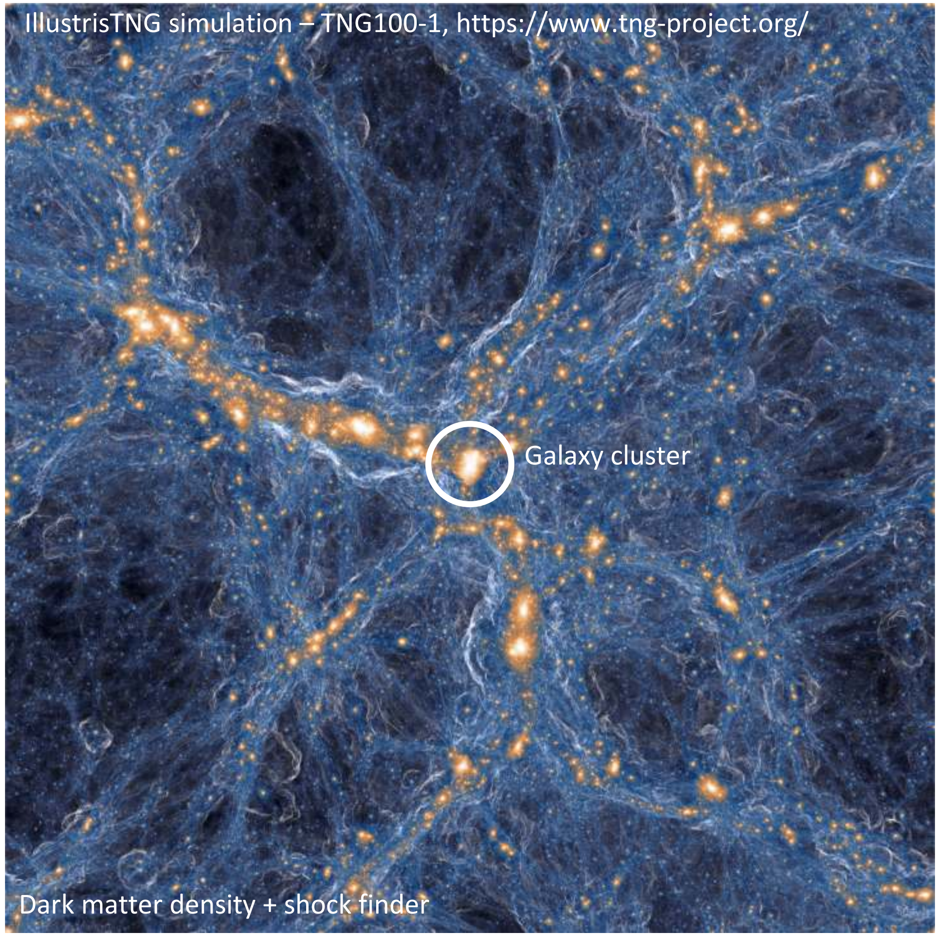

Decay • Best possible targets to consider → $\phi_{DM} \propto \rho_{DM}$

Annihilation • Competitive to other prime targets

Caveat Expected γ-ray emission from astrophysical processes

ASTROPHYSICAL GAMMA-RAY EMISSION IN GALAXY CLUSTERS

- Components:
  - Dark Matter
  - Baryonic Matter
    - Galaxies (~ 3% - 5%)
    - Intra Cluster Medium (~ 15% - 17%)

- Even supposedly virialized objects, a lot of activity
  - Merger events
  - Feedback from galaxies and AGNs
  - Magnetic fields
  - Turbulence

  → Acceleration mechanisms → Cosmic-rays (CRs)

Cosmic-rays (CRs) → Leptons → Diffuse synchrotron emission ✓

Cosmic-rays (CRs) → Hadrons → γ-rays

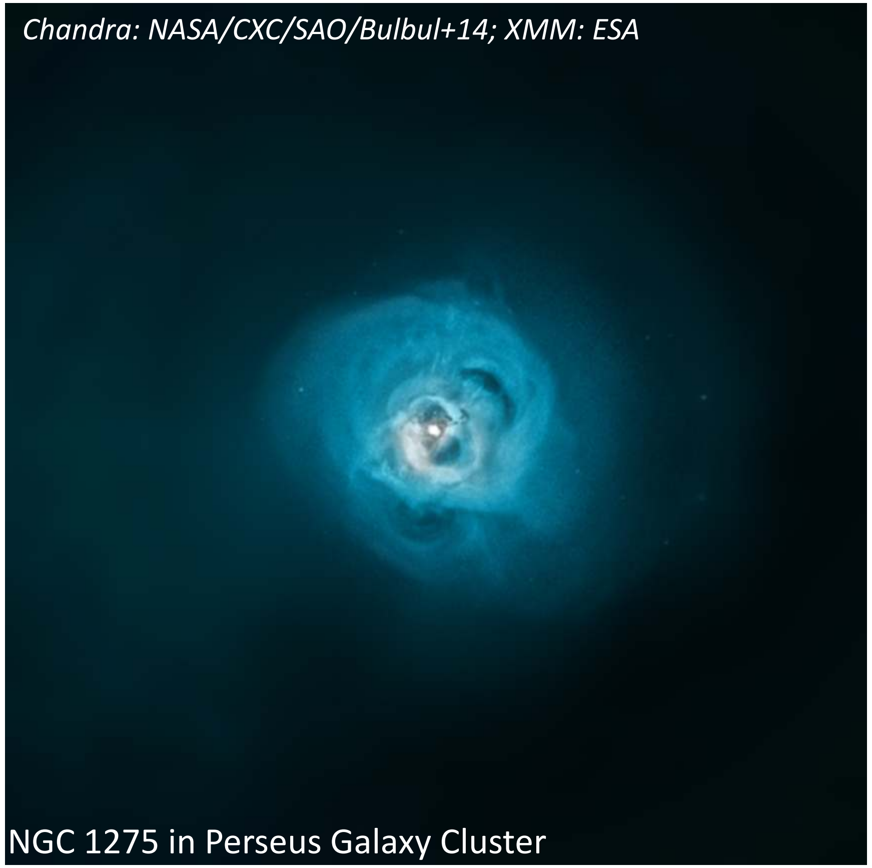

NGC 1275 in Perseus Galaxy Cluster

ASTROPHYSICAL GAMMA-RAY EMISSION IN GALAXY CLUSTERS

- Components:
  - Dark Matter
  - Baryonic Matter
    - Galaxies (~ 3% - 5%)
    - Intra Cluster Medium (~ 15% - 17%)

- Even supposedly virialized objects, a lot of activity
  - Merger events
  - Feedback from galaxies and AGNs
  - Magnetic fields
  - Turbulence

Acceleration mechanisms → Cosmic-rays (CRs)

Leptons → Diffuse synchrotron emission

Hadrons → γ-rays

! → No clear detection but some hints claimed…

Ackermann+15 [Fermi-LAT Collab.], Xi+18, Adam+21

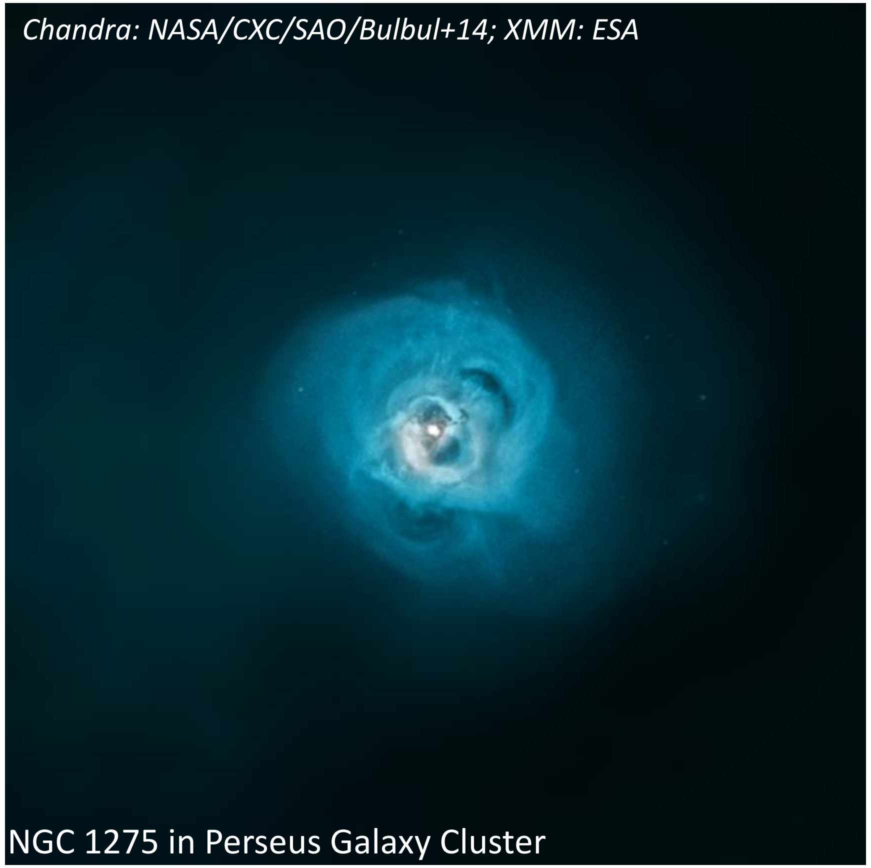

Chandra: NASA/CXC/SAO/Bulbul+14; XMM: ESA

NGC 1275 in Perseus Galaxy Cluster

THE CHERENKOV TELESCOPE ARRAY (CTA)

- Future of Imaging Atmospheric Cherenkov Telescopes for VHE gamma-ray astronomy
- 2 arrays: Northern Array (La Palma, Spain) and Southern Array (Paranal, Chile)
- First LST already in operations!

https://www.cta-observatory.org/

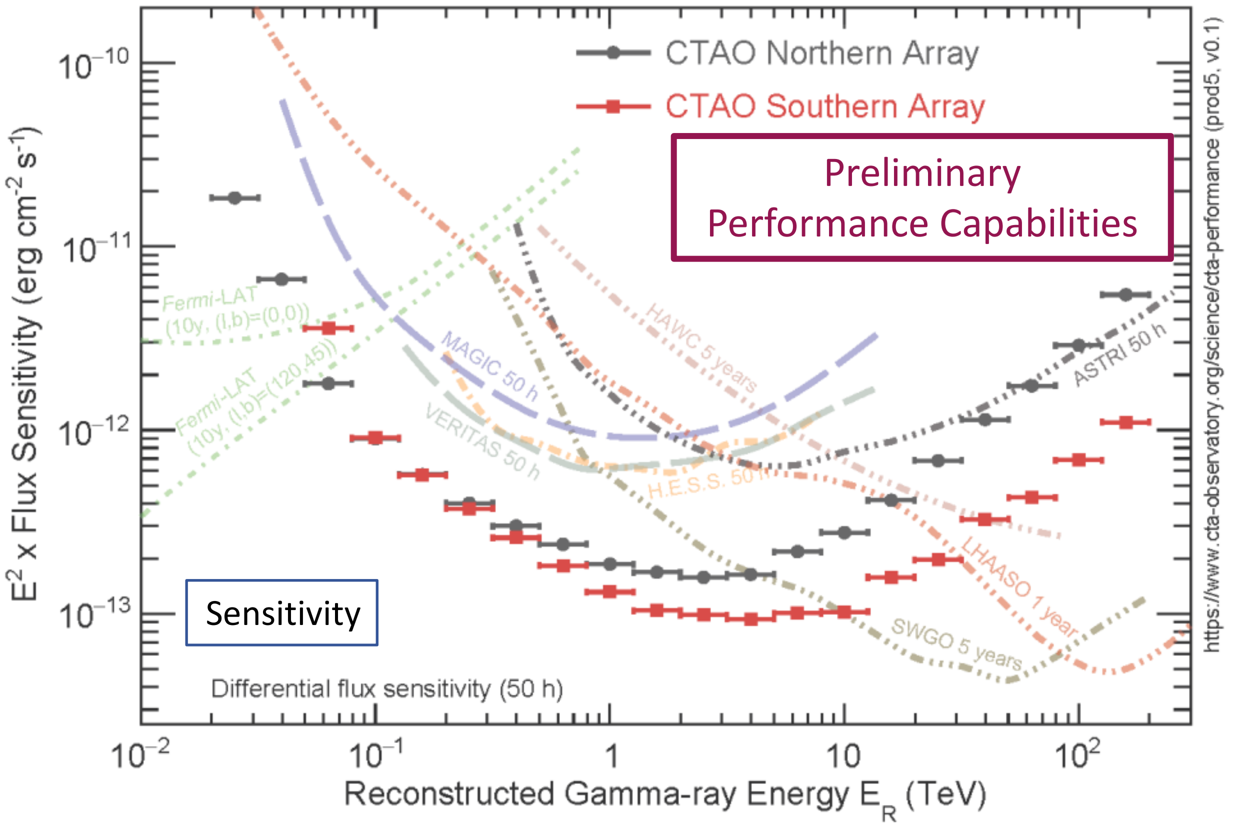

SST	MST	LST	Energy range
5- 300 TeV	150 GeV - 5 TeV	20 - 150 GeV	20 GeV - 300 TeV
$D_{\emptyset}$ = 4.3m	$D_{\emptyset}$ = 11.5m	$D_{\emptyset}$ = 23m	

CTA has superb capabilities for DM gamma-ray searches

PERSEUS GALAXY CLUSTER WITH CTA: A KEY SCIENCE PROJECT (KSP)

- Among local clusters, Perseus is the brightest in X-ray sky
- Cool-cored, relaxed cluster

Object	l [deg]	b [deg]	d_L [Mpc]
Perseus	150.57	-13.26	75.01

- Hosts two Active Galactic Nuclei (AGN), both variable

Object	l [deg]	b [deg]
NGC1275	150.58	-13.26
IC310	150.18	-13.74

NGC 1275 aligned with X-rays centre

Optimal conditions for observation from the northern array

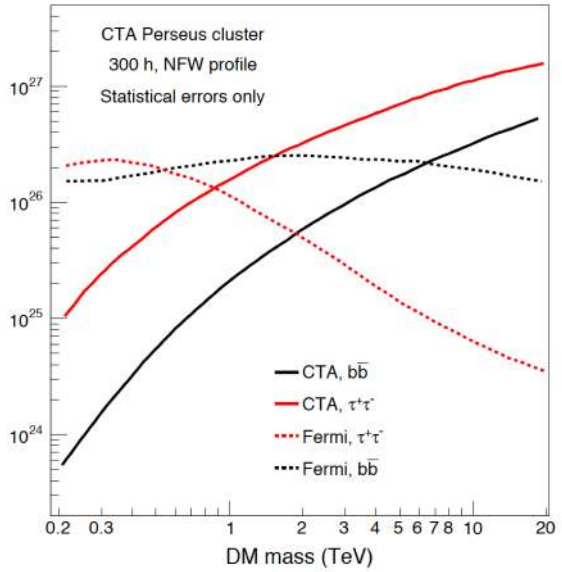

Prospects of constraints for DM decay

Acharya+17 [CTA Cons.]

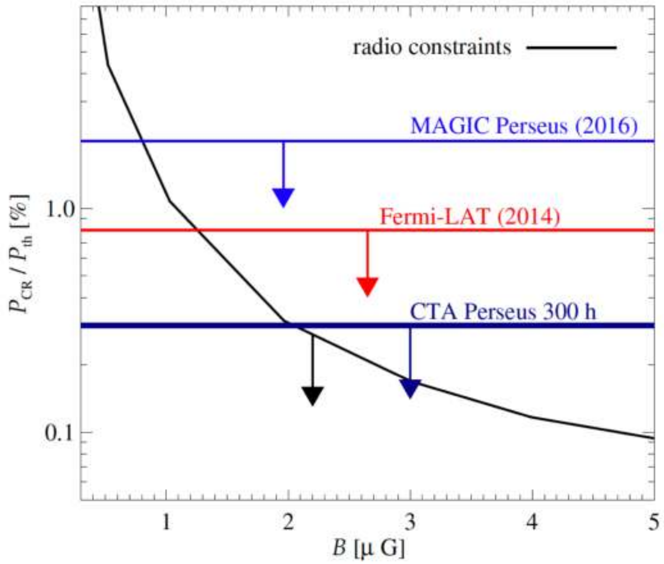

Prospects of constraints for CR models

We use the lastest version of the CTA science tools with the latest Instrument Response Functions (IRFs) to perform the analysis

Prospects for gamma-ray observations of the Perseus galaxy cluster with the Cherenkov Telescope Array
The CTA Consortium and P. de la Torre Luque (corresponding author JPR)
Submmited to JCAP, [arXiv:2309.03712]

DARK MATTER MODELLING

$$\frac{d\Phi_{DM}}{dE}(E, l.o.s, \Delta\Omega, z) = \frac{d\phi}{dE}(E, z) \times \text{Astrophysical factor}$$

DM-induced γ-ray flux from an astrophysical object

Particle Physics Model

Cirelli+12 (EW corrections)

Charbonnier+12, Bonnivard+15, Hütten+18

https://clumpy.gitlab.io/CLUMPY/

Annihilation

$$J(l.o.s, \Delta\Omega, z) = \int_{\Delta\Omega}\int_{l.o.s} \rho^2_{DM}(r)dr \;\rightarrow\; J \propto \frac{M_{200}c^3_{200}}{D^2_{\rm Earth}}$$

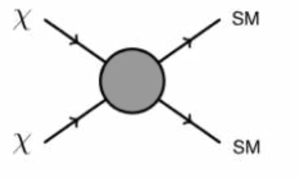

DM density profile

Decay

$$D(l.o.s, \Delta\Omega, z) = \int_{\Delta\Omega}\int_{l.o.s} \rho_{DM}(r)dr \;\rightarrow\; D \propto \frac{M_{200}}{D^2_{\rm Earth}}$$

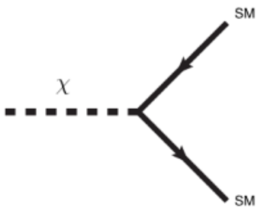

PERSEUS DM MODELLING (I): MAIN HALO

Annihilation

$$J(l.o.s, \Delta\Omega, z) = \int_{\Delta\Omega} \int_{l.o.s} \rho^2_{DM}(r) dr$$

DM density profile

$$D(l.o.s, \Delta\Omega, z) = \int_{\Delta\Omega} \int_{l.o.s} \rho_{DM}(r) dr$$

Decay

- State-of-the-art parametrization of the DM in galaxy clusters:

$$\langle \rho_{\rm tot} \rangle (r) = \rho_{\rm sm}(r) + \langle \rho_{\rm subs} \rangle (r)$$

Assume density profile

$$\rho(r) = \frac{\rho_0}{\left(\frac{r}{r_s}\right)\left(1+\frac{r}{r_s}\right)^2}$$

Navarro – Frenk – White (NFW)
Navarro+96, Navarro+97

  - "Cuspy"-like profile

- To build the DM profile, we assume a concentration-mass relation ($c_{200} - M_{200}$):

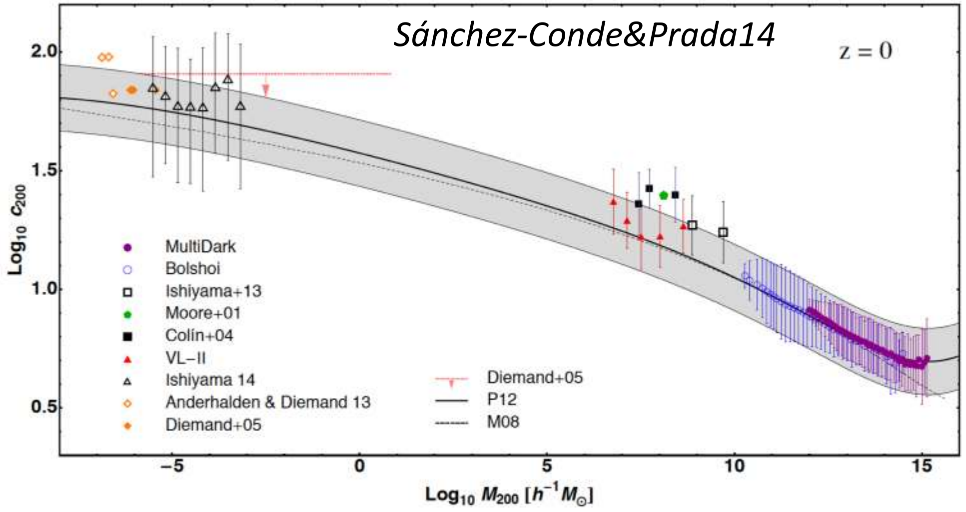

PERSEUS DM MODELLING (II): SUBSTRUCTURE

- Galaxy clusters are the most massive objects today, large amount of substructure expected
- Inclusion through ρ_{DM} using state-of-the-art subhalo models

$$\langle\rho_{\mathrm{tot}}\rangle(r) = \rho_{\mathrm{sm}}(r) + \langle\rho_{\mathrm{subs}}\rangle(r)$$

$$\frac{\mathrm{d}^3 N}{\mathrm{d}V \mathrm{d}M \mathrm{d}c} = N_{\mathrm{tot}} \frac{\mathrm{d}\mathcal{P}_V}{\mathrm{d}V}(r) \cdot \frac{\mathrm{d}\mathcal{P}_M}{\mathrm{d}M}(M) \cdot \frac{\mathrm{d}\mathcal{P}_c}{\mathrm{d}c}(M, c)$$

CLUMPY

DM subhalo profile: NFW

$$\rho(r) = \frac{\rho_0}{(\frac{r}{r_s})[1+\frac{r}{r_s}]^2}$$

PERSEUS DM MODELLING (II): SUBSTRUCTURE

- Galaxy clusters are the most massive objects today, large amount of substructure expected
- Inclusion through ρ_{DM} using state-of-the-art subhalo models

$$\langle\rho_{\mathrm{tot}}\rangle(r) = \rho_{\mathrm{sm}}(r) + \langle\rho_{\mathrm{subs}}\rangle(r)$$

$$\frac{\mathrm{d}^3 N}{\mathrm{d}V\mathrm{d}M\mathrm{d}c} = N_{\mathrm{tot}} \frac{\mathrm{d}\mathcal{P}_V}{\mathrm{d}V}(r) \cdot \frac{\mathrm{d}\mathcal{P}_M}{\mathrm{d}M}(M) \cdot \frac{\mathrm{d}\mathcal{P}_c}{\mathrm{d}c}(M, c)$$

CLUMPY

DM subhalo profile: NFW

$$\rho(r) = \frac{\rho_0}{(\frac{r}{r_s})[1+\frac{r}{r_s}]^2}$$

Subhalo Radial Distribution (SRD)

$$\rho_{\mathrm{sub}}^{VLII}(R) = \frac{\rho_{\mathrm{tot}}^{VLII}(R)\,(R/R_a)}{\left(1+\frac{R}{R_a}\right)}$$

Via Lactea - II
Anti-biased relation
Diemand+08

PERSEUS DM MODELLING (II): SUBSTRUCTURE

- Galaxy clusters are the most massive objects today, large amount of substructure expected
- Inclusion through ρ_{DM} using state-of-the-art subhalo models

$$\langle\rho_{\mathrm{tot}}\rangle(r) = \rho_{\mathrm{sm}}(r) + \langle\rho_{\mathrm{subs}}\rangle(r)$$

$$\frac{\mathrm{d}^3N}{\mathrm{d}V\mathrm{d}M\mathrm{d}c} = N_{\mathrm{tot}}\frac{\mathrm{d}\mathcal{P}_V}{\mathrm{d}V}(r)\cdot\frac{\mathrm{d}\mathcal{P}_M}{\mathrm{d}M}(M)\cdot\frac{\mathrm{d}\mathcal{P}_c}{\mathrm{d}c}(M,c)$$

DM subhalo profile: NFW

$$\rho(r) = \frac{\rho_0}{(\frac{r}{r_s})[1+\frac{r}{r_s}]^2}$$

Subhalo Radial Distribution (SRD)

$$\rho_{\mathrm{sub}}^{VLII}(R) = \frac{\rho_{\mathrm{tot}}^{VLII}(R)\,(R/R_a)}{\left(1+\frac{R}{R_a}\right)}$$

Via Lactea - II
Anti-biased relation
Diemand+08

Subhalo Mass Function (SHMF)

$$dN/dm = A/M(m/M)^{-\alpha}$$

α = 1.9
Springel+08

α = 2.0
Diemand+08

PERSEUS DM MODELLING (II): SUBSTRUCTURE

- Galaxy clusters are the most massive objects today, large amount of substructure expected
- Inclusion through $\rho_{\rm DM}$ using state-of-the-art subhalo models

$$\langle\rho_{\rm tot}\rangle(r) = \rho_{\rm sm}(r) + \langle\rho_{\rm subs}\rangle(r)$$

$$\frac{d^3N}{dV\,dM\,dc} = N_{\rm tot}\frac{d\mathcal{P}_V}{dV}(r)\cdot\frac{d\mathcal{P}_M}{dM}(M)\cdot\frac{d\mathcal{P}_c}{dc}(M,c)$$

DM subhalo profile: NFW

$$\rho(r) = \frac{\rho_0}{(\frac{r}{r_s})[1+\frac{r}{r_s}]^2}$$

Subhalo Radial Distribution (SRD)

$$\rho_{\rm sub}^{VLII}(R) = \frac{\rho_{\rm tot}^{VLII}(R)\,(R/R_a)}{\left(1+\frac{R}{R_a}\right)}$$

Via Lactea - II

Anti-biased relation

Diemand+08

Subhalo Mass Function (SHMF)

$$dN/dm = A/M(m/M)^{-\alpha}$$

α = 1.9

Springel+08

α = 2.0

Diemand+08

Subhalo Concentration-Mass relation (c_{200}-M_{200})

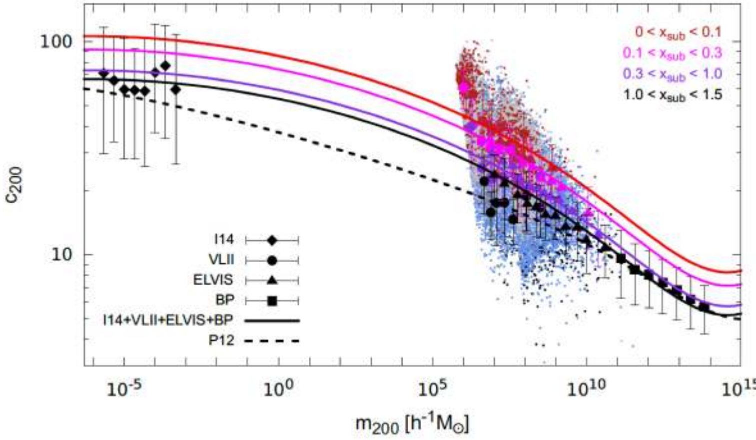

Dependence on the subhalo position

$$c_{200}(m_{200}, x_{\rm sub})$$
$$x_{\rm sub} \equiv R_{\rm sub}/R_\Delta$$

Moliné+17

EXPECTED PERSEUS DM SIGNAL

- Applying modelling formalism we obtain:

Model	SRD	$(c-M)_{sub}$	α	f_{sub}	M_{min}
MIN	-	-	-	0	-
MED	*Antibiased* VL-II (*Diemand+08*)	*Moliné+17*	1.9	0.182	$10^{-6}M_\odot$
MAX	*Antibiased* VL-II (*Diemand+08*)	*Moliné+17*	2.0	0.319	$10^{-6}M_\odot$

Annihilation	$\log_{10} J$ [GeV^{2}cm^{-5}]
MIN	17.42
MED	18.43
MAX	19.20
Decay	$\log_{10} D$ [GeV cm^{-2}]
	19.20

Skymap of the differential J/D-factors

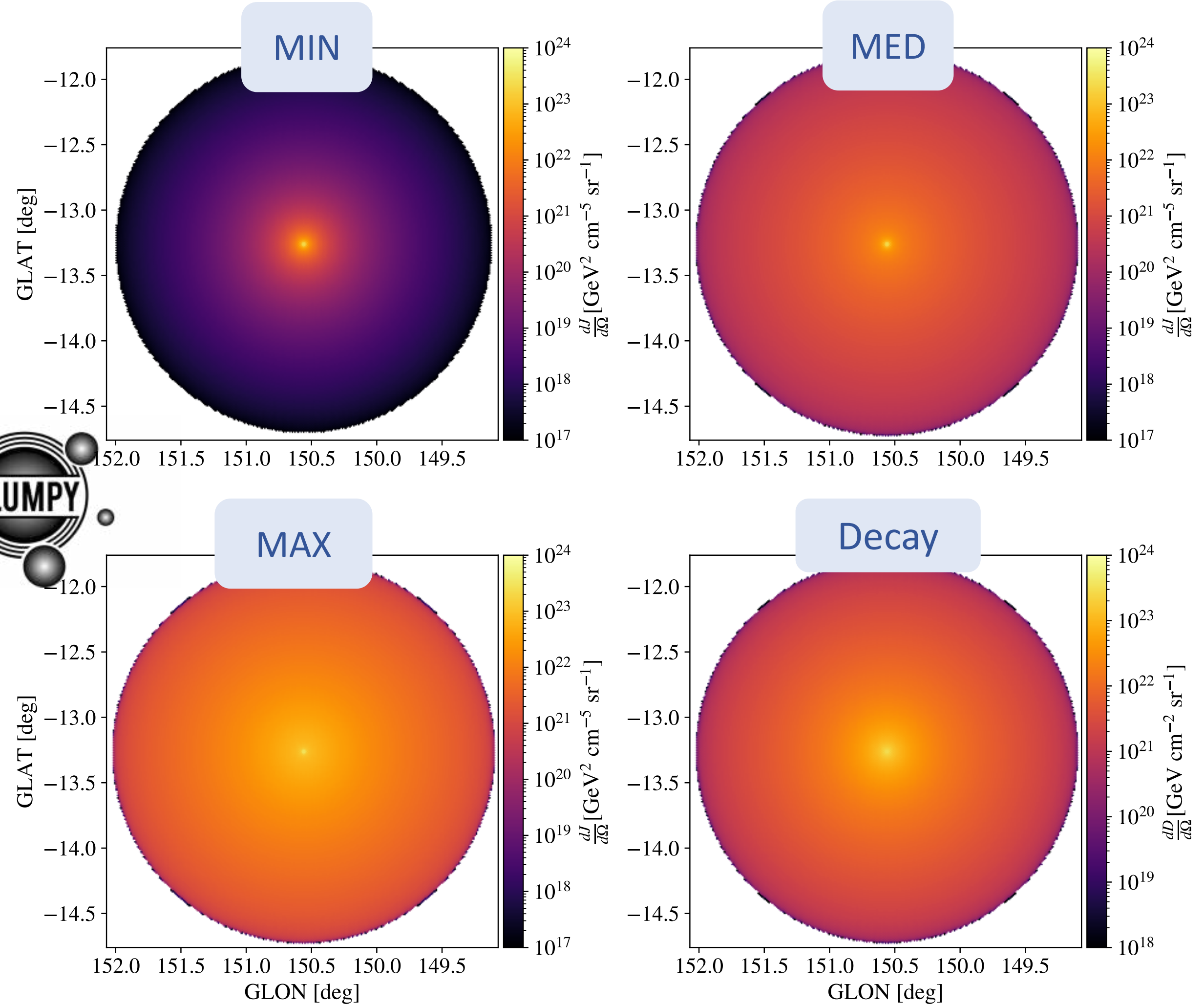

CTA DM ANALYSIS ROADMAP

- Different γ-ray sources in Perseus region:

Total DM-induced $\boldsymbol{\gamma}$-rays

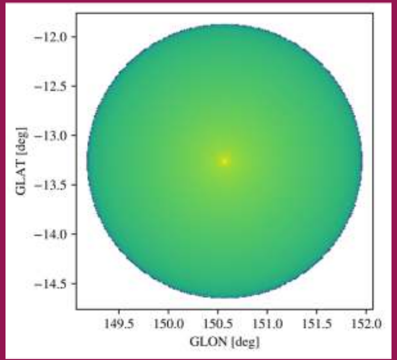

Our signal

Total CR-induced $\boldsymbol{\gamma}$-rays

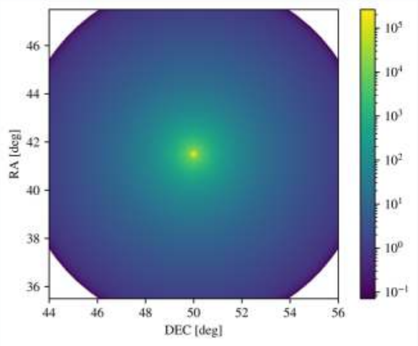

Use as BKG

$\boldsymbol{\gamma}$-rays from AGNs

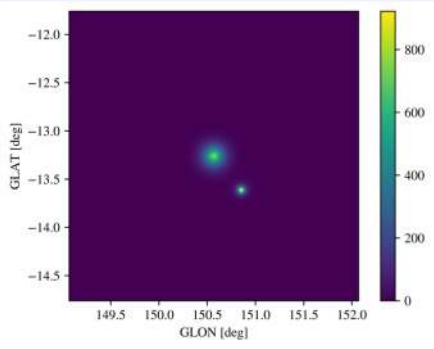

Use as BKG

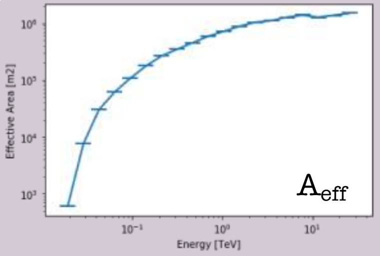

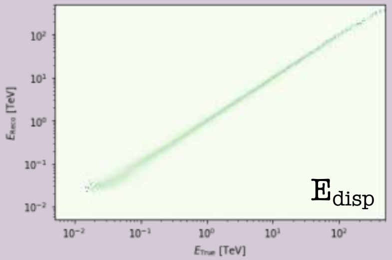

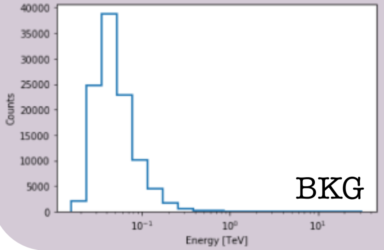

CTA IRFs

https://www.cta-observatory.org/science/cta-performance/

Observation Simulation

If no signal found

Constraints on DM models

$$\frac{d\Phi_\chi^{Ann}}{dE} = \frac{<\sigma v>}{8\pi m_\chi^2}\frac{dN}{dE} \times J$$

$$\frac{d\Phi_\chi^{Decay}}{dE} = \frac{1}{4\pi m_\chi \tau_\chi}\frac{dN}{dE} \times D$$

CTA ANALYSIS CONFIGURATION: TEMPLATE FITTING

- Includes all expected γ-ray sources: DM + CRs + AGNs + Background (BKG) IRFs

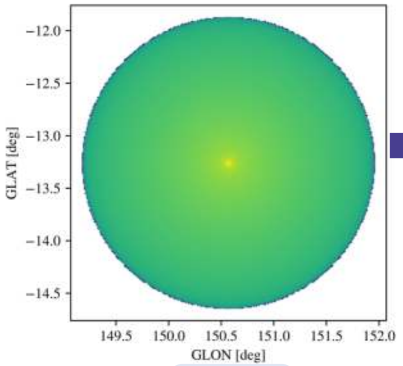

DM

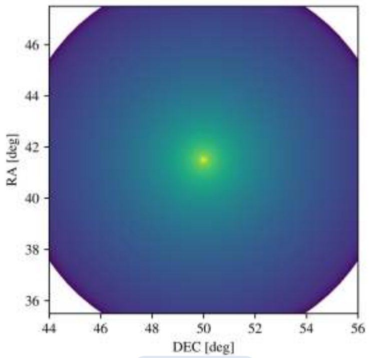

CR

[baseline]

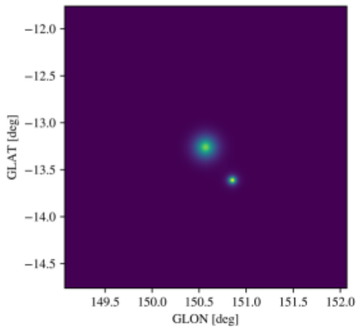

AGNs

[*CTA Cons. 21* – γ-ray propagation]

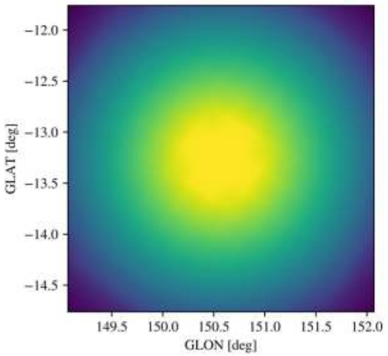

BKG

[from IRFs]

Most realistic physical scenario

- Fitting 8 parameters in total

$$\vec{\theta} \equiv \left(A_\chi, A_{\rm CR}, A_{\rm PS}^{(1,2)}, \alpha_{\rm PS}^{(1,2)}, A_{\rm bkg}, \alpha_{\rm bkg}\right)$$

$$TS = 2\,\log\left[\frac{\mathcal{L}\left(A_\chi, \hat{\hat{\nu}}\right)}{\mathcal{L}_{\rm null}\left(A_\chi = 0, \hat{\nu}\right)}\right]$$

- $TS < 25$ ➡ No signal

- Considers the different morphologies of each emission
- Allows to check correlations between components
- Historically used in *Fermi*-LAT analysis and in a recent CTA analysis (*Acharyya+20* [*CTA Cons.*])

State-of-the-art analysis pipeline

CTA ANALYSIS: DM PROSPECTS FOR CONSTRAINTS

Annihilation 95% C.L Upper Limits

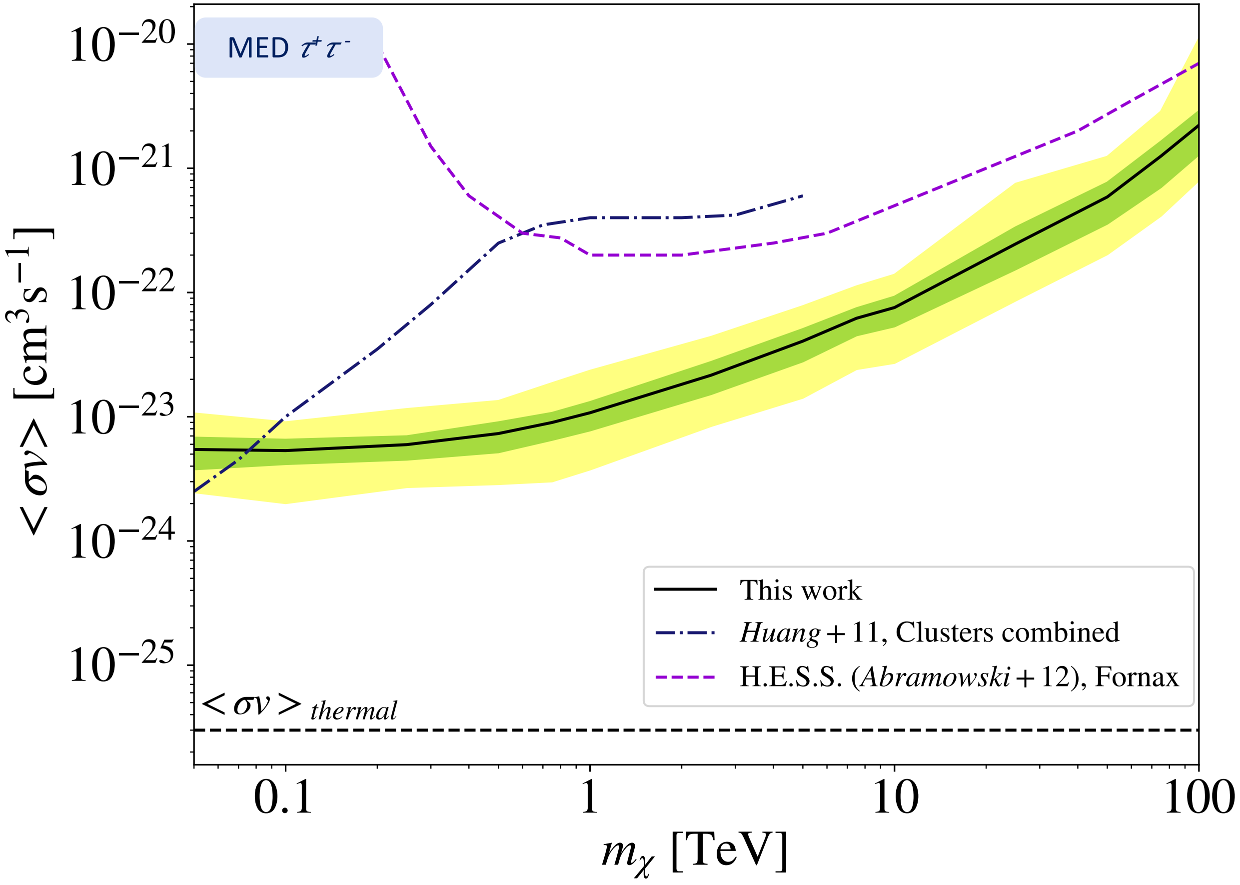

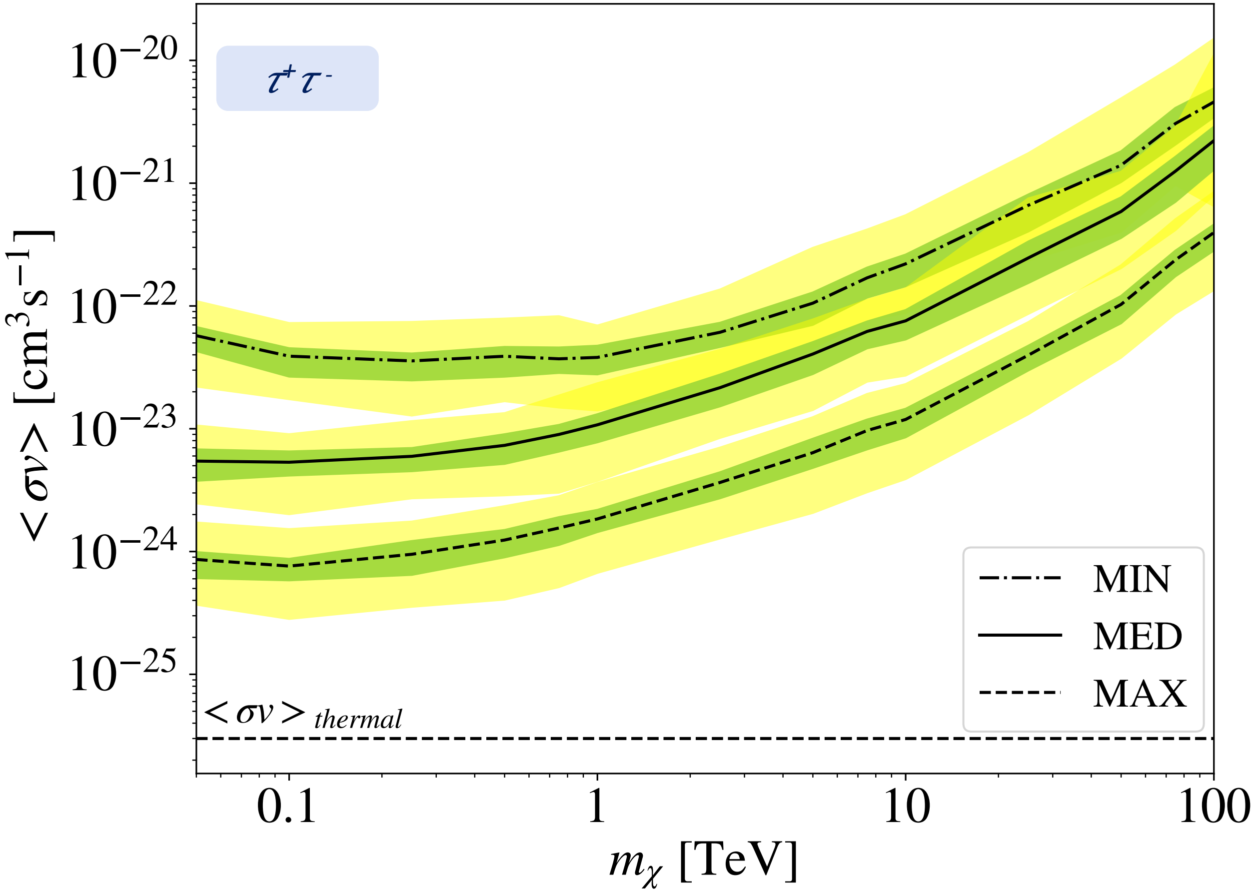

CTA ANALYSIS: DM PROSPECTS FOR CONSTRAINTS

Decay 95% C.L. Lower Limits

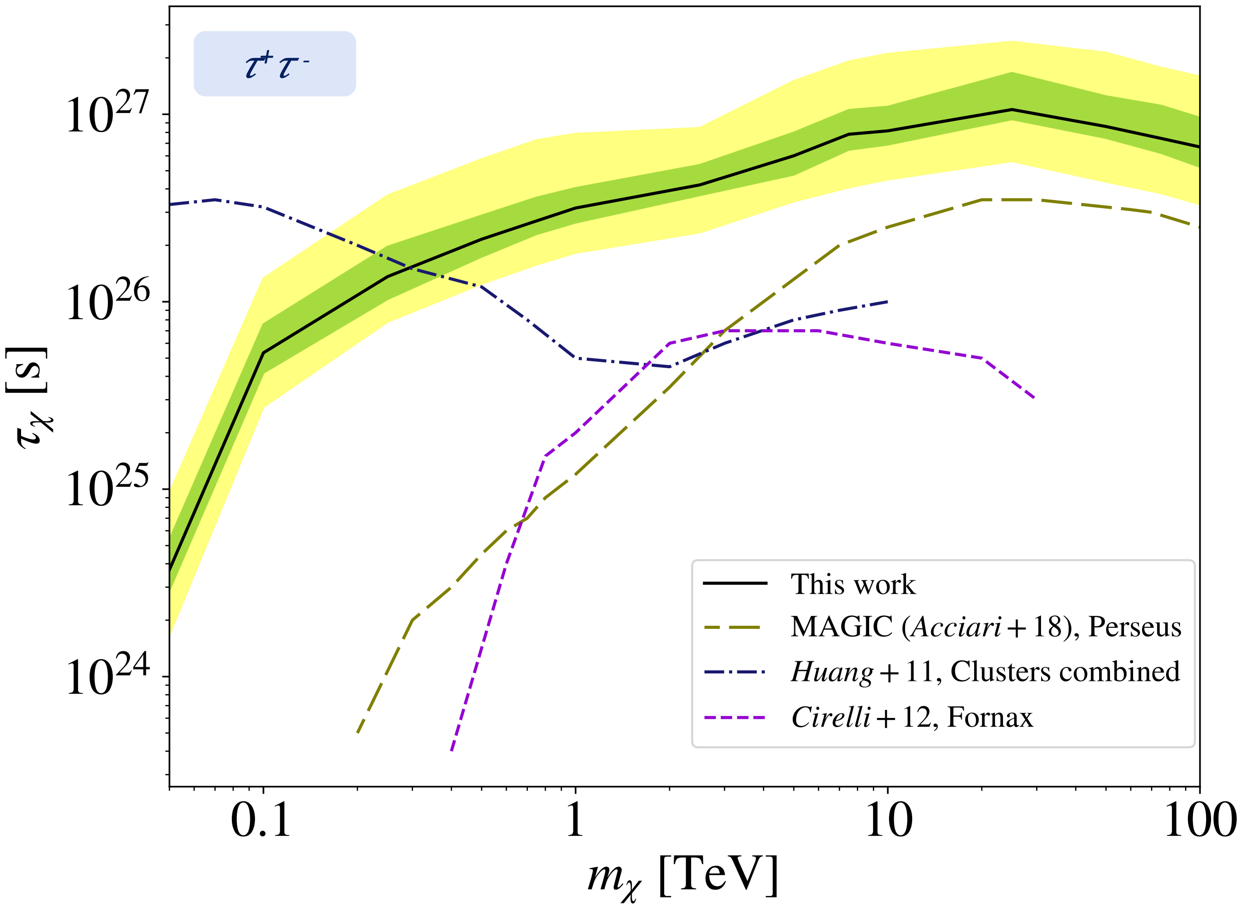

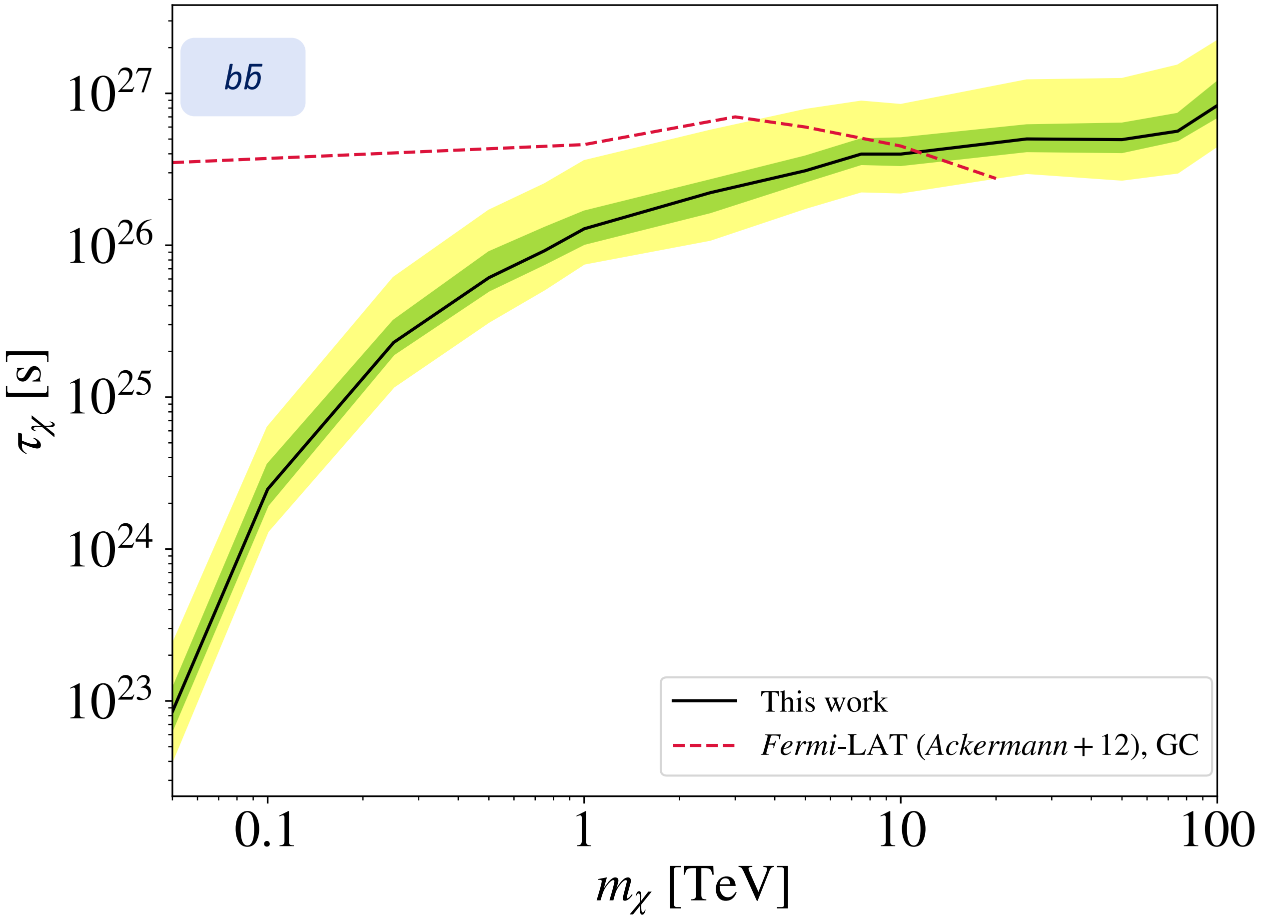

BEYOND THE ORIGINAL KSP: MORE CLUSTERS

- Natural extension of the KSP: why just focus on Perseus for DM searches?
- Similar procedure than KSP applied to few other galaxy clusters
- Based on previous *Fermi*-LAT analysis: *Constraining the dark matter contribution of gamma-rays in cluster of galaxies using Fermi-LAT data*
  M. di Mauro, JPR, M. A. Sánchez-Conde, N. Fornengo
  Phys. Rev. D 107, 083030, [arXiv:2303.16930]

- Selection criteria:
  - Well-known M_{200} from X-rays measurements [*Schellenberger & Reiprich 17*]
  - Local clusters $z < 0.1$
  - Mask of $|b| < 20$ deg to avoid galactic diffuse emission
  - Separation of at least 2 deg to account for cluster extension

Sample of 49 local galaxy clusters

Reiprich & Böhringer 02, Ackermann+10 [Fermi-LAT Coll.], Sánchez-Conde+11, Ackermann+14 [Fermi-LAT Coll.]

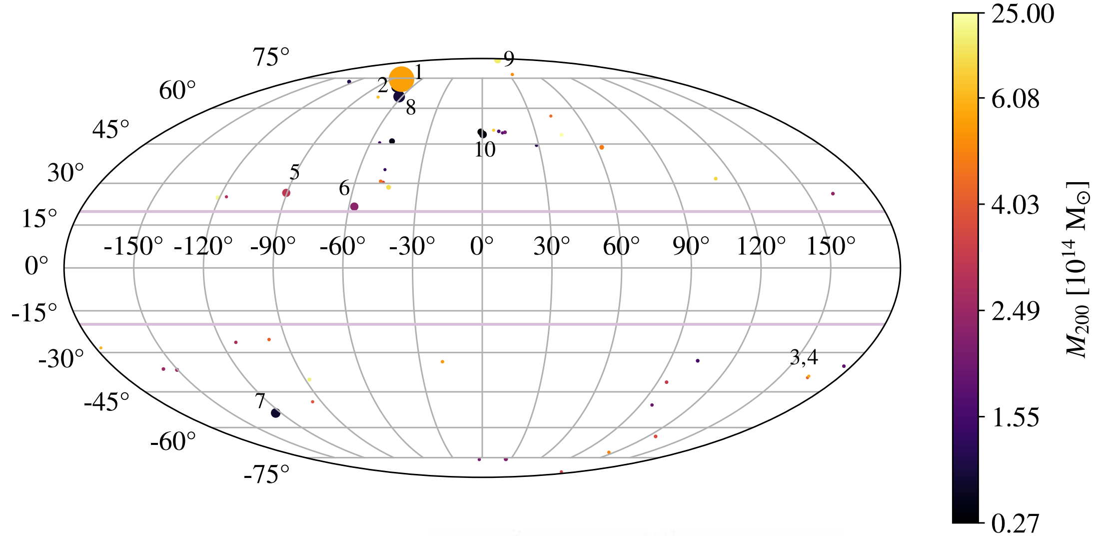

1 - Virgo
2 - M49
3 - A0399
4 - A0401
5 - A1060 - Hydra
6 - A3526 - Centaurus
7 - NGC 1399 - Fornax
8 - NGC 4636
9 - A1656 - Coma
10 - NGC 5813

BEYOND THE ORIGINAL KSP: MORE CLUSTERS

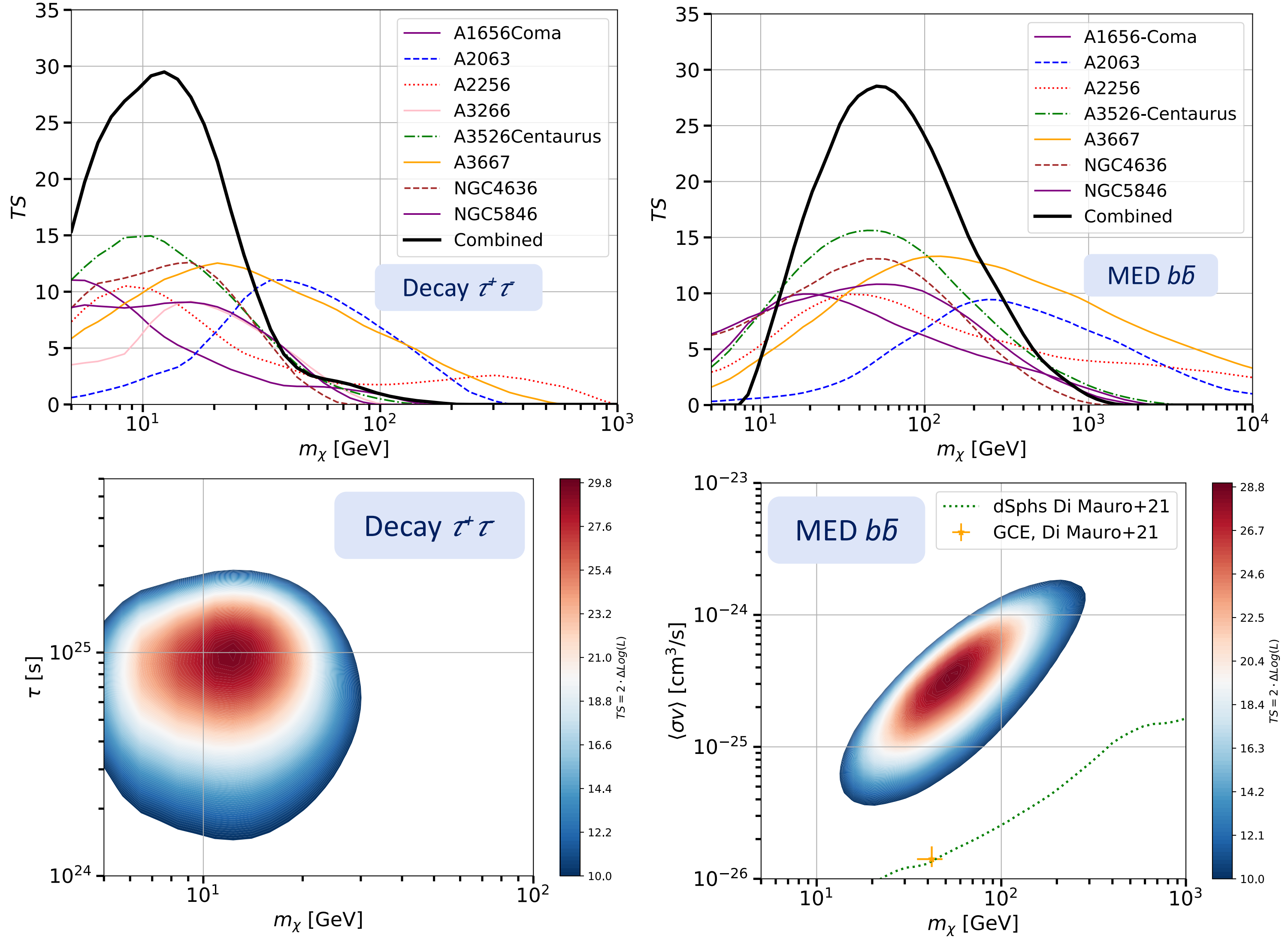

Annihilation

- Not compatible with GC excess
- Ruled out by dSphs

Decay

- Ruled out by Isotropic γ–ray Background (IGRB) and GC

Blanco&Hooper18, Ando&Ishiwata15, Ackermann+12 [Fermi Collab.]

- Build *TS* distribution using 3100 random blank sky directions

Significance around 2.5-3.0σ

GAMMA-RAYS FROM GALAXY CLUSTERS

- Galaxy clusters are excellent target for indirect DM searches (massive, closeby)
- Still no clear gamma-ray signal from clusters detected
- CTA is the future for VHE gamma-ray astronomy, with superb capabilities for WIMP searches
  - Perseus cluster will have 300h of observation time
  - State-of-the-art DM modelling for Perseus including halo substructure
  - Complete and comprehensive study of the different expected emissions: DM+CR+AGNs
  - Fit to $b\bar{b}$ & $\tau^+\tau^-$, annihilation & decay. In the absence of a DM signal:
    - Annihilation:
      - best 95% C.L. upper limits for $\tau^+\tau^-$,2-4 orders of magnitude above $<\sigma v>_{thermal}$;
      - different prescriptions for subhalos (MIN-MED-MAX) change our results a factor ~O(10)
    - Decay:
      - best 95% C.L. lower limits for $\tau^+\tau^-$, with τ_χ~10^{27}s, most competitive for m_χ~TeV
- Recent analysis with *Fermi*-LAT provided very promising results for the observation of clusters with CTA, it hints to being closer to a signal than ever!

THANKS FOR YOUR ATTENTION

BACK UP MATERIAL

DARK MATTER (DM) EVIDENCE

Galactic scales

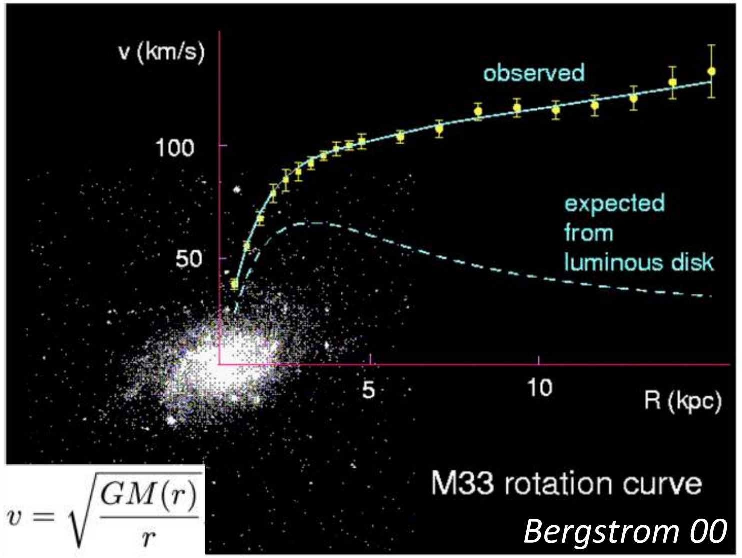

Bergstrom 00

- Rotational curves
- Velocity dispersion

Galaxy cluster scales

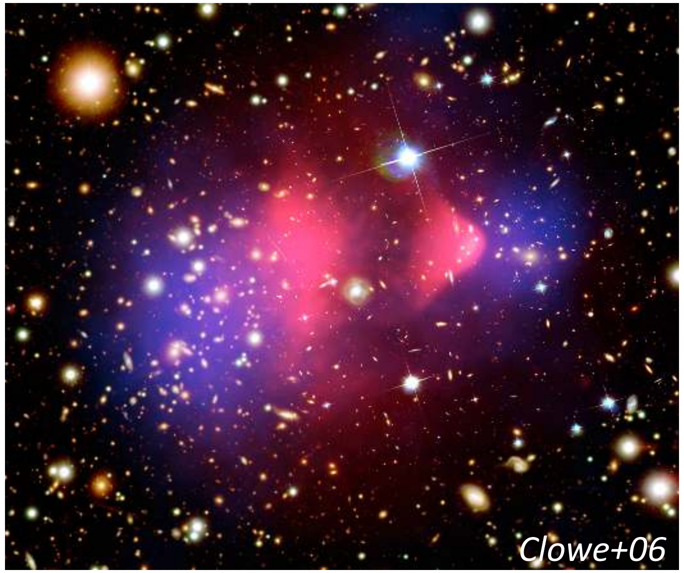
Clowe+06

- Peculiar velocity flows
- Mass tracers (X-rays, Sunyaev–Zeldovich, strong&weak lensing)
- Dynamical systems

Cosmological scales

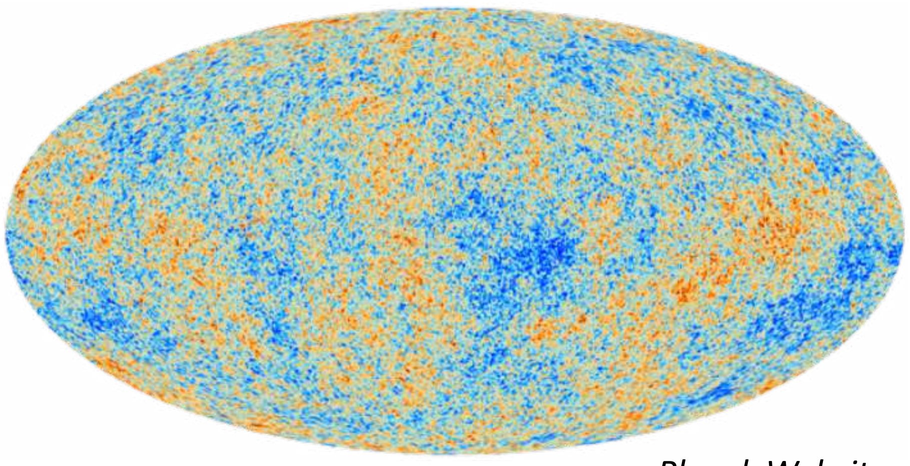
Planck Website

- Cosmic Microwave Background (CMB) anisotropies
- Large Scale Structure (LSS)

HALO AND SUBHALO PROPERTIES

Main halos

- Fundamental non-linear units of cosmic structures
- Inner density profile

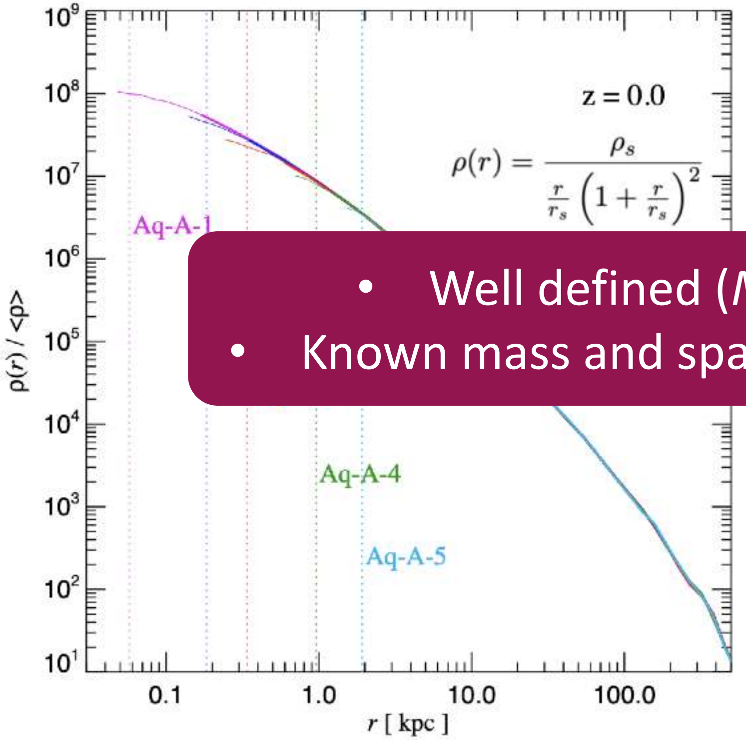

- Mass distribution

dn ... $\propto M^\alpha$

- Concentration

$c(M)$

- Well defined (M_{200}, R_{200})
- Known mass and spatial distribution

Subhalos

- The later halos that do not get to merge with the rest
- Fall in the potential wells of main halos

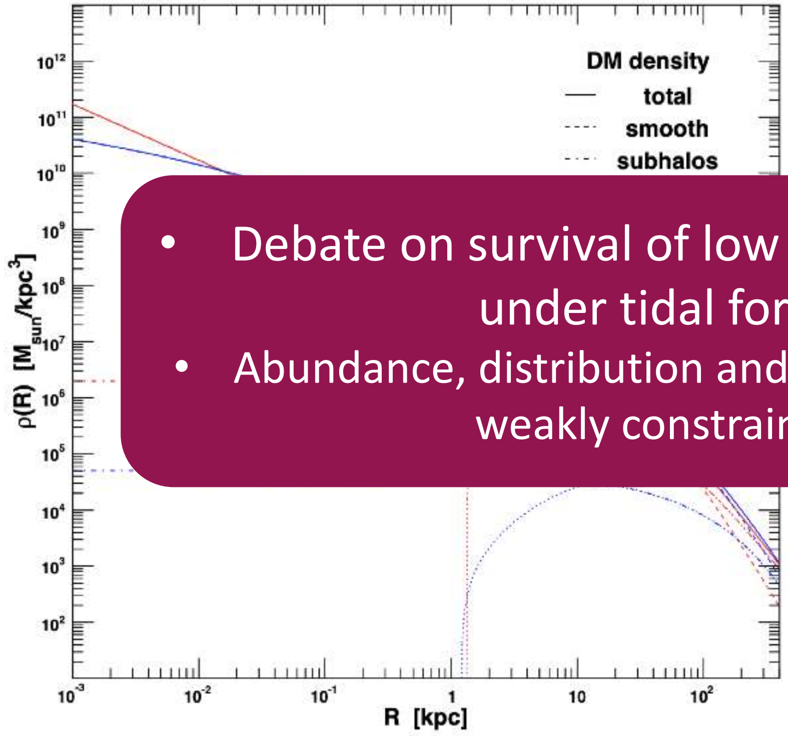

- Mass distribution

... M^α_{sub}

...]

$c_{sub}(M_{sub}, r_{sub})$

- Debate on survival of low mass subhalos under tidal forces
- Abundance, distribution and inner structure weakly constrained

PREVIOUS γ-RAY DM SEARCHES IN GALAXY CLUSTERS

Fermi-LAT - Annihilation

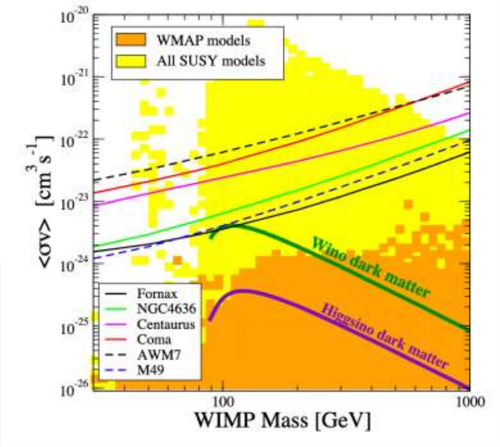

Ackermann+10 [*Fermi-LAT Collab.*]

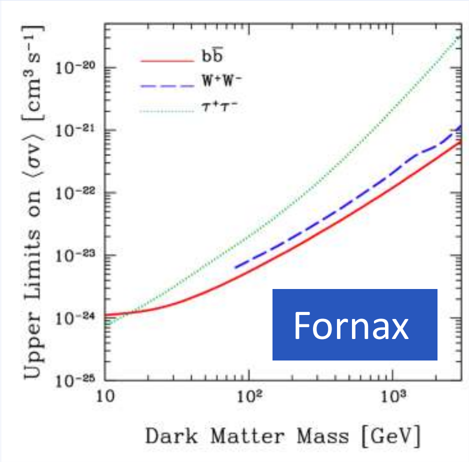

Ando&Nagai12

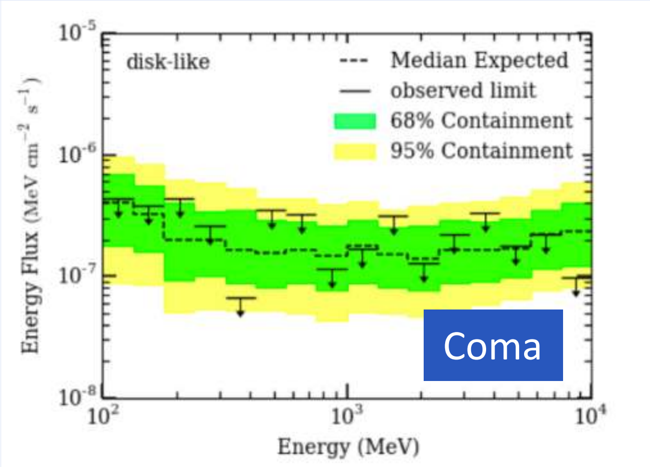

Ackermann+16 [*Fermi-LAT Collab.*]

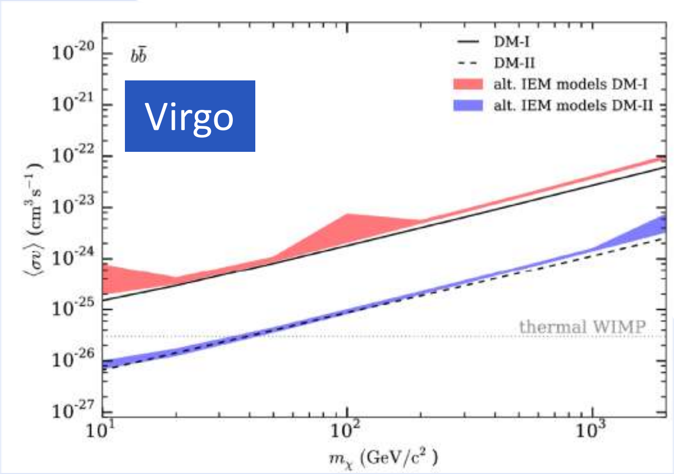

Ackermann+15 [*Fermi-LAT Collab.*]

- Last word about gamma-ray searches in a big sample of galaxy clusters: CR focused (*Ackermann+14* [*Fermi-LAT Collab.*])

MAGIC - Decay

Best constraints so far!

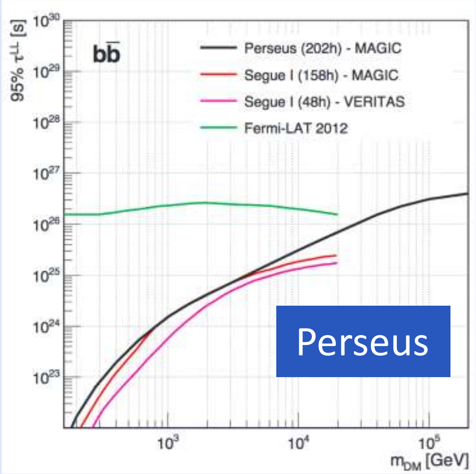

Acciari+18 [*MAGIC Collab.*]

PREVIOUS γ-RAY DM SEARCHES IN GALAXY CLUSTERS

- For annihilation of WIMPs:
  - $\phi_{DM} \propto \rho_{DM}^2$
  - $\phi_{DM} \propto 1/d^2$

DM distribution becomes extremely relevant

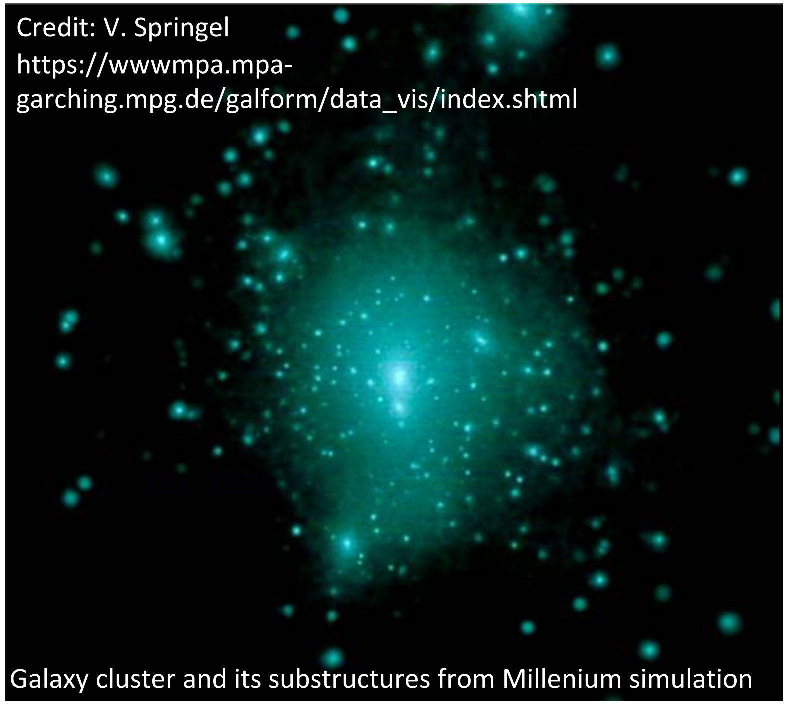

Considering:
- Smooth component
  +
- Substructure

Object	Type	J_{tot} (GeV^2cm^{-5})
Fornax	Cluster	1.48×10^{18}
Willman 1	DSPH	8.51×10^{17}
Coma	Cluster	6.92×10^{17}
Perseus	Cluster	5.37×10^{17}
Segue 1	DSPH	5.13×10^{17}
Draco	DSPH	3.72×10^{17}

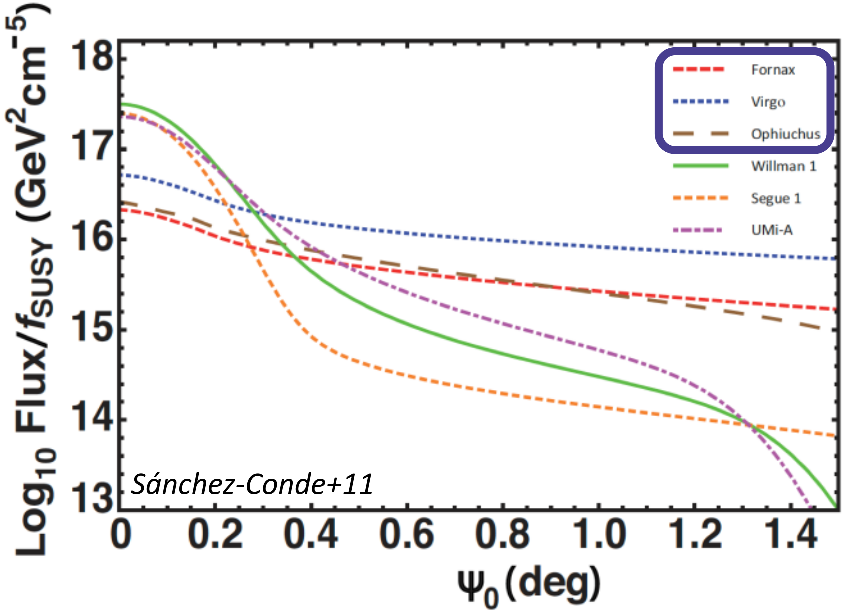

OBTENTION OF DM MODEL PARAMETERS

- State-of-the-art parametrization of the DM in galaxy clusters: $\langle\rho_{\rm tot}\rangle(r) = \rho_{\rm sm}(r) + \langle\rho_{\rm subs}\rangle(r)$

1. Assume a DM profile $\rho(r) = \frac{\rho_0}{(\frac{r}{r_s})[1+\frac{r}{r_s}]^2}$ NFW

2. Assume a concentration-mass relation ($c_{200} - M_{200}$): *Sánchez-Conde&Prada14* $c_{200}(M_{200}, z=0) = \sum_{i=0}^{5} c_i \times \left[\ln\left(\frac{M_{200}}{h^{-1}M_\odot}\right)\right]^i$

3. Assume spherical collapse from an overdensity Δ = 200 over the critical density $\Delta_{200} = \frac{3M_{200}}{4\pi R_{200}^3 \rho_{crit}}$

4. Compute remaining parameters

Scale density

$$\rho_0 := \frac{2\Delta_{200}\rho_{crit}c_{200}}{3F(c_{200})}$$

with

$$F(c_{200}) = \frac{2}{c_{200}^2}\left(\ln(1+c_{200}) - \frac{c_{200}}{1+c_{200}}\right)$$

Scale radius

$$c_{200} = \frac{R_{200}}{r_s}$$

Angular extension

$$\theta_{200} = \tan\left(\frac{R_{200}}{d_L}\right)$$

PERSEUS DIFFERENTIAL ANNIHILATION FLUX PROFILE

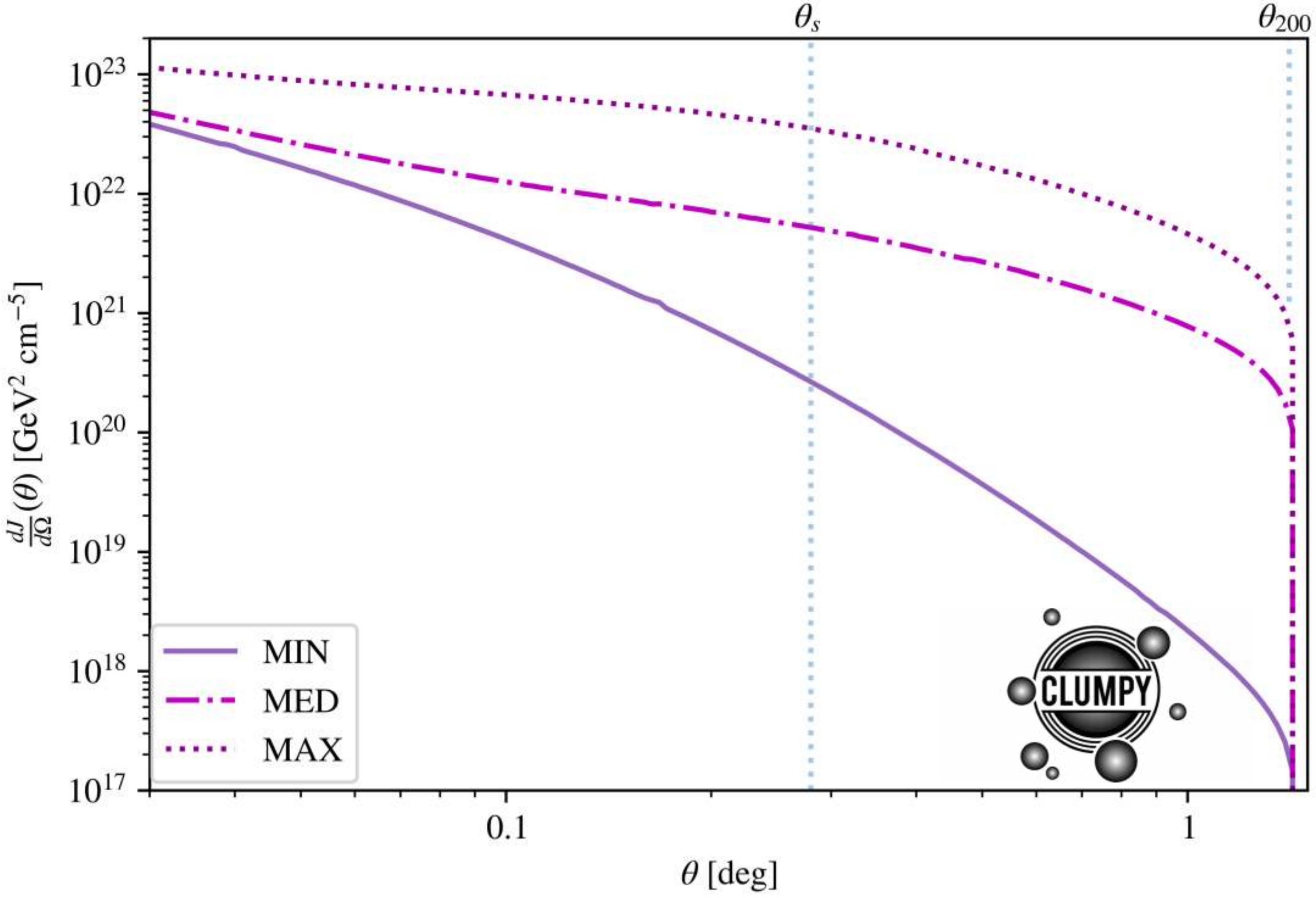

General parameters

Hitomi Coll.18	z	0.017284	l, b	150.58 deg, -13.26 deg
Urban+14	M_{200}	7.52×10^{14} $M_\odot$	R_{200}	1865.0 kpc
Sánchez-Conde & Prada 14	c_{200}	5.03	θ_{200}	1.42 deg
	r_s	370.82 kpc	θ_s	0.28 deg
Flat ΛCDM	d_L	75.01 Mpc	ρ_s	299581 $M_\odot$/kpc^3

Annihilation	$\log_{10} J$ [GeV^{2}cm^{-5}]
MIN	17.42
MED	18.43
MAX	19.20
Decay	$\log_{10} D$ [GeV cm^{-2}]
	19.20

MORPHOLOGY OF THE DM SIGNAL FROM PERSEUS

- Skymaps of the differential J/D-factors

Annihilation

- Boost factor

$B = J^X / J^{\mathrm{MIN}} - 1$ →

B_{MED} = 9 (B~9 – *Moliné+17*)
B_{MAX} = 59 (B~72 – *Moliné+17*)

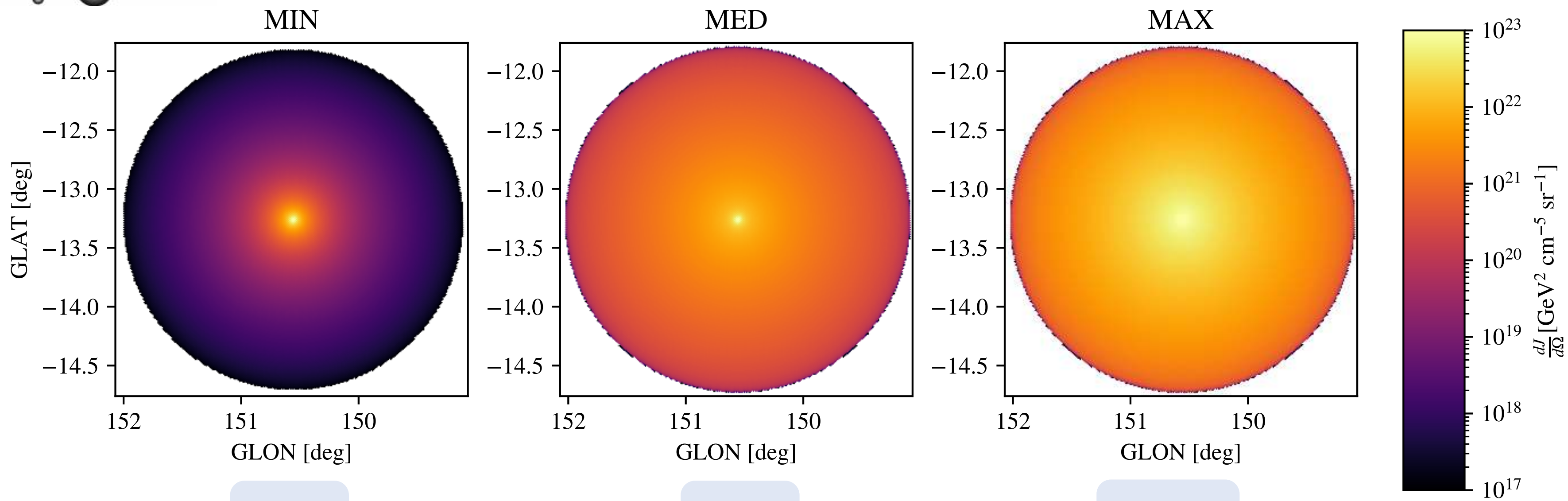

MIN MED MAX

Decay

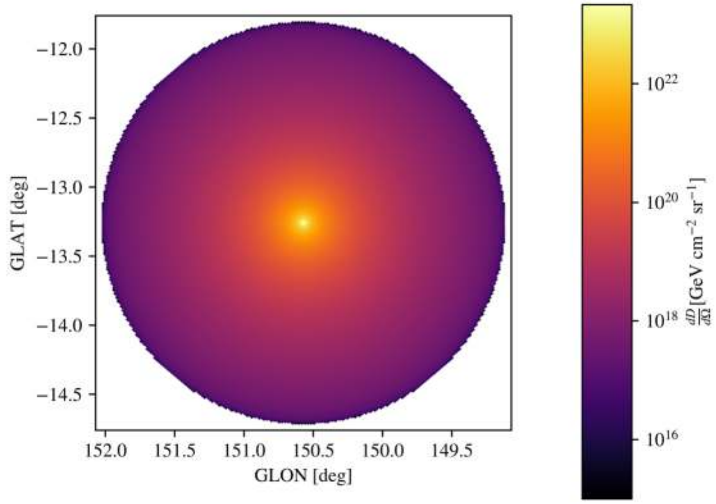

UNCERTAINTIES FOR CLUSTER'S DM MODELS

- Uncertainties in the J/D-factor enter through:

X-rays measurements → *Urban+14* Mass modelling and extrapolations → *c(M) – M* scatter →

- Masses from other methods
- Other X-rays measurements

- ~ O(0.14) dex for *Sánchez-Conde & Prada 14*

	σ_J	σ_D
$M_{min} + c_{200,min}$	0.2	0.003
M_{min}	0.002	0.0
M_{max}	0.005	0.0
$M_{max} + c_{200,max}$	0.2	0.0

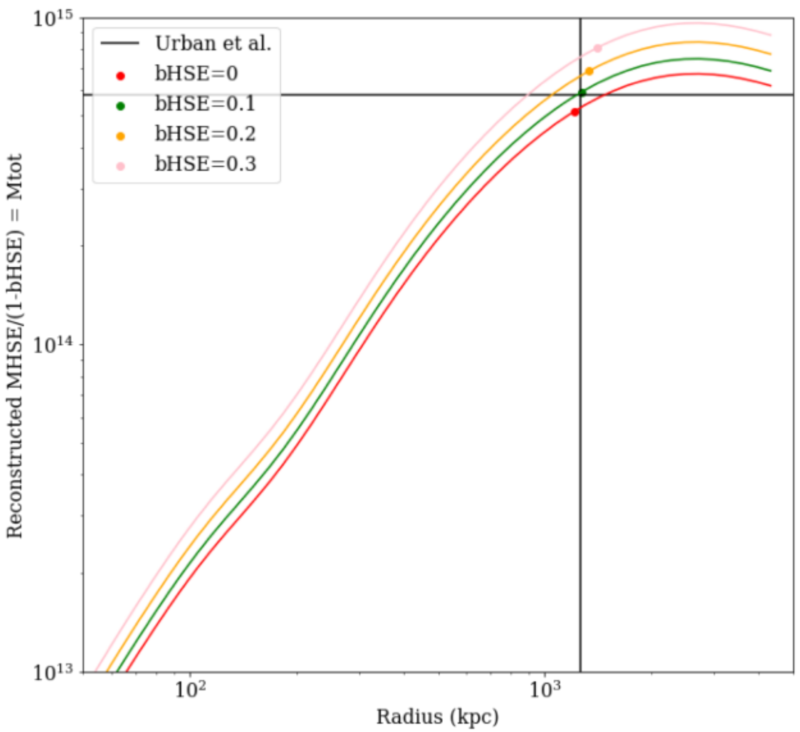

$$\mathcal{J}(J\,|\,J_{\rm obs},\sigma_J) = \frac{1}{\ln(10)J_{\rm obs}\sqrt{2\pi}\sigma_J} \times e^{-\left(\log_{10}(J)-\log_{10}(J_{\rm obs})\right)^2/2\sigma_J^2}$$

Gaussian prior in J-factor uncertainty

CHARACTERISTICS OF THE SIMULATIONS

- Background models: CR baseline model + NGC1275 & IC310 + CTA IRFs instrumental

  - From simulations by *Pinzke&Pfrommer 2010:* π^0 decay + Inverse Compton

Model	X_{500} (%)	$\alpha_{\rm CRp}$	$\eta_{\rm CRp}$	$F^{\rm (had)}_{500,E_\gamma>150\ \rm GeV}$	$F^{\rm (IC)}_{500,E_\gamma>150\ \rm GeV}$ [10^{-14} cm^{-2} s^{-1}]
	reference value, [min, max]				
Baseline	1.0, [0.0, 20.0]	2.30, [2.0, 3.0]	1.0, [0.0, 1.5]	70.2, [0, 11373.8]	2.1, [0, 625.4]

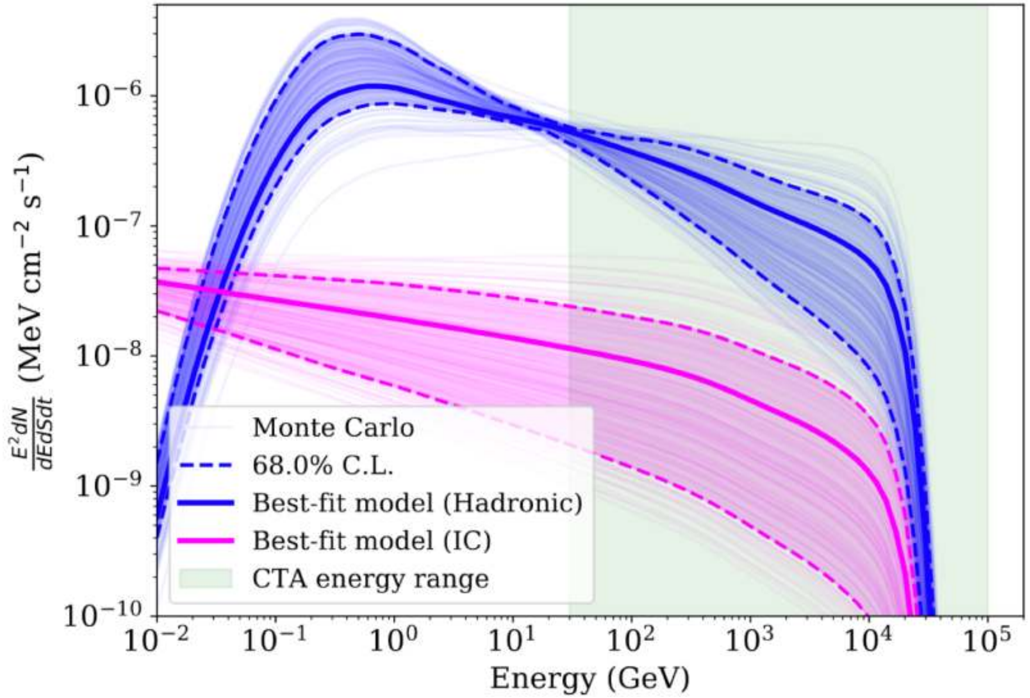

- Quiescent states

  - NGC 1275 (*Ahnen+16*)

$$\frac{dN}{dEdSdt} = 2.1 \times 10^{-11} \left(\frac{E}{200\ \mathrm{GeV}}\right)^{-3.6} \mathrm{cm^{-2}s^{-1}TeV^{-1}}$$

  - IC 310 (*Alecksic+14*)

$$\frac{dN}{dEdSdt} = 0.741 \times 10^{-12} \left(\frac{E}{1\ \mathrm{TeV}}\right)^{-1.81} \mathrm{cm^{-2}s^{-1}TeV^{-1}}$$

CHARACTERISTICS OF THE SIMULATIONS

- Input models:

DM Annihilation (thermal cross-section)
DM Decay (τ_χ = 10^{27}s)
m_χ = 10 TeV
$b\bar{b}$

+ CR baseline model

NGC1275
&
IC310

+ EBL
Domínguez+11

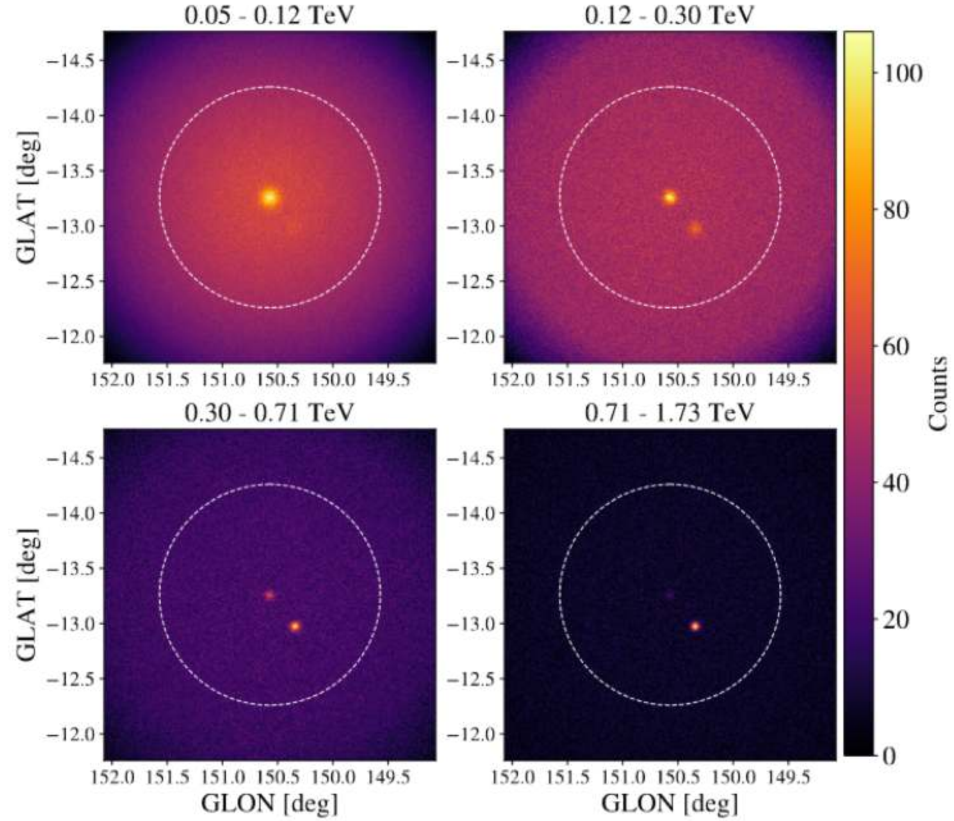

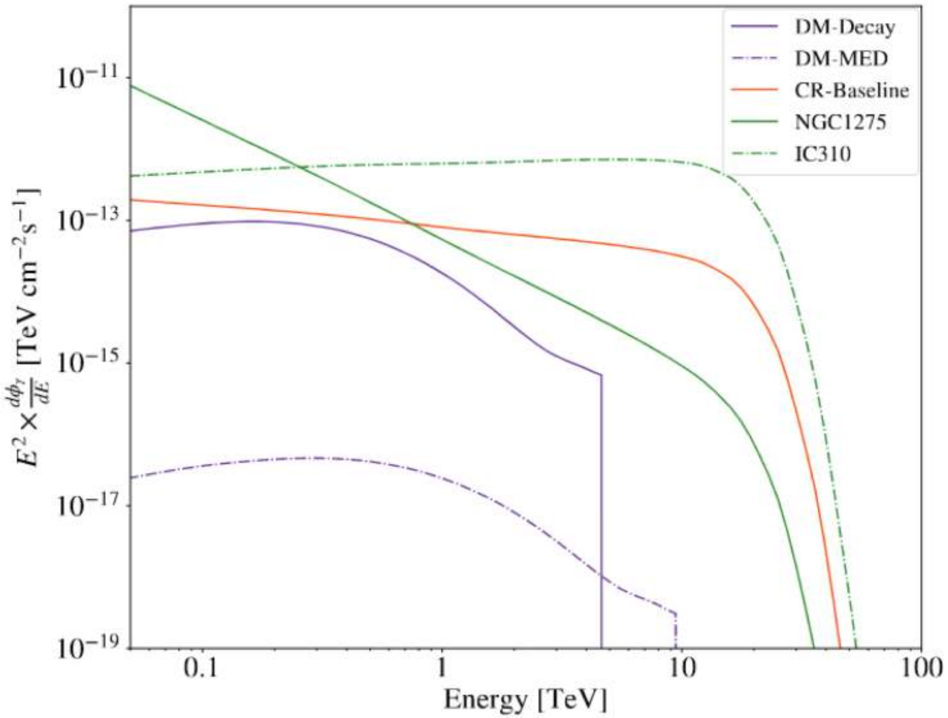

CTA ANALYSIS CONFIGURATION: TEMPLATE FITTING

- Includes all expected γ-ray sources: DM + CRs + AGNs + Background (BKG) IRFs

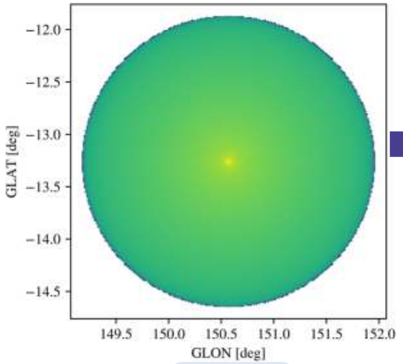

DM

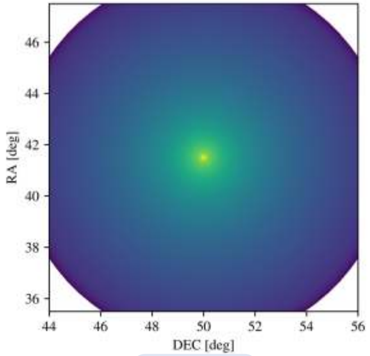

CR

[baseline]

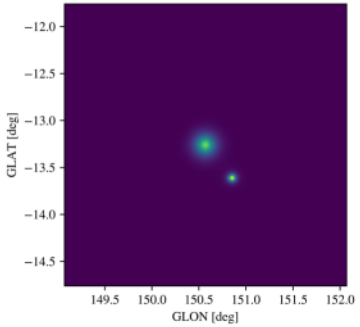

AGNs

[*CTA Cons. 21* – γ-ray propagation]

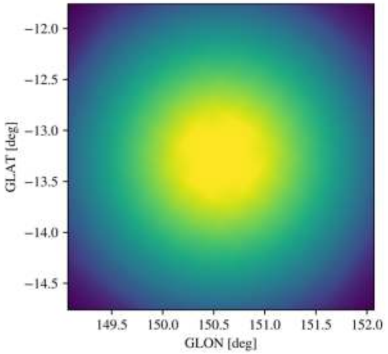

BKG

[from IRFs]

Most realistic physical scenario

- Fitting 8 parameters in total

$$\vec{\theta} \equiv \left(A_\chi, A_{\rm CR}, A_{\rm PS}^{(1,2)}, \alpha_{\rm PS}^{(1,2)}, A_{\rm bkg}, \alpha_{\rm bkg}\right)$$

- Use likelihood ratio test to fit the models to the simulated data:

$$\ln\mathcal{L}(\vec{\theta}|D) = \sum_i \tilde{M}_i(\vec{\theta}) - d_i \ln(\tilde{M}_i(\vec{\theta}))$$

Poissonian likelihood for each parameter

$$TS = 2\,\log\left[\frac{\mathcal{L}\left(A_\chi, \hat{\hat{\nu}}\right)}{\mathcal{L}_{\rm null}\left(A_\chi = 0, \hat{\nu}\right)}\right]$$

- *TS* < 25 ➡ No signal

DMtools

N_{obs}	100
T_{obs} [h]	300
IRFs	`North_z20_50h, prod5`
Energy range [TeV]	0.03 - 100

CTA ANALYSIS ELEMENTS

- https://docs.gammapy.org/0.19/stats/fit_statistics.html

- Likelihood ratio test:

$$TS = 2\,\log\left[\frac{\mathcal{L}\left(A_\chi, \hat{\hat{\nu}}\right)}{\mathcal{L}_{\rm null}\left(A_\chi = 0, \hat{\nu}\right)}\right]$$

  - *TS* < 25 ⟶ No signal

Template fitting: Poisson likelihood for each component, *Cash* statistics (*Cash 79*)

$$\ln\mathcal{L}(\vec{\theta}|D) = \sum_i \tilde{M}_i(\vec{\theta}) - d_i \ln(\tilde{M}_i(\vec{\theta})) \qquad \vec{\theta} \equiv \left(A_\chi, A_{\rm CR}, A_{\rm PS}^{(1,2)}, \alpha_{\rm PS}^{(1,2)}, A_{\rm bkg}, \alpha_{\rm bkg}\right)$$

ON-OFF analysis: Poisson likelihood for signal and background, *Wstat* statistics (*XSpec manual*)

$$\mathcal{L}(A_\chi|D) = \prod_{ij} \frac{(N^S_{ij} + \kappa_{ij} N^B_{ij})^{N^{ON}_{ij}}}{N^{ON}_{ij}!} e^{-(N^S_{ij} + \kappa_{ij} N^B_{ij})} \times \frac{(N^B_{ij})^{N^{OFF}_{ij}}}{N^{OFF}_{ij}!} e^{-N^B_{ij}}$$

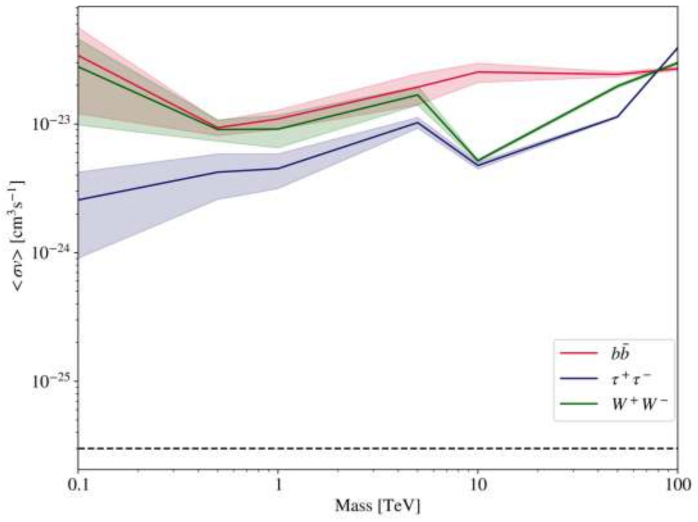

Caveat

- Since WStat takes into account background estimation uncertainties and makes no assumption such as a background model, it usually gives larger statistical uncertainties on the fitted parameters. If a background model exists, to properly compare with parameters estimated using the Cash statistics, one should include some systematic uncertainty on the background model.
- Note also that at very low counts, WStat is known to result in biased estimates. This can be an issue when studying the high energy behaviour of faint sources. When performing spectral fits with WStat, it is recommended to randomize observations and check whether the resulting fitted parameters distributions are consistent with the input values.

CTA ANALYSIS ELEMENTS

- Role of the Galactic diffuse emission:
  - Perseus is located "close" to the galactic plane (150.57, -13.26) deg
  - Baseline model for the galactic diffuse emission provided by D. Gaggero & P. de la Torre Luque
  - Integrated up to different radius and compared to CR baseline model
  - Worst case scenario, still factor ~few 10 below the expected CR emission

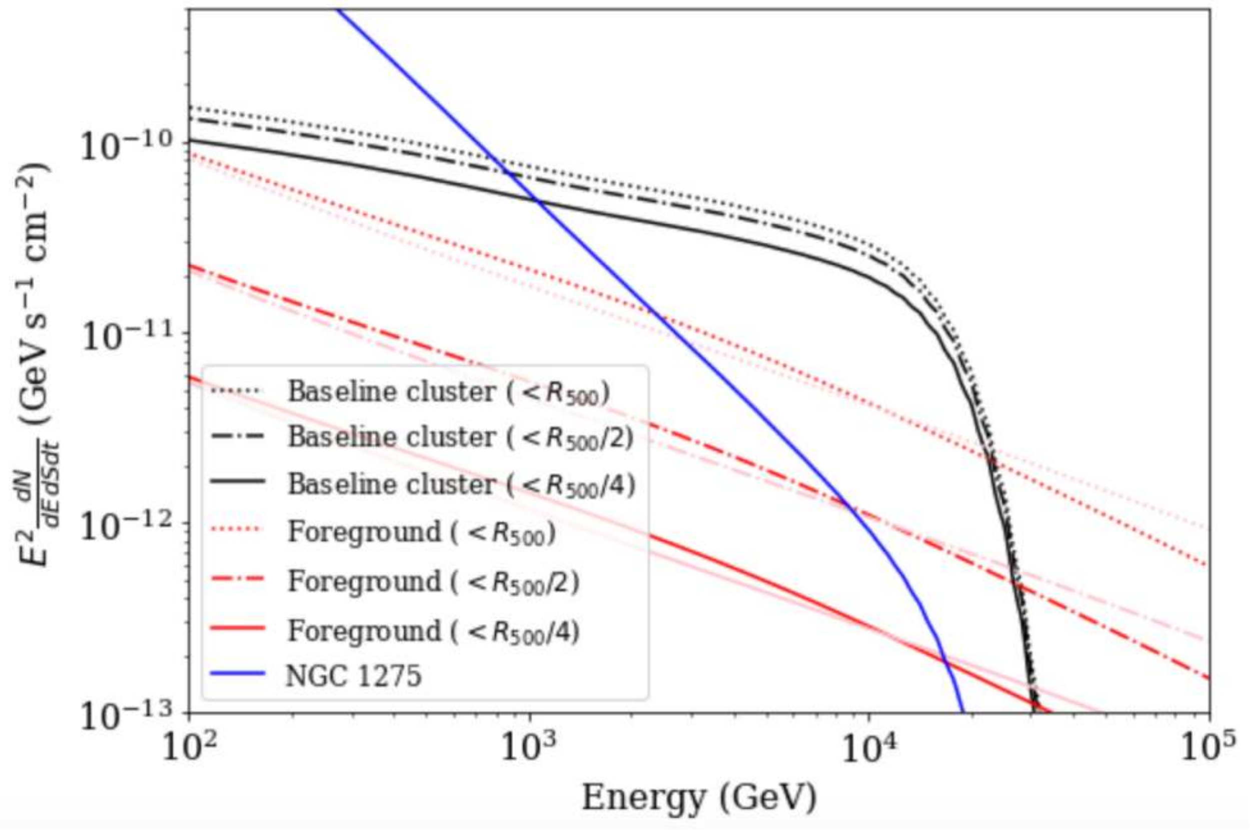

CTA ANALYSIS APPROACHES: DMTOOLS

- Most DM projects within CTA with same needs in terms of analysis tools and statistical treatment

Common set of tools

- Unified definitions, methodology
- Avoids repetition of same coding
- Allows easy comparison of results.
- Everyone can potentially contribute

- Creation & coordination of *DMTools Task Force* within CTA
- Gammapy beta-testing and software development

Since v-0.8 to v-1.0 (15 versions)

- Gammapy embedded functions:
  - DarkMatterAnnihilationSpectralModel
- GitHub repository:
  - Gammapy-DMTools
  https://github.com/peroju/dmtools_gammapy
- Gammapy coding sprints

CTA ANALYSIS APPROACHES: DMTOOLS

ON-OFF/Wobble Analysis

Standard for IACTs

Point-like

- Lowest complexity
- Most constraining results

Extended

- More complex and realistic than point-like approach
- Benefits from CTA large FoV and angular resolution

Template fitting

State-of-the-art pipeline

Minuit

- Already embedded in `Gammapy`
- Historically used fitter (`iminuit`) and very well documented (stability)

MCMC

- Flexible definition of likelihood and priors
- Easy analysis of correlations

CTA ANALYSIS APPROACHES: DMTOOLS

Basic functioning of the pipelines

Input DM model

- Spectral (based on Cirelli+12)
- Spatial (point-like, analytical, FITS files)

+

Combine with observation set-up

- IRFs
- Observation time
- Backgrounds

→

- Simulated Observation (Poisson realization)
- Observation

Enter the DM fit loop

1. For each realization, consider a list of channels and for each, a list of DM masses
2. Perform a likelihood fit to this specific model
3. Check $TS(H_{null}) \geq 25$
4. Compute $<\sigma v>$ upper limits with $TS(\mathrm{H}_{\text{best-fit}}) = 2.71$

INSIGHT RESULTS: CR ANALYSIS SUMMARY

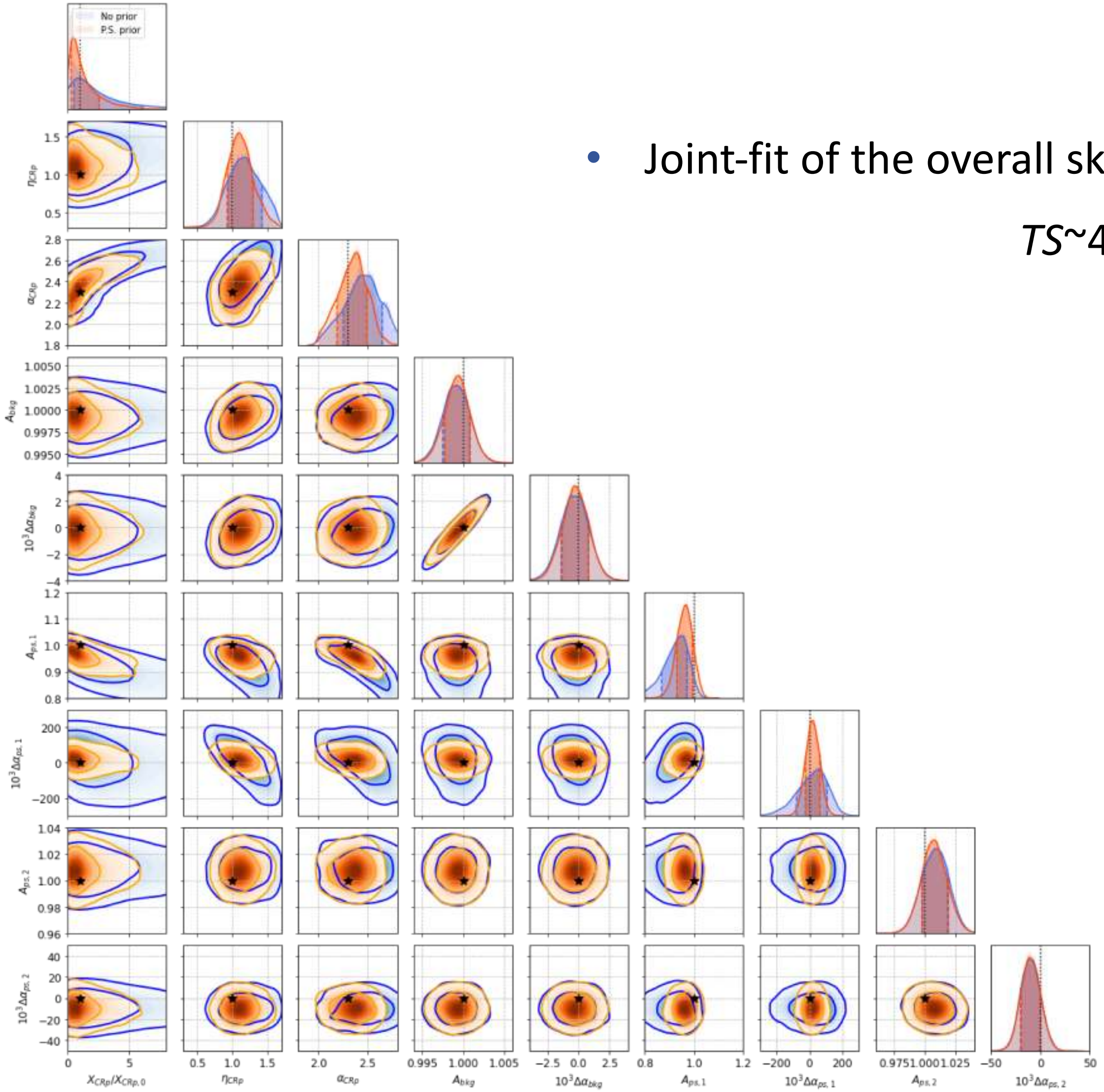

- Joint-fit of the overall sky model simultaneously

TS~42

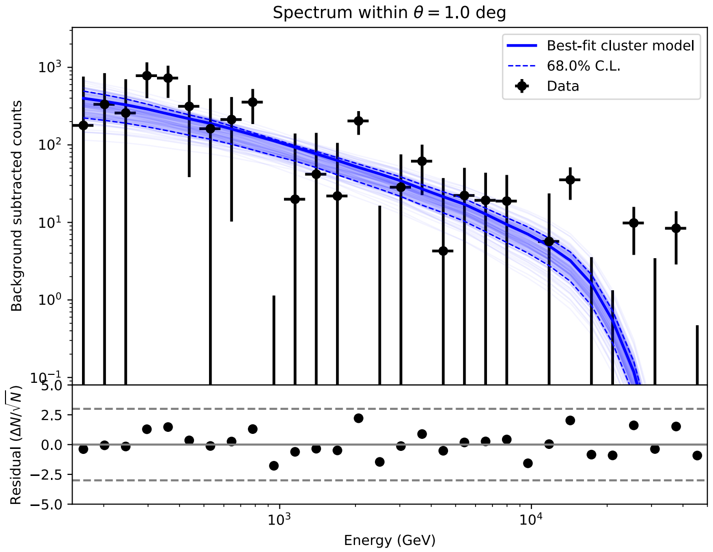

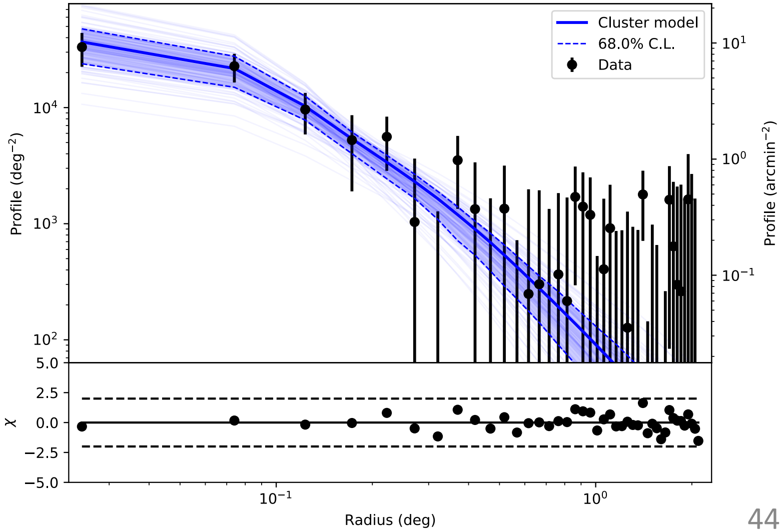

INSIGHT RESULTS: DM CONSTRAINTS

Annihilation (MED)

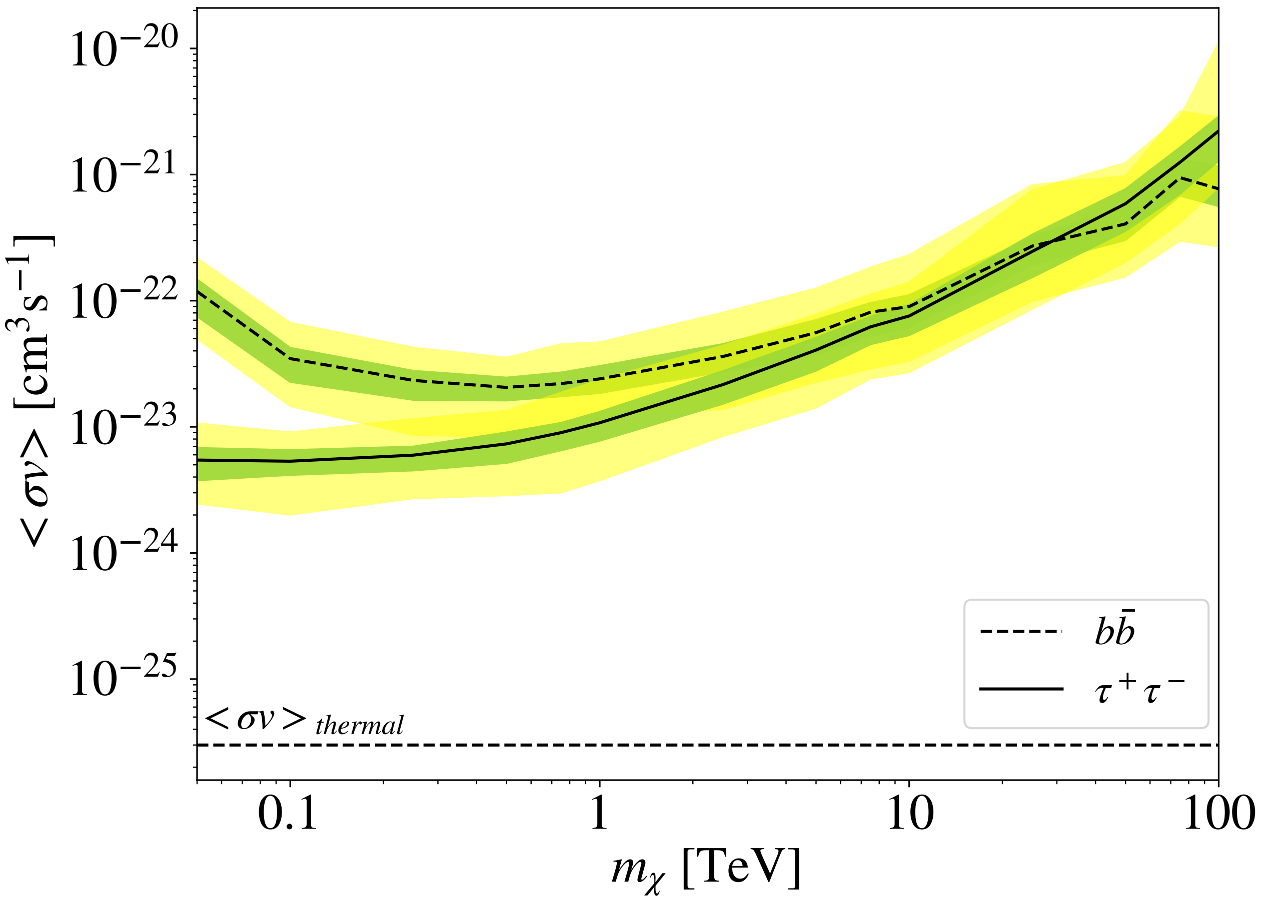

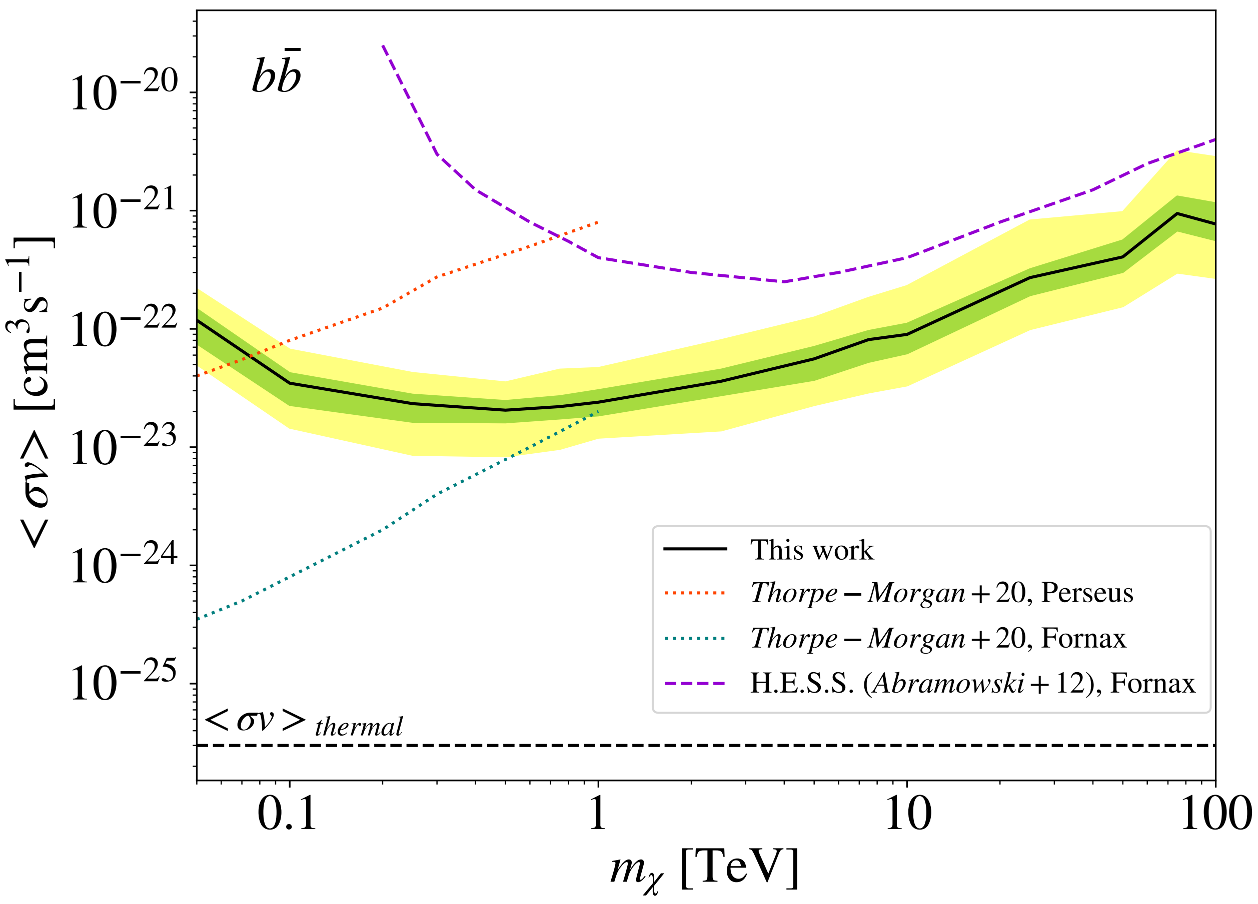

INSIGHT RESULTS: DM CONSTRAINTS

Annihilation (MED)

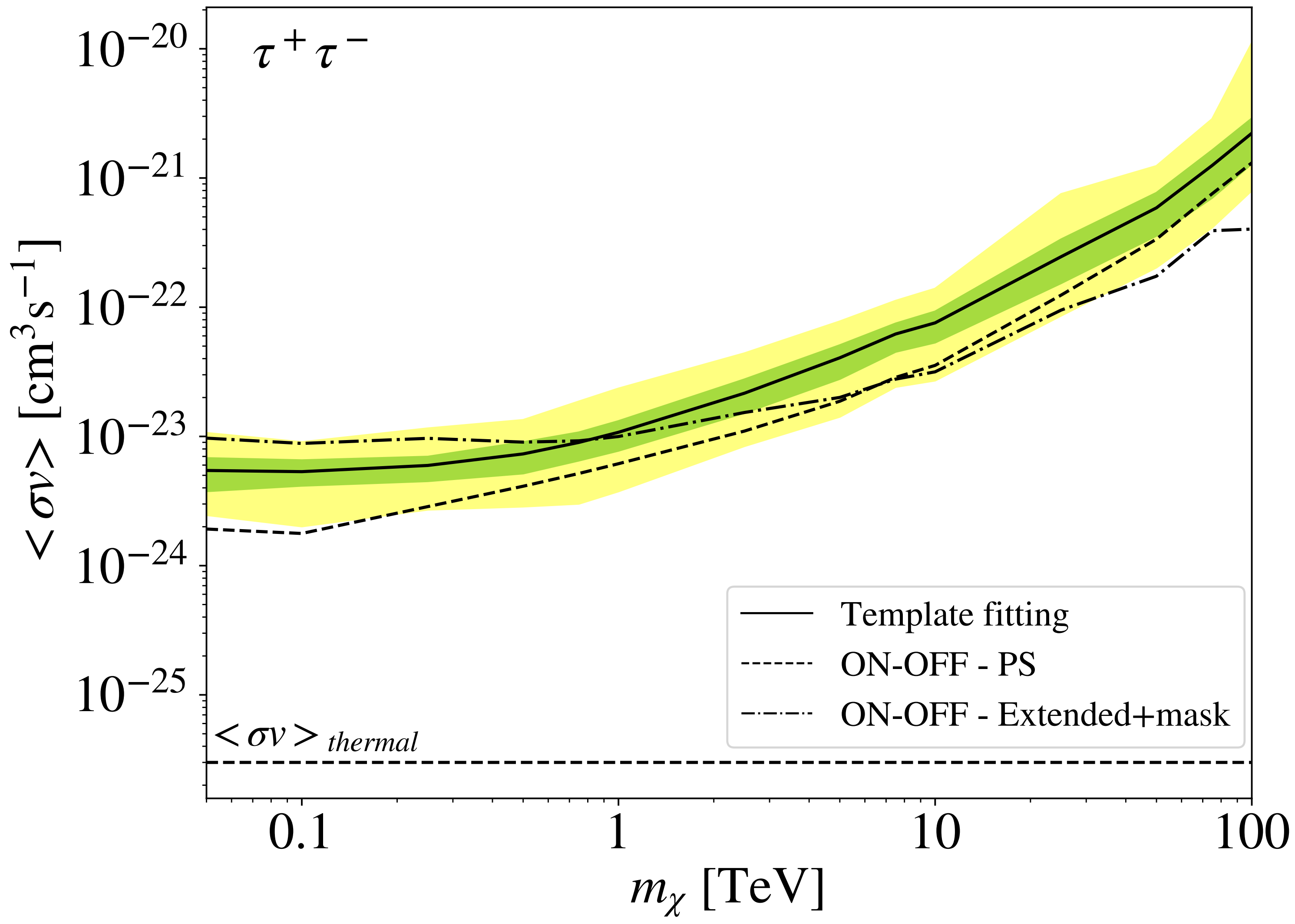

INSIGHT RESULTS: DM CONSTRAINTS

Decay

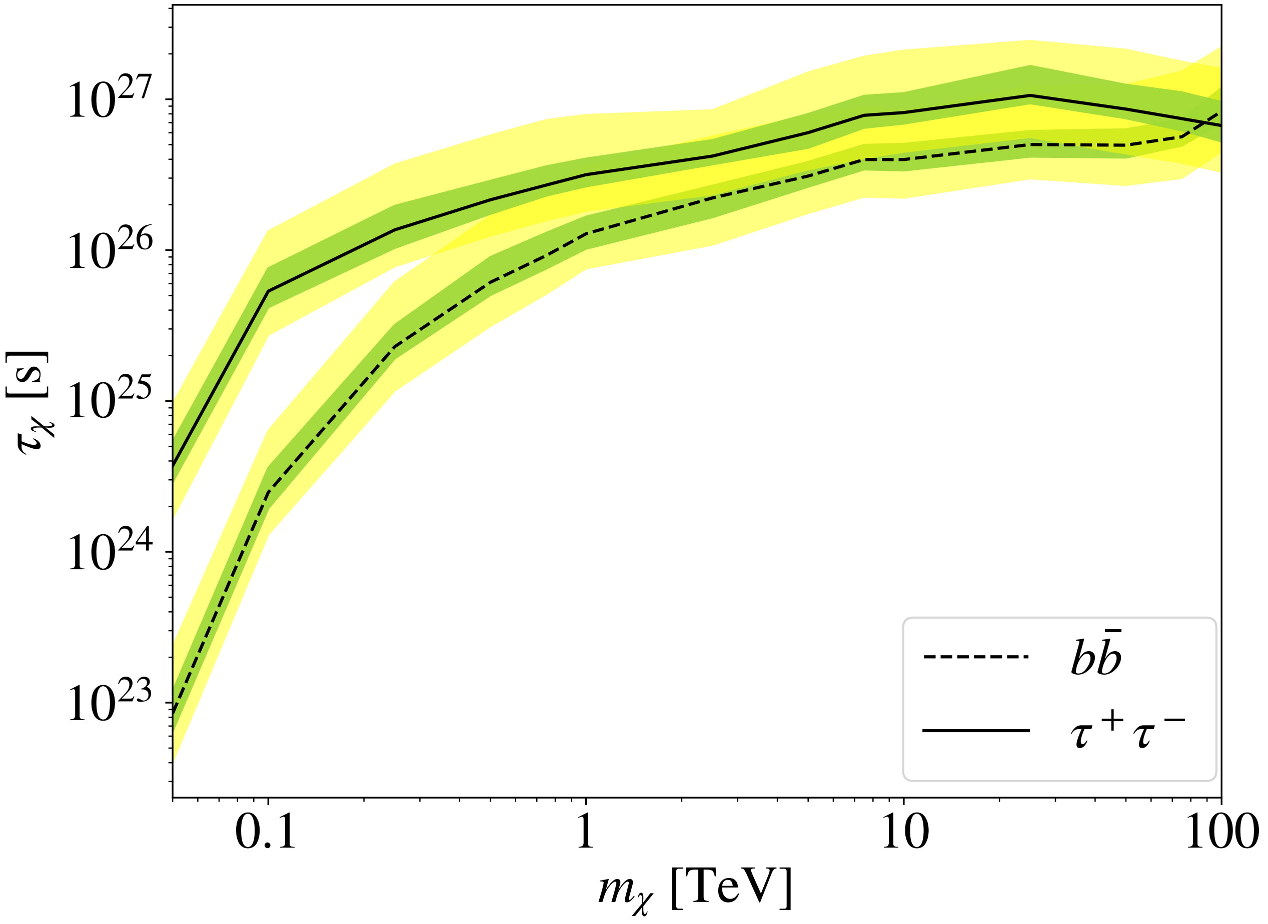

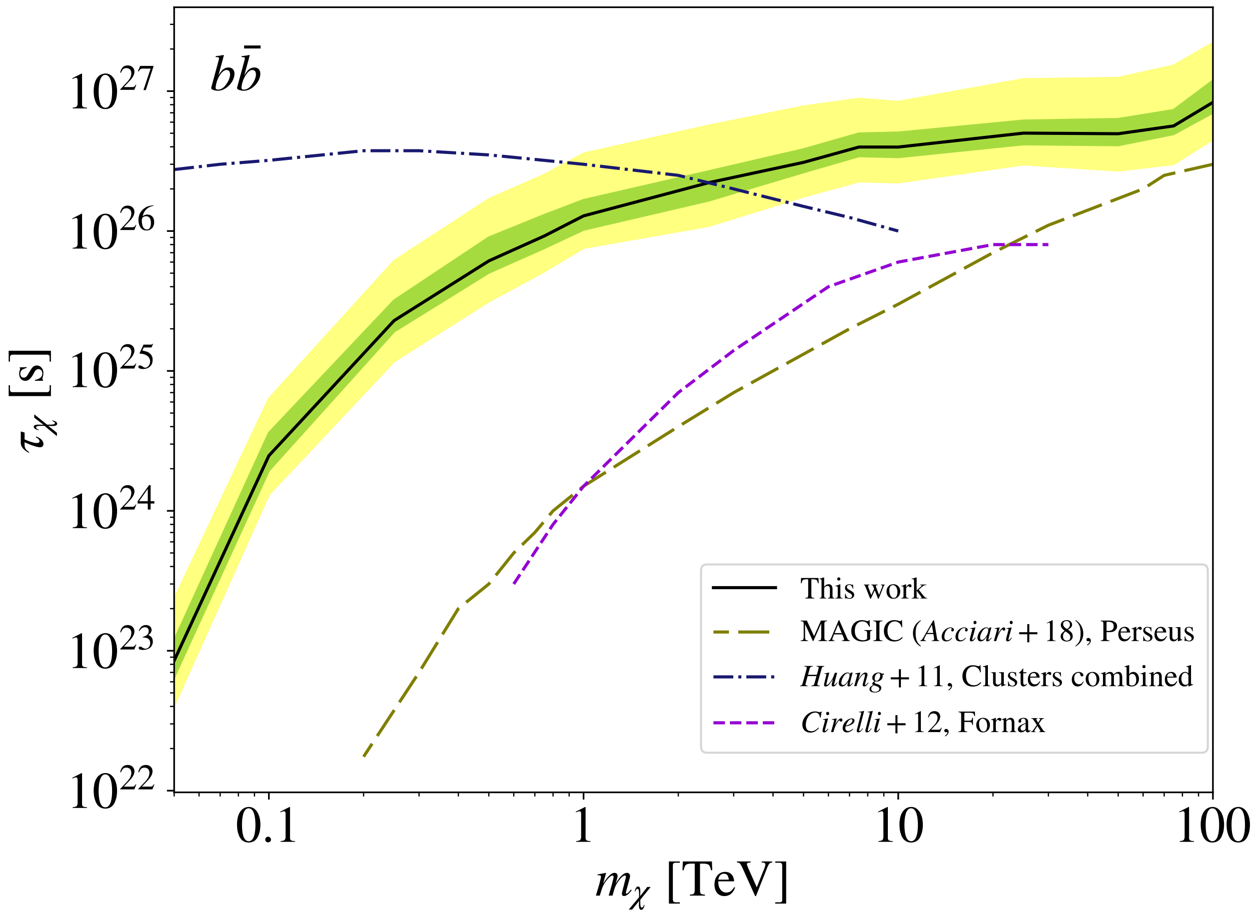

INSIGHT RESULTS: DM CONSTRAINTS

Decay

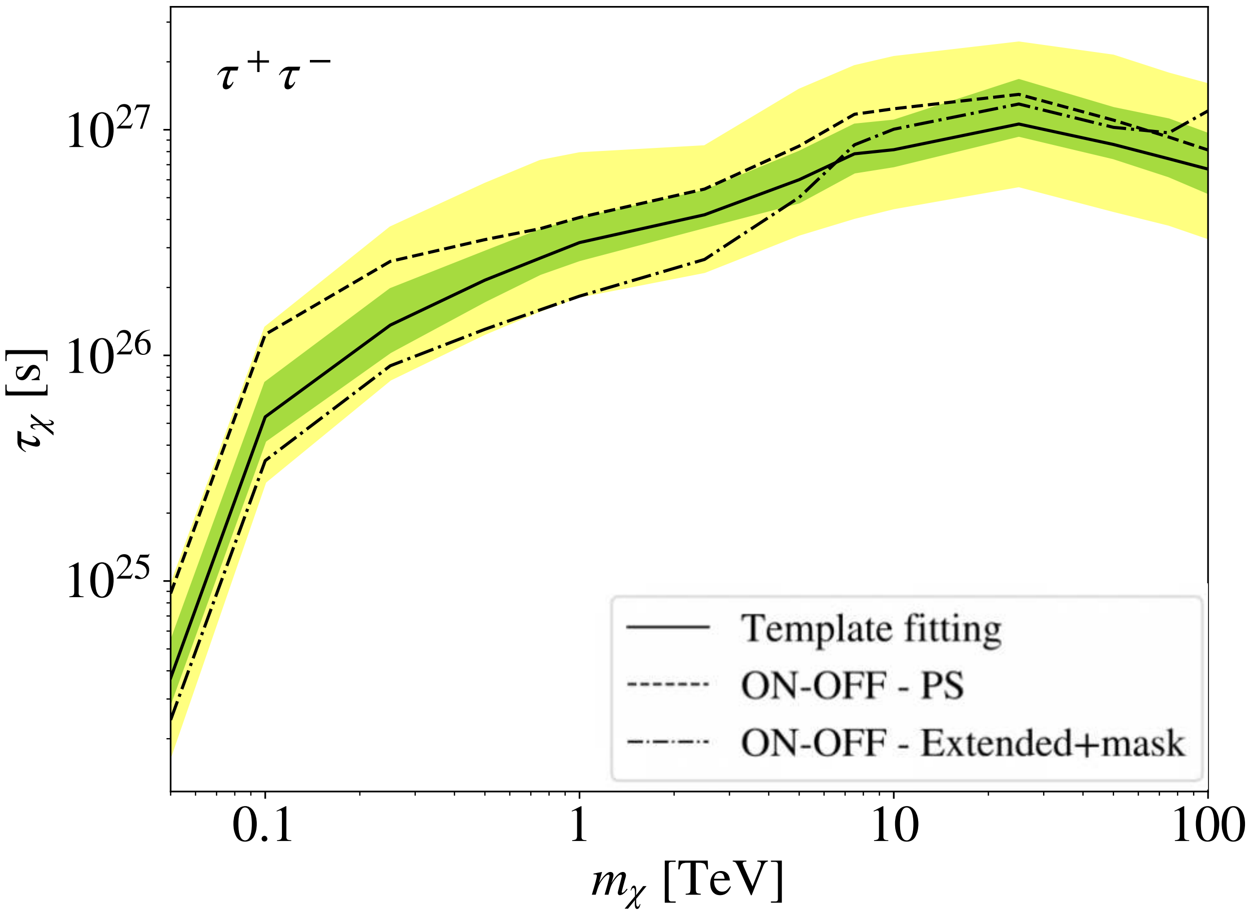

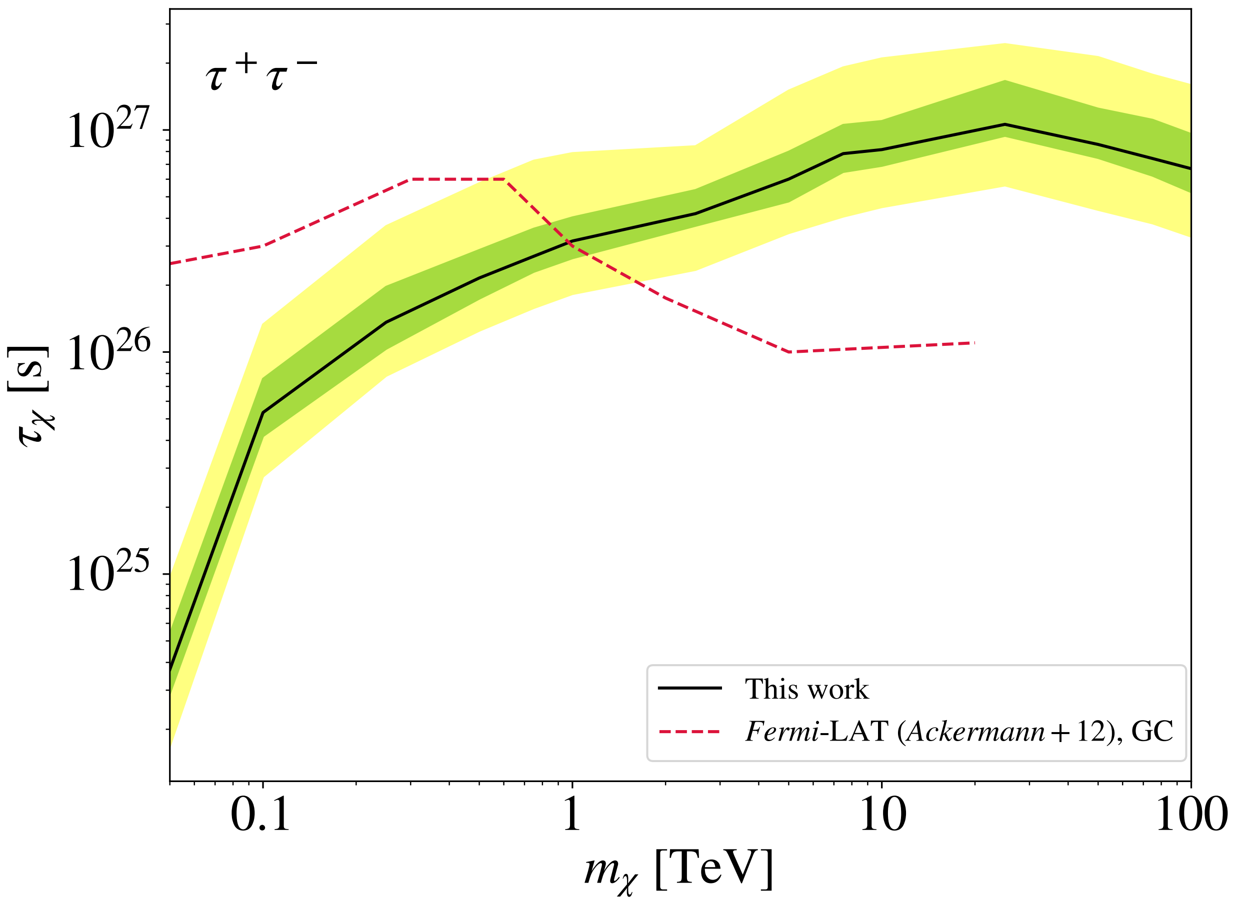

DM CONSTRAINTS: SCATTER BANDS

One-sided 1σ & 2 σ scatter bands evolution with the number of realizations
(annihilation MED model, template fitting)

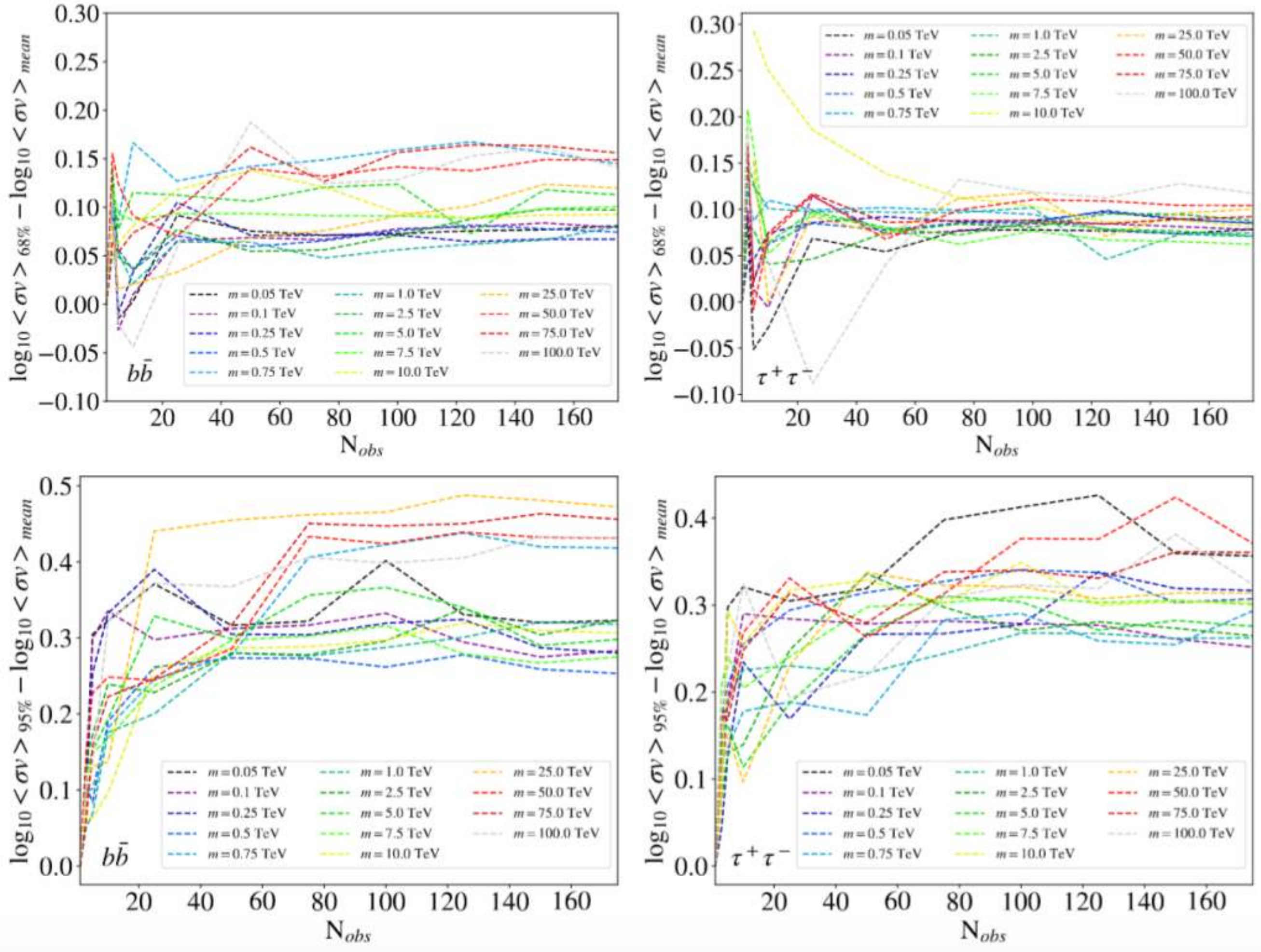

CTA ANALYSIS: INTERPLAY BETWEEN COMPONENTS

$\tau^+\tau^-$ annihilation channel and m_χ = 1TeV

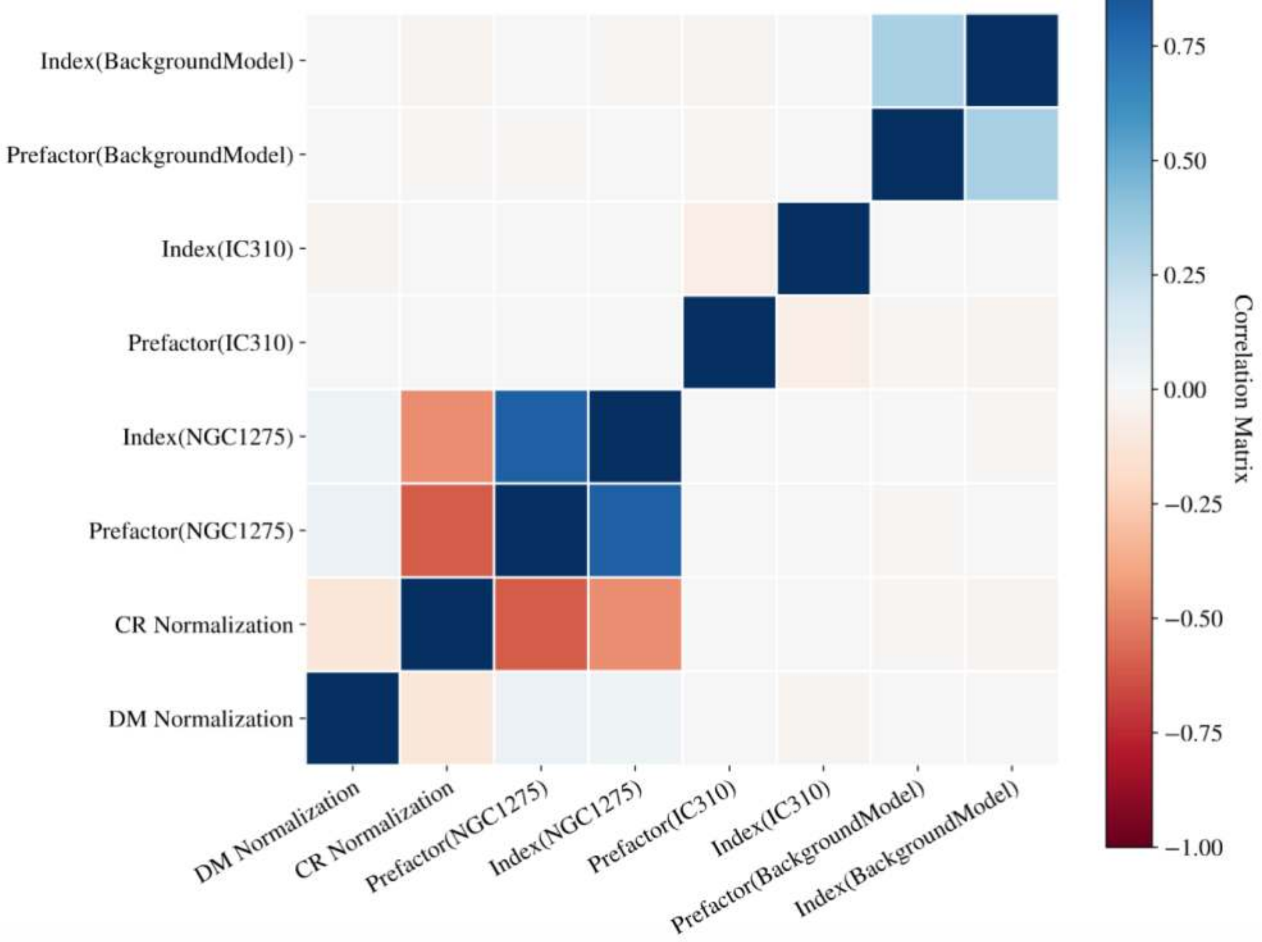

- Recovered mean values for CRs, NGC 1275, IC 310 and IRF-BKG within 1σ, independently of the channel or m_χ
- May be dependent on the considered DM scenario (annihilation/decay), channel or m_χ
- DM flux should not be neglected, as it seems to affect the correlations of CR normalization and NGC 1275

CTA ANALYSIS CONFIGURATION (II): ON-OFF ANALYSIS

- First analysis approach
  - Only includes γ-ray emission from DM and background from IRFs
  - Assumes the DM emission template
  - Circular mask of 0.1 deg in the centre
  - Historically used in Imaging Air Cherenkov Telescopes (IACTs) as MAGIC → Direct comparisons

Lowest level of complexity, more constraining results

- Different set-ups tested, best results for:

Regions	1 On/3 Off
Regions radius [deg]	0.5
Pointing (l, b) [deg]	(150.57, -13.26)
Offset [deg]	1

N_{obs}	100
T_{obs} [h]	300
IRFs	North_z20_50h, prod5
Energy range [TeV]	0.03 - 100

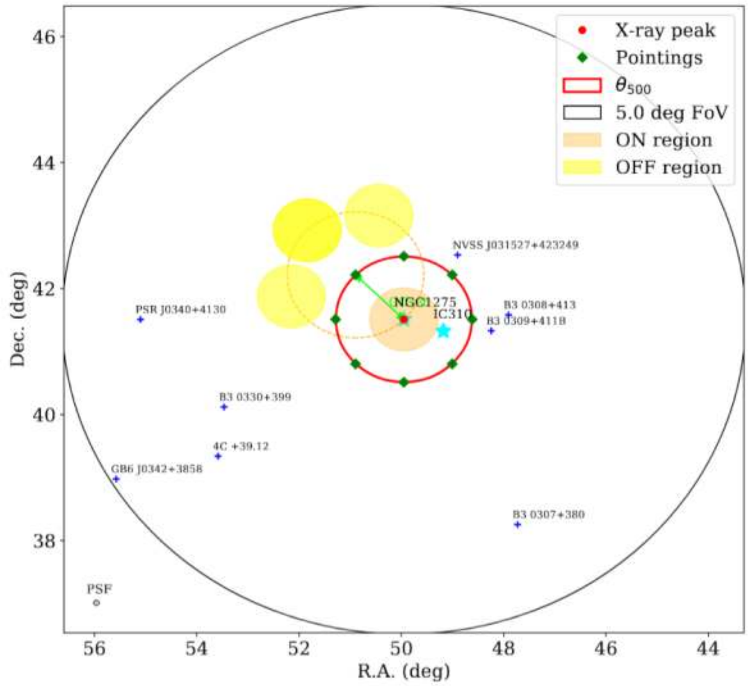

DM CONSTRAINTS: ON-OFF SET-UPS

Different configurations tested with the ON-OFF set-up

Case	$\theta_{pointing}$ [deg]	θ_{ON} [deg]	N_{OFF}	κ
1	**1**	**0.5**	**3**	**3**
2	0	1	3	3
3	0.5	0.5	3	3
4	1	0.5	5	5

Limits for Perseus for MED annihilation model (DM template + mask)

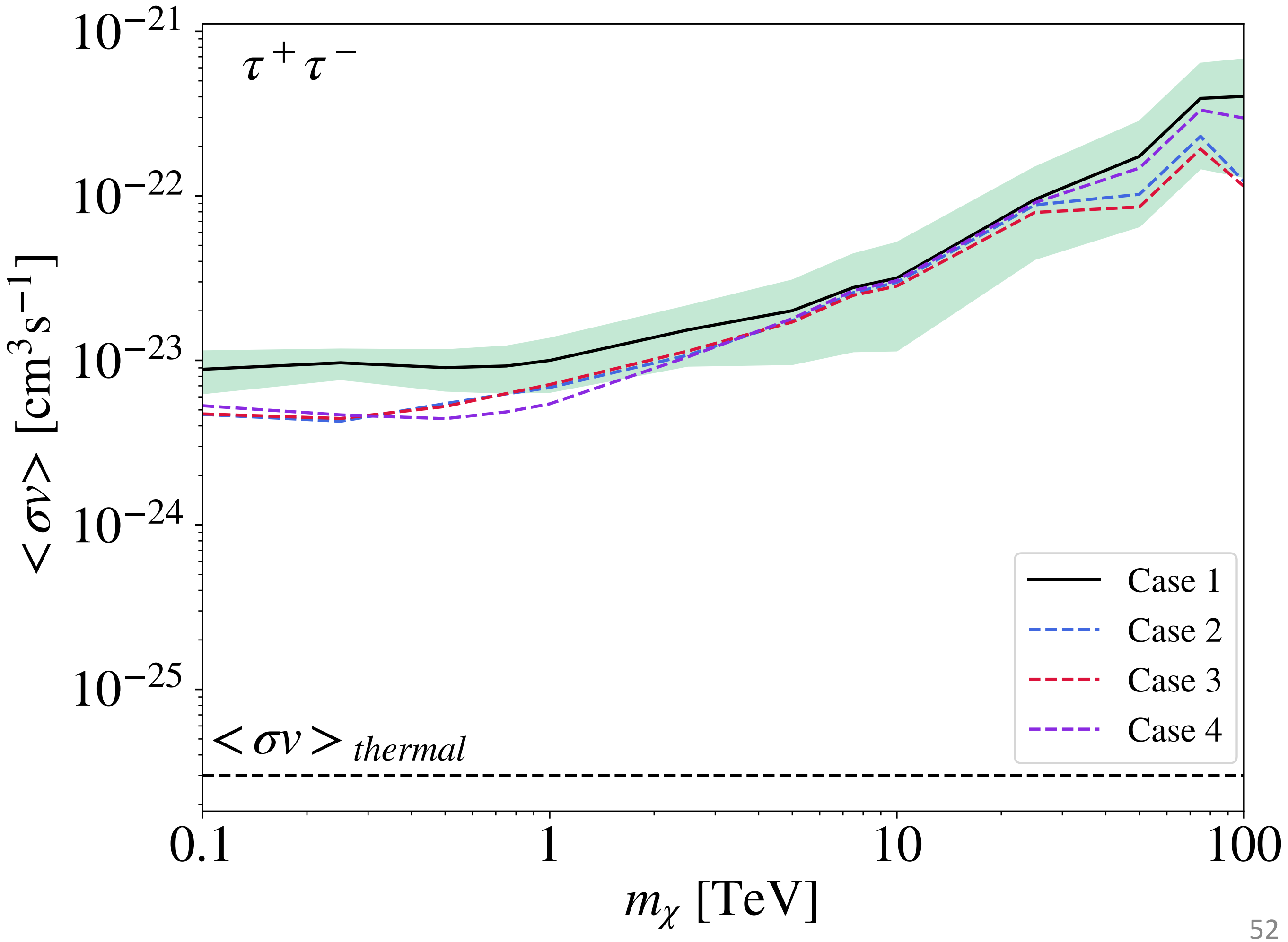

ON-OFF RESULTS: DM CONSTRAINTS

Annihilation (MED)

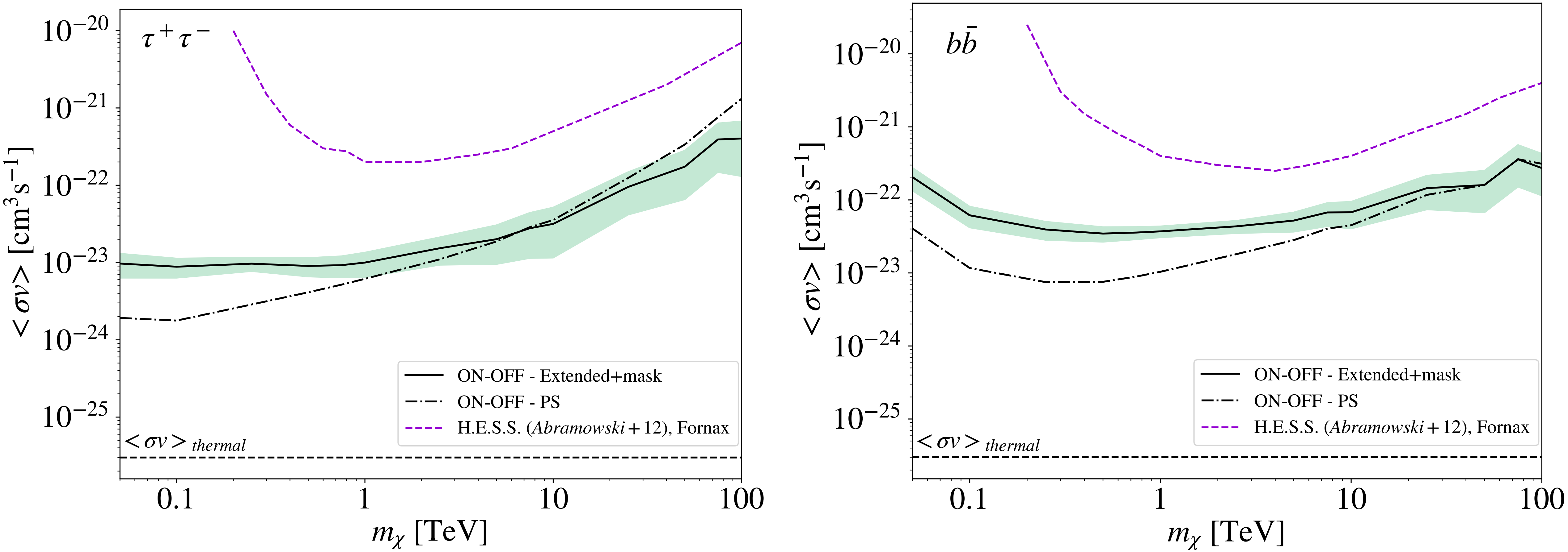

ON-OFF RESULTS: DM CONSTRAINTS

Decay

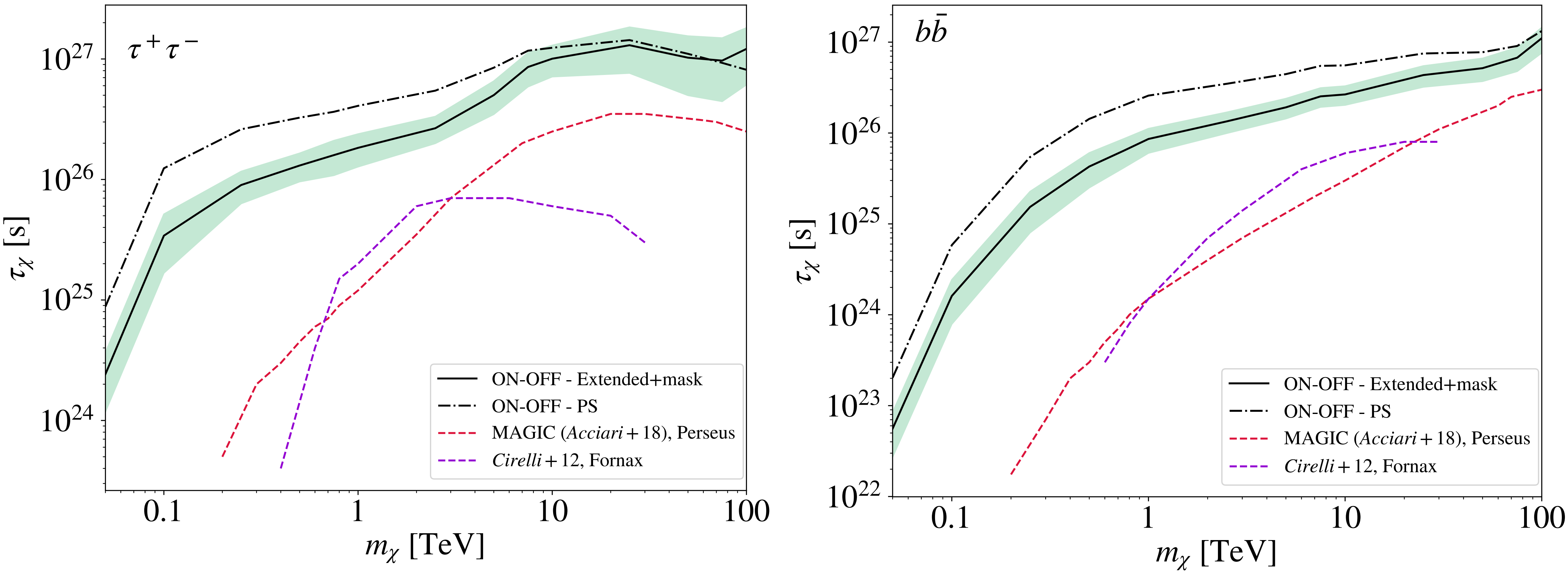

ON-OFF RESULTS : SCATTER BAND

One-sided 1σ band evolution with the number of realizations
(annihilation MED model, ON-OFF - Extended+mask)

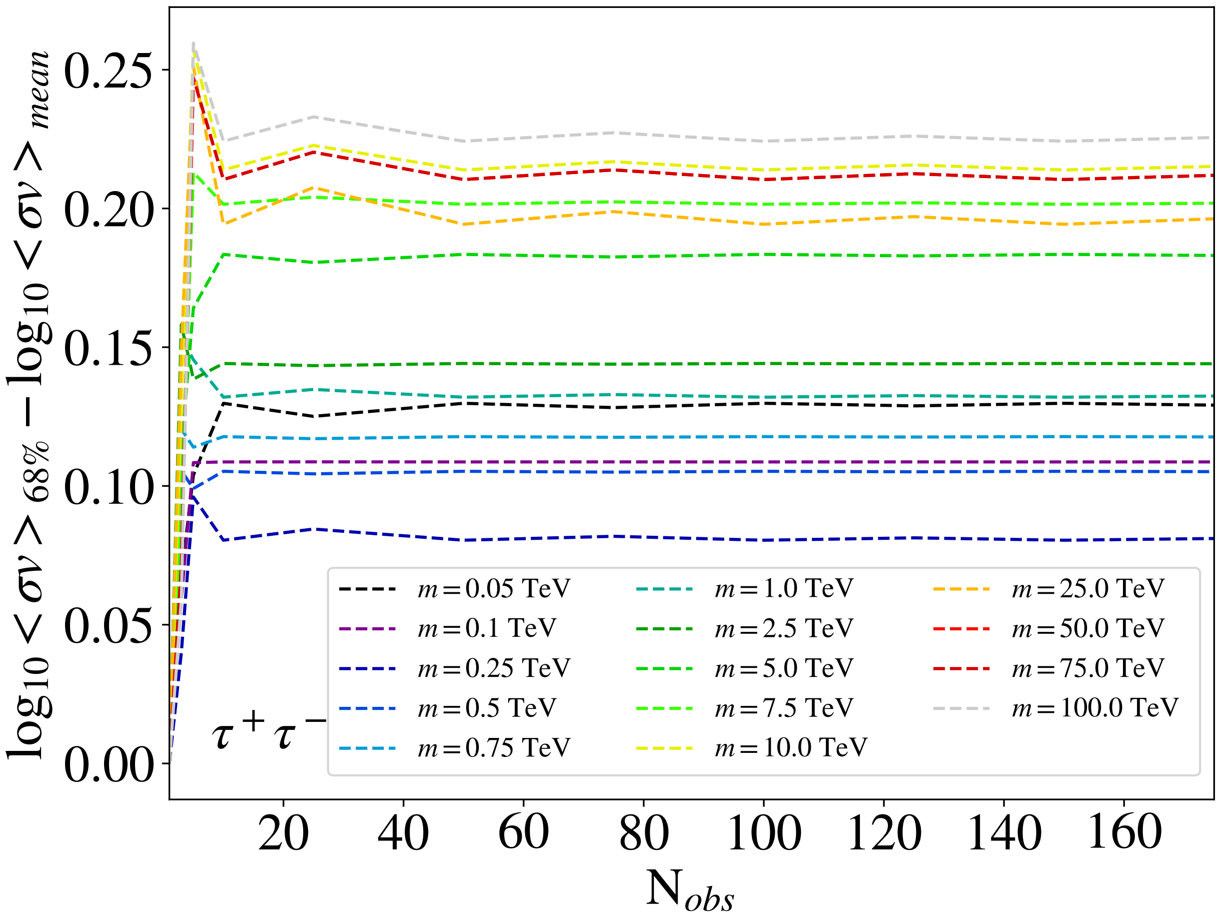

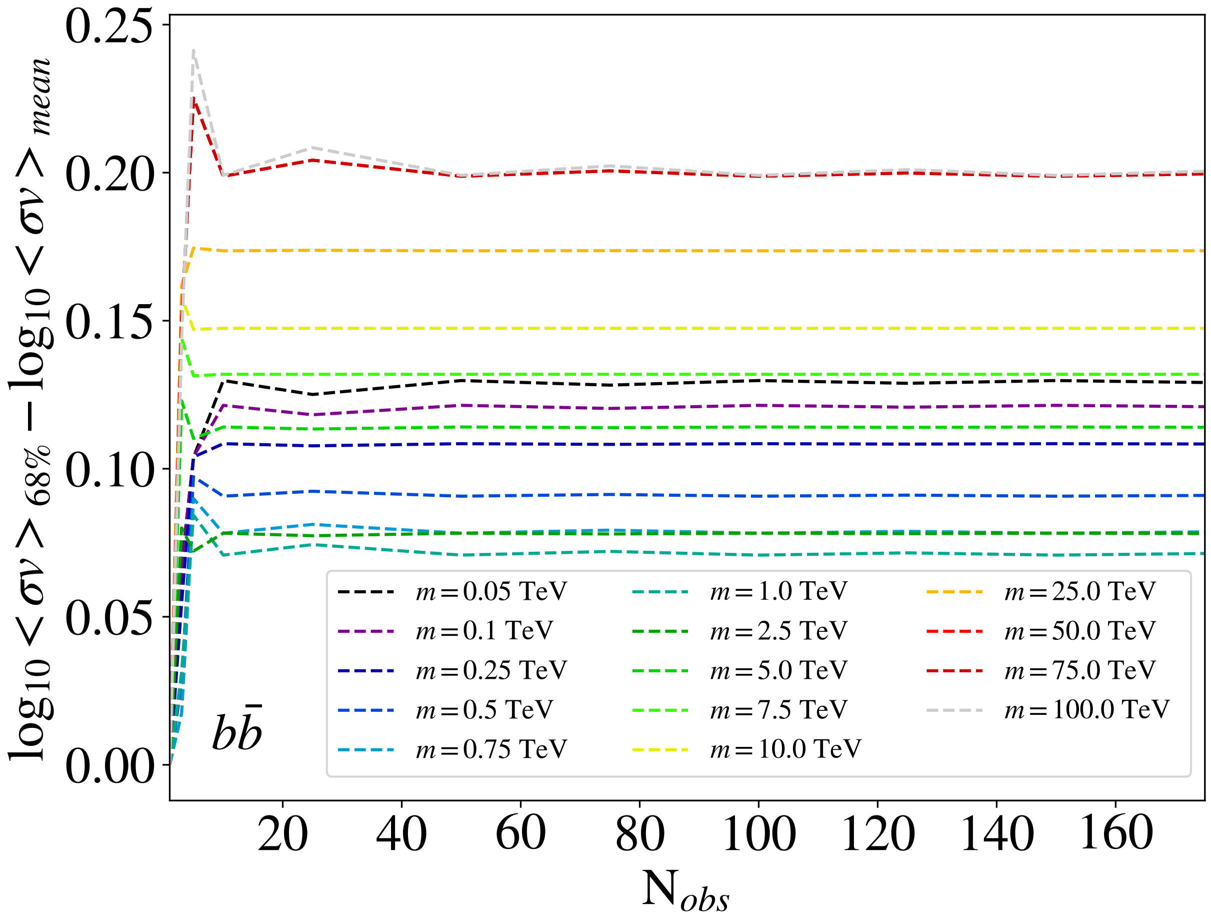

FERMI LARGE AREA TELESCOPE (LAT)

- Satellite-based telescope launched in June 2008 – 14 years of γ-ray data
- All sky survey mode, image of whole sky every 3 hours
- The γ–ray produces a pair of electron-positron, tracked and used to determine the energy of the primary γ-ray

https://fermi.gsfc.nasa.gov/

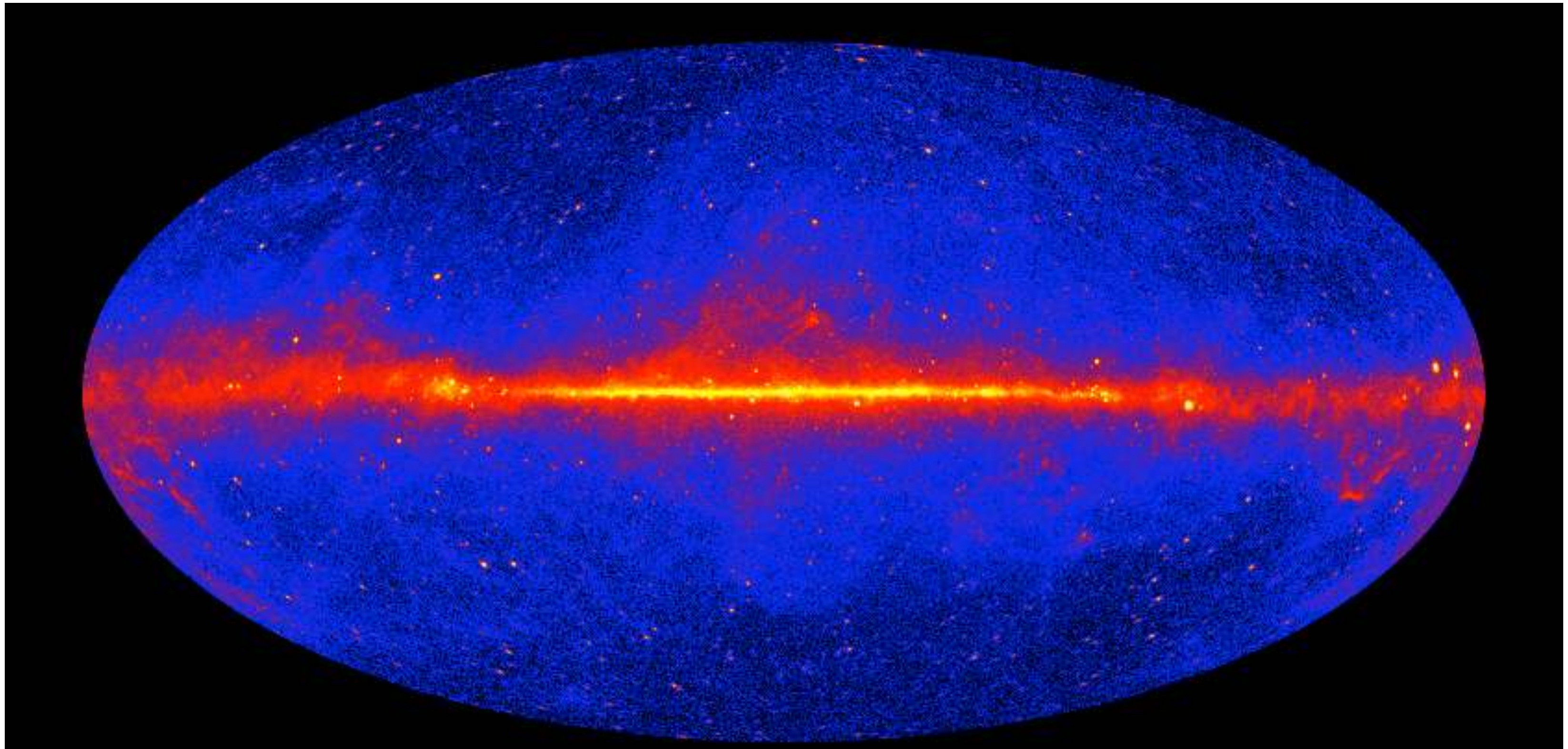

12 years of γ–ray data above 1 TeV

FERMI-LAT PERFORMANCE

10y Performance Capabilities

https://www.slac.stanford.edu/exp/glast/groups/canda/lat_Performance.htm

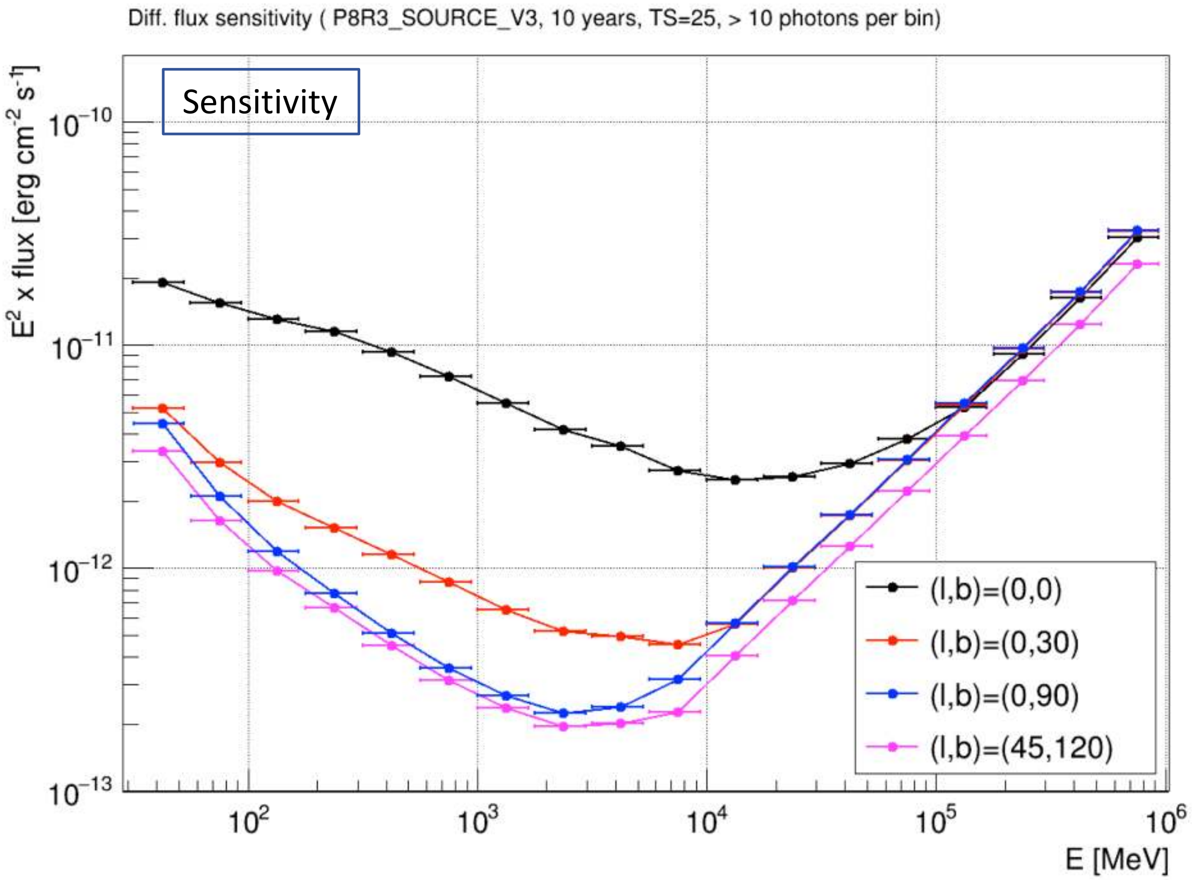

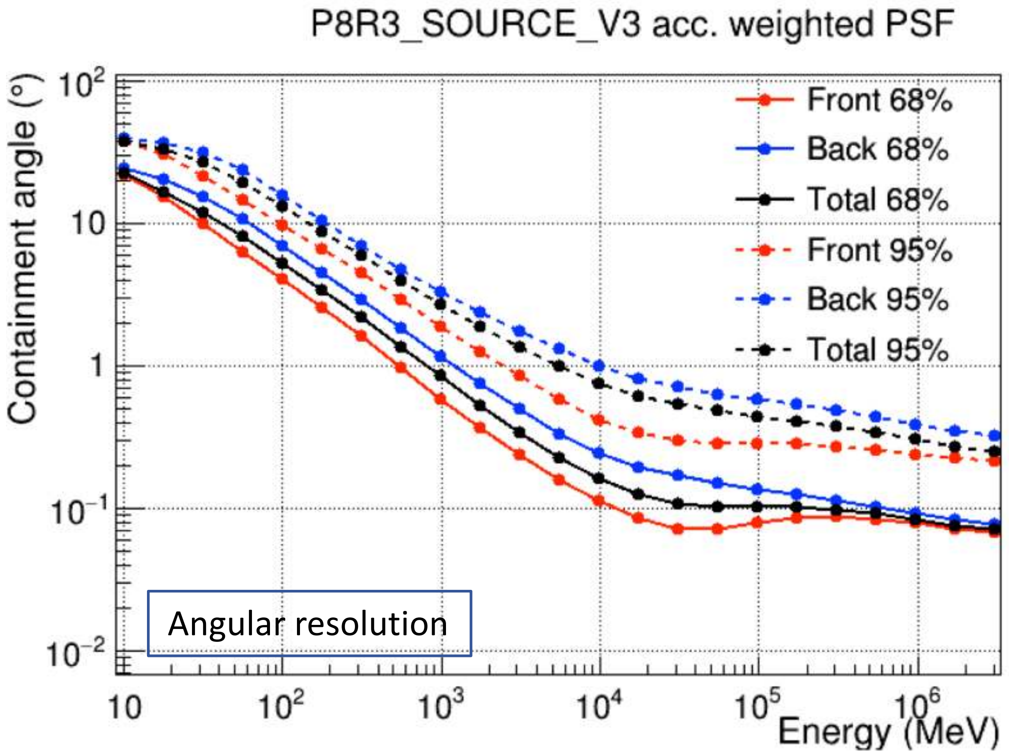

BEYOND THE ORIGINAL KSP: MORE CLUSTERS

- Natural extension of the KSP: why just focus on Perseus for DM searches?
- Will follow similar procedure than KSP, just applied to few other galaxy clusters and DM focused.
- Based on previous *Fermi*-LAT analysis: *Constraining the dark matter contribution of gamma-rays in cluster of galaxies using Fermi-LAT data*
  M. di Mauro, JPR, M. A. Sánchez-Conde, N. Fornengo
  Phys. Rev. D 107, 083030, [arXiv:2303.16930]

- Selection criteria:
  - Well-known M_{200} from X-rays measurements

    Masses from *Schellenberger&Reiprich17* (X-rays data from Chandra)

  - Local clusters

    $z < 0.1$

  - Mask of $|b| < 20$ deg to avoid galactic diffuse emission
  - Separation of at least 2 deg to account for cluster extension

HIFLUGCS catalogue (*Reiprich&Böhringer02*)

- 50 local clusters
- $f_x \geq 1.7 \cdot 10^{-11}$ erg s^{-1} cm^{-2}
- biased towards cool-cored clusters (*Käfer+19*)

+

- Clusters used in previous searches:

  Ackermann+10 [Fermi-LAT Coll.]

  Sánchez-Conde+11

  Ackermann+14 [Fermi-LAT Coll.]

Sample of 49 local galaxy clusters

CLUSTERS SAMPLE

Cluster	d_L	M_{200}	c_{200}	ρ_s	r_s	R_{200}	θ_{200}	$\log_{10} J_{MIN}$	$\log_{10} J_{MED}$	B_{MED}	$\log_{10} J_{MAX}$	B_{MAX}	$\log_{10} D$	TS
	[Mpc]	[10^{14} $M_\odot$]		[$M_\odot/kpc^3$]	[kpc]	[kpc]	[deg]	[GeV^2cm^{-5}]	[GeV^2cm^{-5}]		[GeV^2cm^{-5}]		[GeV cm^{-2}]	
A478	387.29	6.08	5.06	303795	345.37	1747.71	0.30	16.05	17.00	9.03	17.77	52.90	17.74	0.00
A399	320.39	4.03	5.14	314222	296.58	1523.16	0.31	16.02	17.00	9.54	17.76	54.90	17.72	5.69
A2065	325.13	4.73	5.10	309802	314.87	1607.11	0.33	16.08	17.05	9.46	17.82	55.00	17.78	4.94
A1736	203.92	1.45	5.40	352863	200.77	1084.70	0.33	15.96	16.98	10.50	17.71	56.70	17.65	4.89
A1644	208.50	1.55	5.38	349910	205.81	1107.83	0.33	15.96	16.98	10.50	17.72	56.70	17.66	1.90
A401	339.38	5.92	5.06	304380	342.03	1732.25	0.34	16.14	17.11	9.34	17.88	54.90	17.84	8.07
A2029	348.92	6.59	5.05	302105	355.64	1795.26	0.34	16.16	17.13	9.21	17.90	54.40	17.86	0.26
Hydra-A	240.76	2.60	5.24	328469	251.56	1317.25	0.35	16.06	17.07	10.20	17.82	57.70	17.76	3.74
ZwCl1215	339.38	6.54	5.05	302272	354.58	1790.34	0.35	16.18	17.15	9.32	17.92	55.00	17.88	0.00
MKW3S	199.34	1.66	5.36	346794	211.39	1133.45	0.36	16.02	17.05	10.60	17.78	57.60	17.72	0.00
A133	254.68	3.35	5.18	319842	276.74	1432.35	0.36	16.12	17.12	10.10	17.88	57.70	17.83	2.46
A3158	263.99	3.97	5.14	314620	295.06	1516.19	0.37	16.16	17.16	9.99	17.92	57.70	17.87	5.39
A4059	203.92	2.19	5.28	334997	235.56	1244.13	0.38	16.12	17.14	10.50	17.89	58.90	17.83	0.06
A1795	278.01	5.17	5.09	307558	325.36	1655.37	0.38	16.23	17.22	9.81	17.99	57.50	17.94	0.42
A2657	176.55	1.69	5.36	345942	212.97	1140.70	0.40	16.13	17.16	10.80	17.90	58.90	17.84	4.53
A2147	153.91	1.17	5.47	363492	184.45	1009.48	0.40	16.09	17.13	11.00	17.86	58.70	17.79	5.72
A3376	199.34	2.58	5.24	328779	250.74	1313.53	0.41	16.20	17.23	10.60	17.98	59.90	17.92	0.84
A3562	222.29	3.53	5.16	318132	282.44	1458.40	0.41	16.24	17.26	10.40	18.02	59.70	17.96	0.03
A85	250.04	5.09	5.09	307918	323.62	1647.33	0.42	16.30	17.31	10.10	18.07	59.00	18.03	0.31
A3391	236.13	4.51	5.11	311034	309.49	1582.37	0.43	16.29	17.30	10.30	18.07	59.90	18.02	0.11
A3667	250.04	5.30	5.08	306940	328.42	1669.45	0.43	16.31	17.32	10.10	18.09	59.50	18.04	13.31
A2052	153.91	1.63	5.37	347614	209.89	1126.58	0.45	16.22	17.26	11.00	18.00	60.10	17.93	0.03
2A0335	153.91	1.66	5.36	346659	211.64	1134.59	0.45	16.23	17.27	11.00	18.01	60.20	17.95	5.44
A2589	185.64	2.99	5.20	323540	265.28	1379.98	0.46	16.31	17.34	10.70	18.10	61.20	18.04	0.13
EXO0422	172.01	2.49	5.25	330093	247.36	1298.09	0.47	16.30	17.33	10.80	18.09	61.30	18.02	0.18

CLUSTERS SAMPLE

Cluster	d_L	M_{200}	c_{200}	ρ_s	r_s	R_{200}	θ_{200}	$\log_{10} J_{MIN}$	$\log_{10} J_{MED}$	B_{MED}	$\log_{10} J_{MAX}$	B_{MAX}	$\log_{10} D$	TS
	[Mpc]	[10^{14} $M_\odot$]		[$M_\odot$/kpc^3]	[kpc]	[kpc]	[deg]	[GeV^{2}cm^{-5}]	[GeV^{2}cm^{-5}]		[GeV^{2}cm^{-5}]		[GeV cm^{-2}]	
A576	167.47	2.37	5.26	331959	242.73	1276.91	0.47	16.31	17.34	10.90	18.09	61.30	18.03	0.99
A2063	153.91	1.97	5.31	339288	226.15	1201.08	0.48	16.29	17.34	11.00	18.08	61.00	18.01	9.44
A3558	213.09	4.89	5.10	308961	318.70	1624.70	0.48	16.41	17.42	10.30	18.19	60.90	18.14	0.35
A2142	411.48	28.03	4.97	291172	585.57	2908.46	0.48	16.66	17.57	8.15	18.38	51.70	18.36	0.00
A119	194.77	3.96	5.14	314731	294.64	1514.28	0.49	16.33	17.39	11.20	18.15	65.60	18.09	8.49
A2634	135.92	1.55	5.38	349762	206.07	1109.02	0.50	16.30	17.35	11.20	18.09	60.90	18.02	4.31
A2256	268.66	10.17	4.99	294929	415.33	2074.55	0.50	16.53	17.52	9.65	18.31	59.10	18.26	9.91
A496	144.90	2.56	5.24	329080	249.96	1309.96	0.55	16.45	17.49	11.10	18.25	63.50	18.18	0.00
A3266	263.99	13.44	4.97	292052	457.72	2276.43	0.55	16.67	17.65	9.57	18.44	59.60	18.40	8.19
A1367	95.81	0.88	5.57	379136	164.49	916.83	0.57	16.36	17.42	11.50	18.14	60.80	18.06	0.99
A4038	122.49	2.23	5.28	334336	237.08	1251.09	0.62	16.53	17.58	11.30	18.33	64.00	18.26	0.71
A754	236.13	25.00	4.96	290649	564.09	2799.56	0.75	17.14	18.05	8.23	18.86	52.70	18.82	0.28
A2199	131.44	5.07	5.09	308030	323.08	1644.84	0.76	16.80	17.85	11.10	18.62	66.00	18.56	1.86
A3571	162.95	10.90	4.99	294084	425.60	2123.16	0.80	16.95	17.97	10.50	18.77	65.20	18.71	0.00
NGC 5044	38.81	0.41	5.88	428317	121.16	711.87	1.07	16.82	17.90	11.90	18.60	60.50	18.51	0.00
NGC 5813	27.55	0.27	6.06	460583	102.21	619.60	1.31	16.96	18.03	11.80	18.72	58.30	18.62	4.10
A1656-Coma	100.24	13.16	4.97	292223	454.37	2260.40	1.35	17.42	18.46	11.00	19.26	69.60	19.20	9.93
NGC 5846	26.25	0.38	5.91	434293	117.22	692.90	1.53	17.13	18.20	11.90	18.91	60.40	18.81	10.81
A1060-Hydra	47.51	2.97	5.20	323860	264.34	1375.66	1.70	17.43	18.51	12.00	19.27	70.00	19.19	5.41
A3526-Centaurus	43.16	2.27	5.27	333726	238.51	1257.60	1.70	17.41	18.49	12.10	19.25	69.20	19.16	15.62
NGC 1399-Fornax	21.50	0.51	5.79	413641	131.82	762.97	2.05	17.41	18.50	12.20	19.21	62.60	19.11	4.01
M49	18.91	0.46	5.82	419644	127.27	741.24	2.26	17.49	18.57	12.10	19.28	62.00	19.18	0.00
NGC 4636	17.18	0.53	5.77	409991	134.72	776.79	2.61	17.63	18.71	12.20	19.43	63.00	19.33	13.09
VIRGO	15.46	5.60	5.07	305646	335.10	1700.27	6.32	18.65	19.74	12.30	20.52	74.80	20.44	1.05

CLUSTERS DM MODELLING

- Follow similar strategy:
  I. Model de main halo;
  II. Model de substructure population defining benchmark models

$$\langle\rho_{\rm tot}\rangle(r) = \rho_{\rm sm}(r) + \langle\rho_{\rm subs}\rangle(r)$$

$$J(l.o.s, \Delta\Omega, z) = \int_{\Delta\Omega}\int_{l.o.s} \rho^2_{DM}(r)dr$$

$$D(l.o.s, \Delta\Omega, z) = \int_{\Delta\Omega}\int_{l.o.s} \rho_{DM}(r)dr$$

$\rho_{\rm sm}$ → NFW

$$\rho(r) = \frac{\rho_0}{\left(\frac{r}{r_s}\right)\left(1+\frac{r}{r_s}\right)^2}$$

Navarro+96, Navarro+97

+ ($c_{200} - M_{200}$) *Sánchez-Conde &Prada14*

$\langle\rho_{\rm subs}\rangle$

$$\frac{d^3N}{dVdMdc} = N_{\rm tot}\frac{d\mathcal{P}_V}{dV}(r)\cdot\frac{d\mathcal{P}_M}{dM}(M)\cdot\frac{d\mathcal{P}_c}{dc}(M,c)$$

MIN → No substructure considered

MED → Best guess according to most recent results

MAX → Educated upper bound

Model	SRD	α	$c(M)$	M_{min}	f_{sub}
MIN	-	-	-	-	-
MED	VL-II (*Diemand+08*)	1.9	*Moliné+17*	$10^{-6}\ M_\odot$	0.18
MAX	Aquarius (*Springer+08*)	2.0	*Moliné+17*	$10^{-9}\ M_\odot$	0.34

DM ANNIHILATION FLUXES OF THE SAMPLE

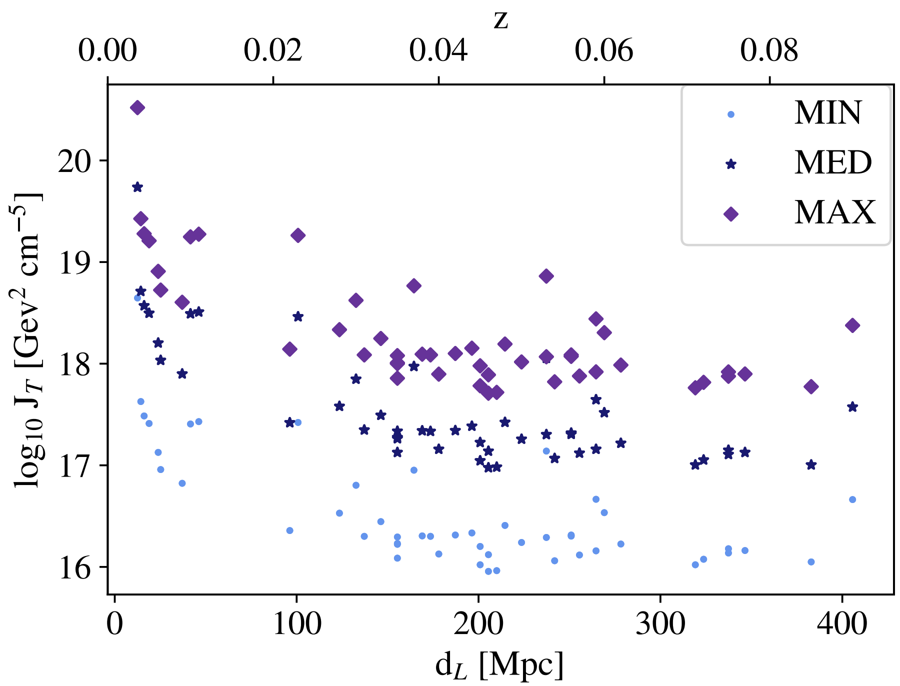

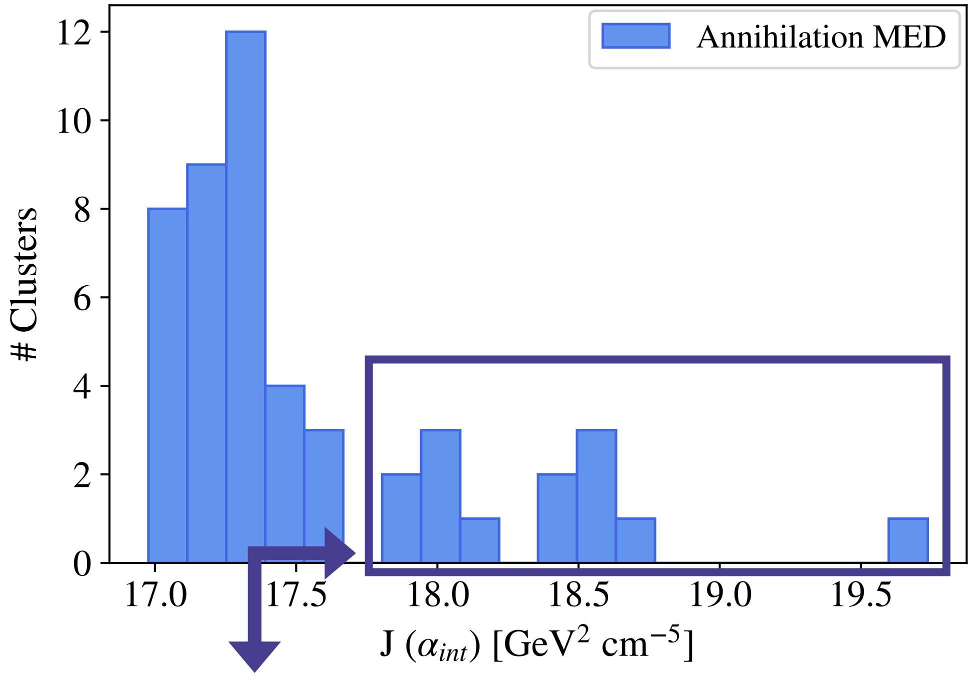

Cluster	z	M_{200} $[10^{14}\ M_\odot]$	R_{200} [kpc]	θ_{200} [deg]	$\log_{10} J_{MIN}$ $[\mathrm{GeV^2 cm^{-5}}]$	$\log_{10} J_{MED}$ $[\mathrm{GeV^2 cm^{-5}}]$	$\log_{10} J_{MAX}$ $[\mathrm{GeV^2 cm^{-5}}]$	$\log_{10} D$ $[\mathrm{GeV\ cm^{-2}}]$
Virgo	0.0036	5.60	1700	6.32	18.65	19.74	20.52	20.44
NGC 4636	0.004	0.53	777	2.61	17.63	18.71	19.43	19.33
M49	0.0044	0.46	741	2.26	17.49	18.57	19.28	19.18
A1060-Hydra	0.011	2.97	1376	1.70	17.43	18.51	19.27	19.19
A1656-Coma	0.023	13.16	2260	1.35	17.42	18.46	19.26	19.20
NGC 1399-Fornax	0.005	0.51	763	2.05	17.41	18.50	19.21	19.11
A3526-Centaurus	0.01	2.27	1258	1.70	17.41	18.49	19.25	19.16
A754	0.053	25.00	2800	0.75	17.14	18.05	18.86	18.82
NGC 5813	0.0064	0.27	620	1.31	16.96	18.03	18.72	18.62
A3571	0.037	10.90	2123	0.80	16.95	17.97	18.77	18.71

DM DECAY FLUXES OF THE SAMPLE

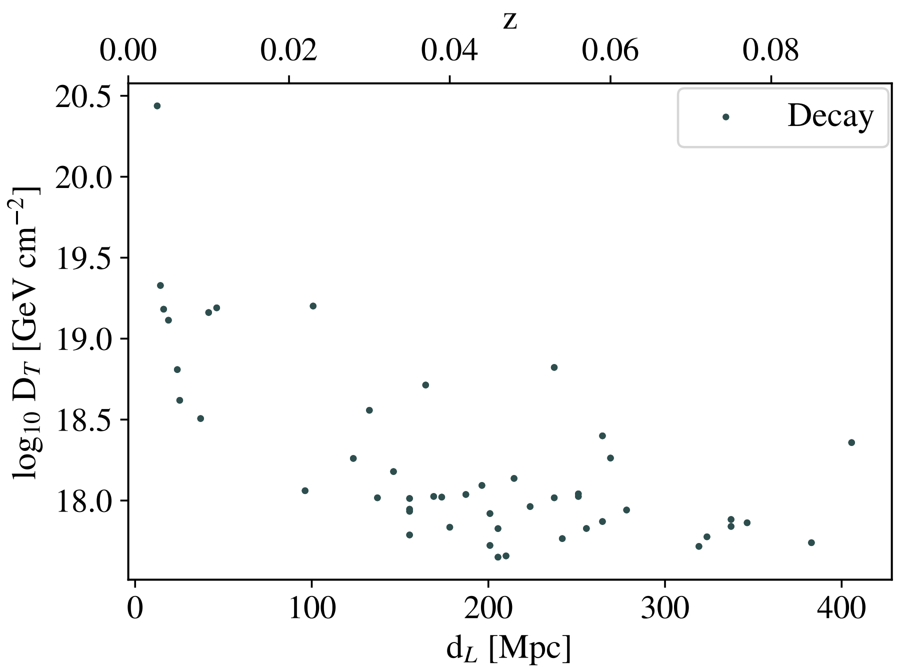

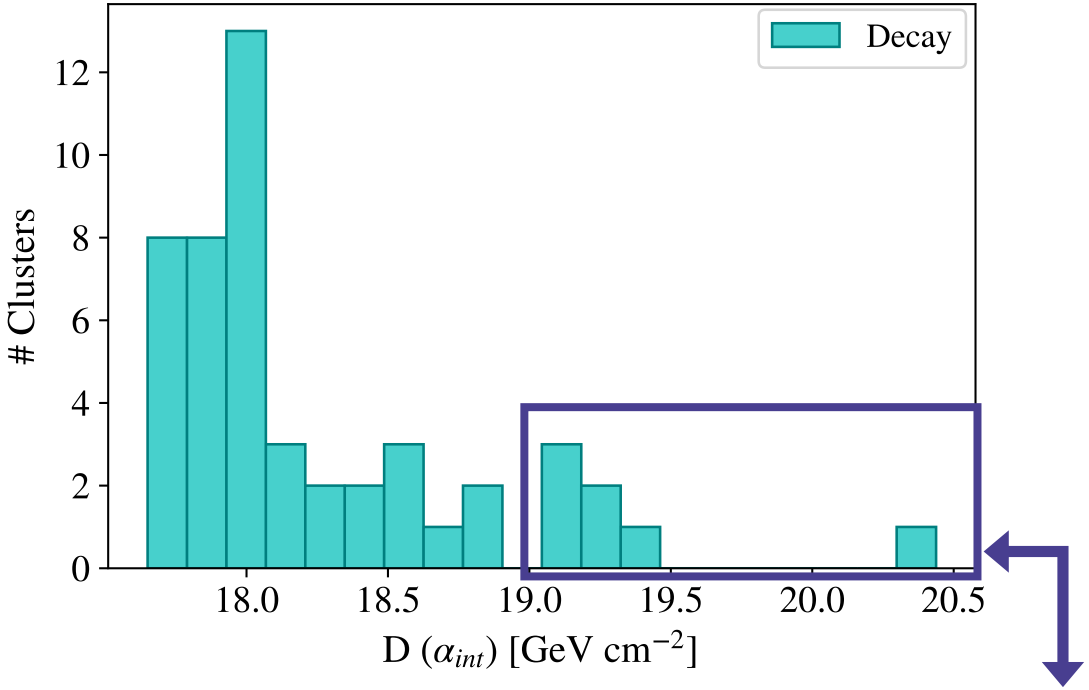

Cluster	z	M_{200} [10^{14} $M_\odot$]	R_{200} [kpc]	θ_{200} [deg]	$\log_{10} J_{MIN}$ [$GeV^2 cm^{-5}$]	$\log_{10} J_{MED}$ [$GeV^2 cm^{-5}$]	$\log_{10} J_{MAX}$ [$GeV^2 cm^{-5}$]	$\log_{10} D$ [GeV cm^{-2}]
Virgo	0.0036	5.60	1700	6.32	18.65	19.74	20.52	20.44
NGC 4636	0.004	0.53	777	2.61	17.63	18.71	19.43	19.33
M49	0.0044	0.46	741	2.26	17.49	18.57	19.28	19.18
A1060-Hydra	0.011	2.97	1376	1.70	17.43	18.51	19.27	19.19
A1656-Coma	0.023	13.16	2260	1.35	17.42	18.46	19.26	19.20
NGC 1399-Fornax	0.005	0.51	763	2.05	17.41	18.50	19.21	19.11
A3526-Centaurus	0.01	2.27	1258	1.70	17.41	18.49	19.25	19.16
A754	0.053	25.00	2800	0.75	17.14	18.05	18.86	18.82
NGC 5813	0.0064	0.27	620	1.31	16.96	18.03	18.72	18.62
A3571	0.037	10.90	2123	0.80	16.95	17.97	18.77	18.71

DARK MATTER FLUXES OF THE SAMPLE

Example of skymaps of the differential J/D-factors for NGC 1399-Fornax

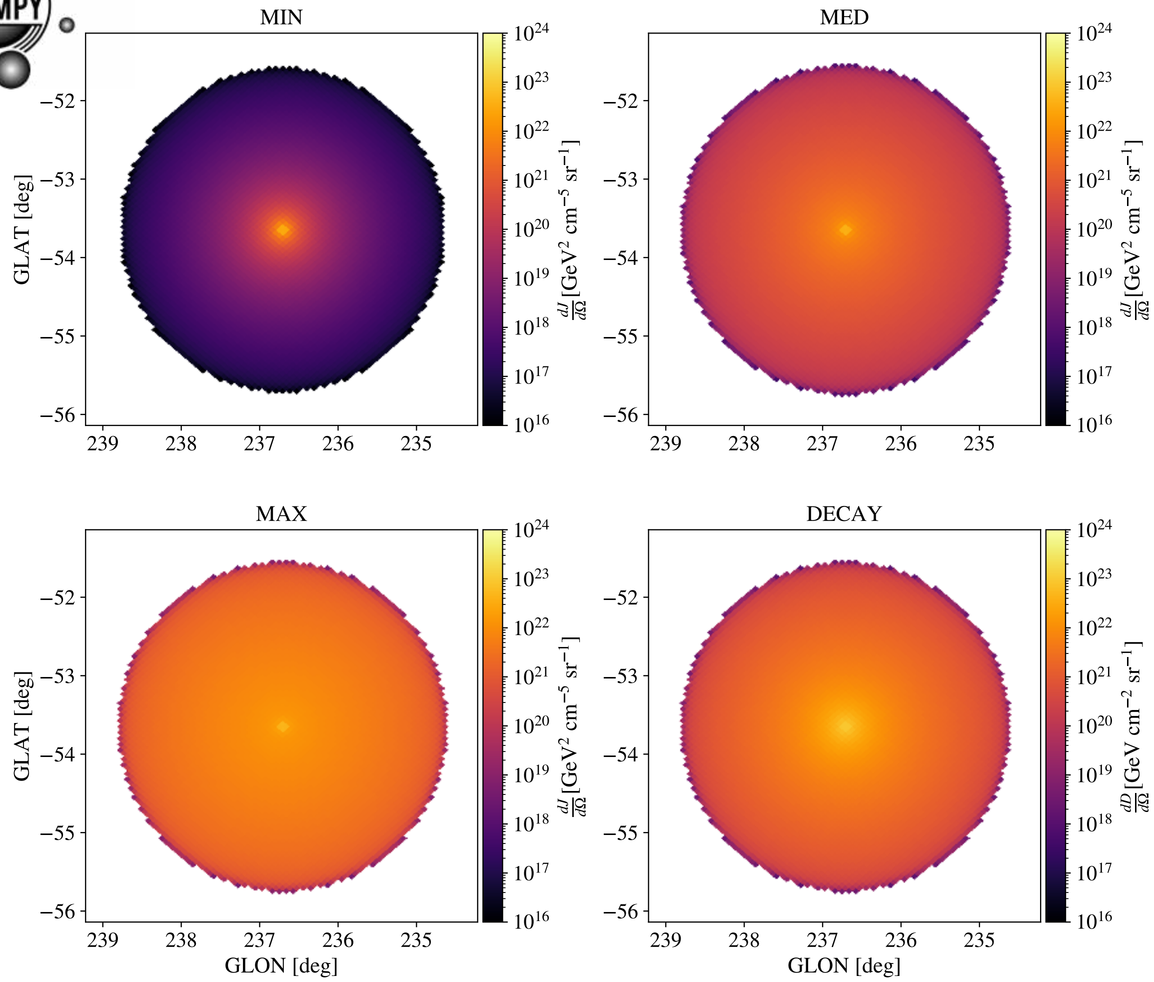

- Effects of substructure:
  - Most relevant in outskirts
  - Mean boost values:

B_{MED} = 11 (B~9 – *Moliné+17*)
B_{MAX} = 60 (B~65 – *Moliné+17*)

FERMI-LAT ANALYSIS SET-UP

Baseline set-up

Years of *Fermi* data	12
IRFs	P8R3_SOURCEVETO_V2
Energy range [GeV]	0.5 – 1000
Bins per decade	8
Region of Interest (ROI) [deg^2]	20 x 20
Pixel size [deg]	0.08
Catalogue	4FGL-DR2

- Standard template Fermi analysis
- Combined likelihood:

$$\log(\mathcal{L}_j\,(\mu_\chi,\nu_j|\mathcal{D}_j)) = \sum_i \log(\mathcal{L}_{i,j}\,(\mu_\chi,\nu_{i,j}|\mathcal{D}_{i,j}))$$

- Tested different set-ups for energy range, ROI, IRFs and BKG models
- Background components:
  - Individual PS LAT sources (4FGL-DR2)
  - Fermi bubbles
  - Loop I + Sun + Moon
  - Isotropic emission
  - Galactic Interstellar Emission (IEM)

Divided in: Bremsstrahlung + π^0 + Inverse Compton (CMB + starlight + Infrared)
Ackerman+17 [Fermi Collab.]

TS OF THE BENCHMARK MODELS

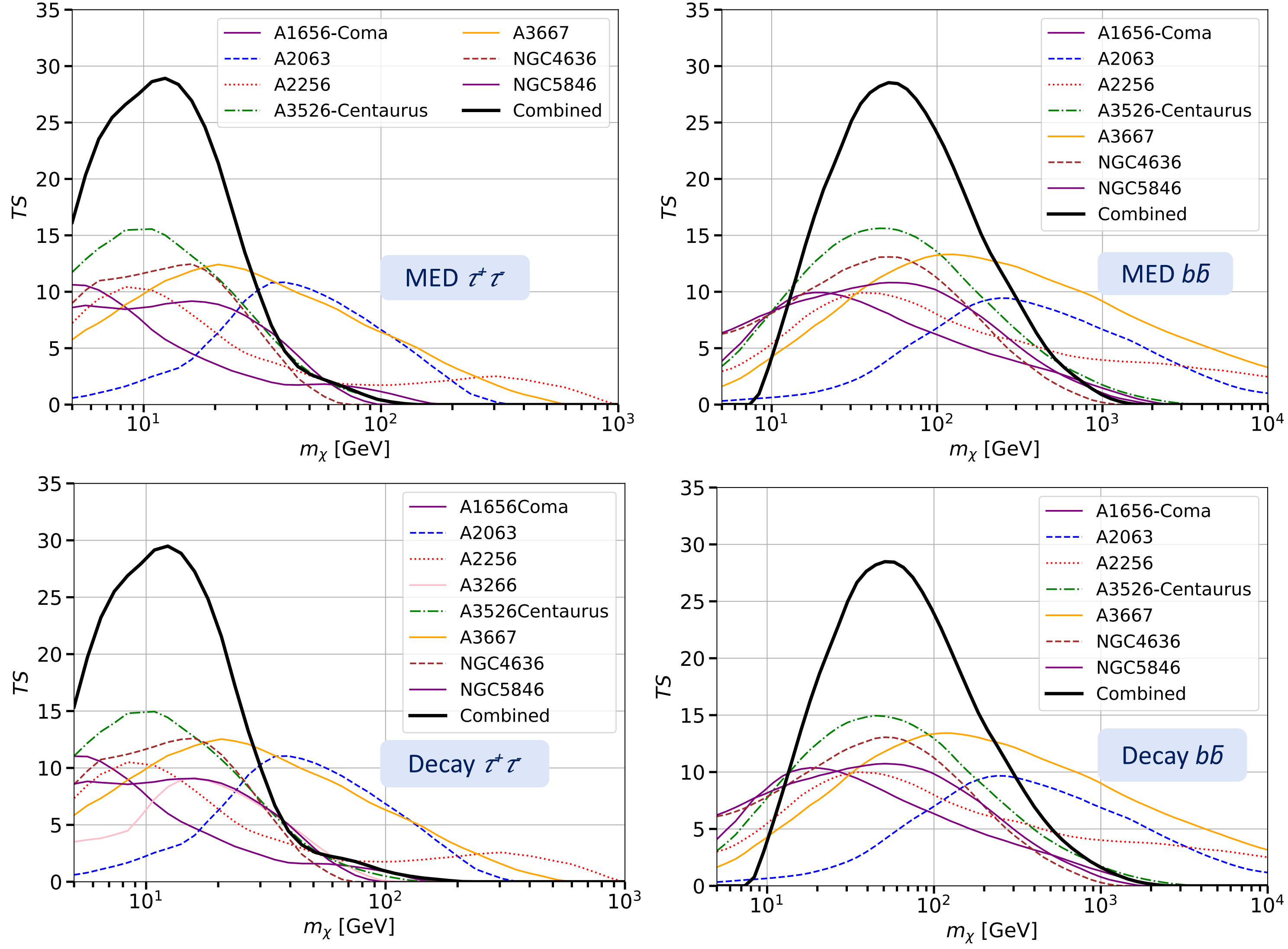

Individual *TS*

- Highest **A3526-Centaurus** – *TS* = 15
- A1656-Coma – *TS* ~10 (*Ackermann+17 [Fermi Collab.]*)

Combined *TS*

MIN	No sig.
MED	*TS* = 27
MAX	*TS* = 23
DECAY	*TS* = 28

TS VALUES INTERPRETED AS DM

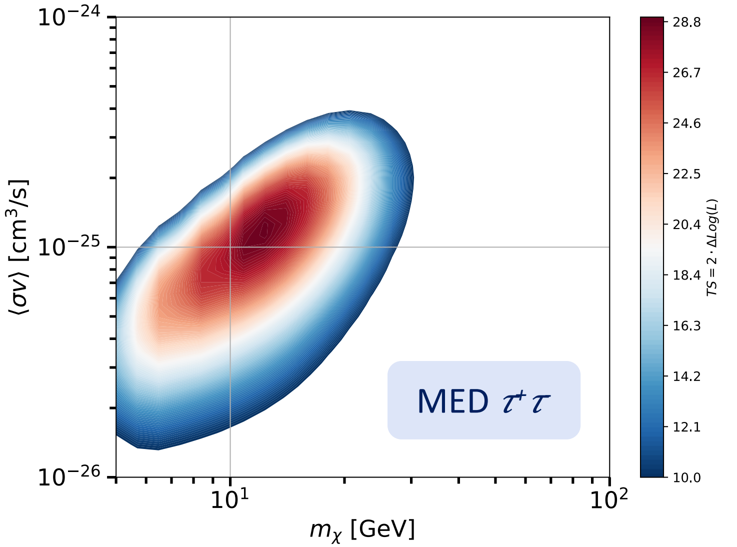

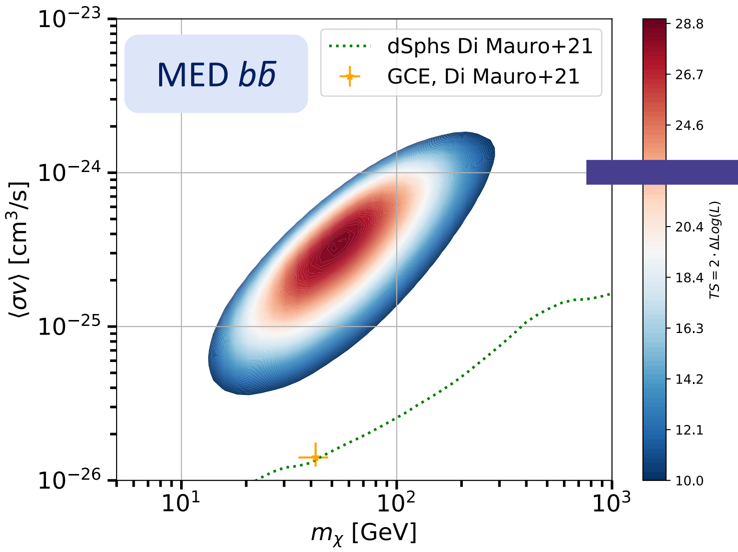

- Not compatible with GC excess
- Ruled out by dSphs

	$b\bar{b}$ (40 - 60 GeV)	$\tau^+\tau^-$ (8-20 GeV)
MED	2-4 x 10^{-25} cm^{3}s^{-1}	8-20 x 10^{-26} cm^{3}s^{-1}
MAX	4-9 x 10^{-26} cm^{3}s^{-1}	1-3 x 10^{-26} cm^{3}s^{-1}
DECAY	5-8 x 10^{24} s	8-12 x 10^{24} s

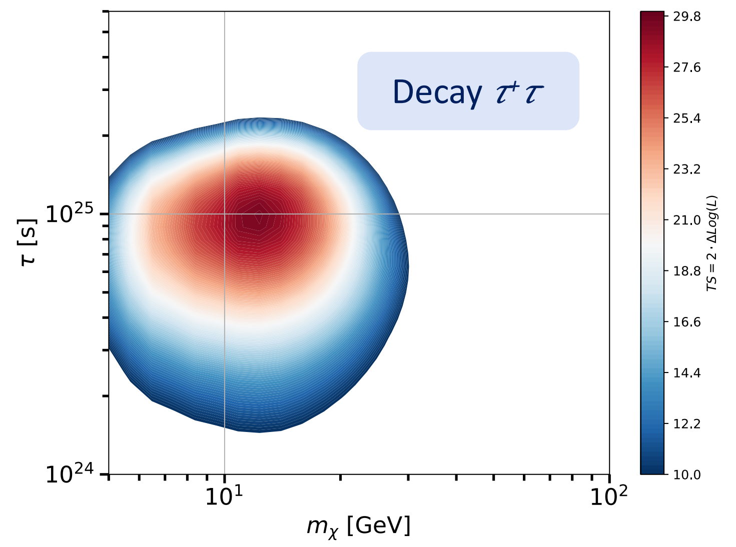

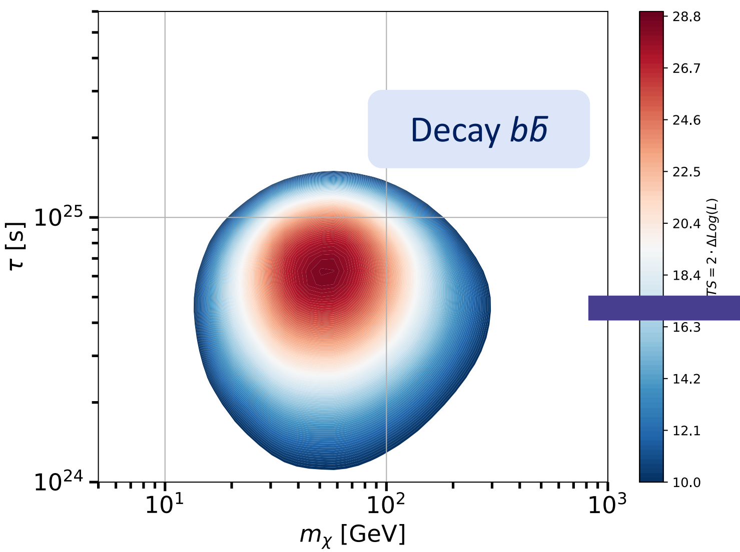

- Ruled out by Isotropic γ–ray Background (IGRB) and GC

Blanco&Hooper18, Ando&Ishiwata15, Ackermann+12 [Fermi Collab.]

NULL HYPOTHESIS FOR *TS* DISTRIBUTION

- Ideal knowledge of BKGs → *TS* distribution described as $\chi^2_2/2$ *Chernoff 54* → BUT → Analysis of real data at low energies for extended sources

- Build *TS* distribution using 3100 random blank sky directions
  - Remove directions with $|b|$<20 deg
  - Farther than 2 deg from known sources
  - Limited to extension of sources and ROI

- For each ROI, fit MED DM template and $b\bar{b}$ annihilation for m_χ=50 GeV

$$N_{\rm norm}(TS) = 0.22 \times (TS)^{-1.29-0.31\log(TS/2.55)}$$

TS = 27 for MED → p –value = 3.1 x 10^{-3} (local) → 2.7σ

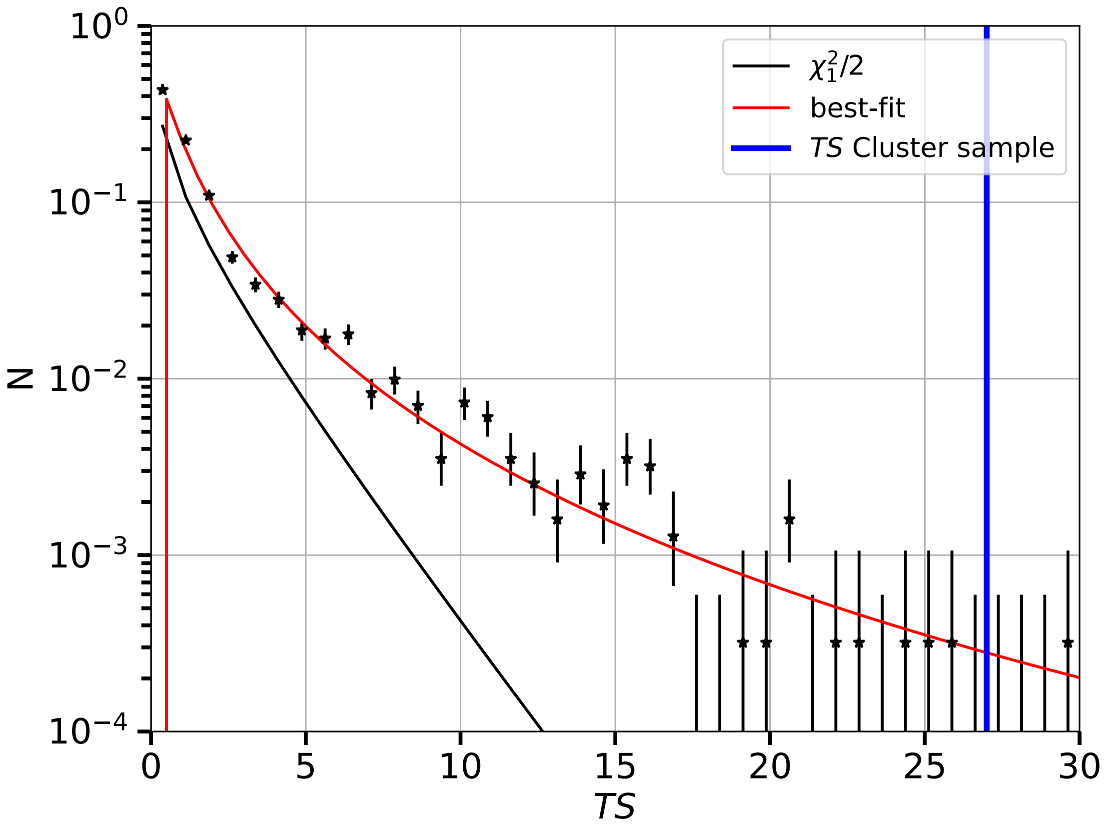

DM CONSTRAINTS FROM COMBINED CLUSTERS ANALYSIS

- The signal is not significant and if interpreted as DM, is not compatible with existing limits
  - Annihilation 95% C.L Upper Limits
  - Decay 95% C.L Lower Limits

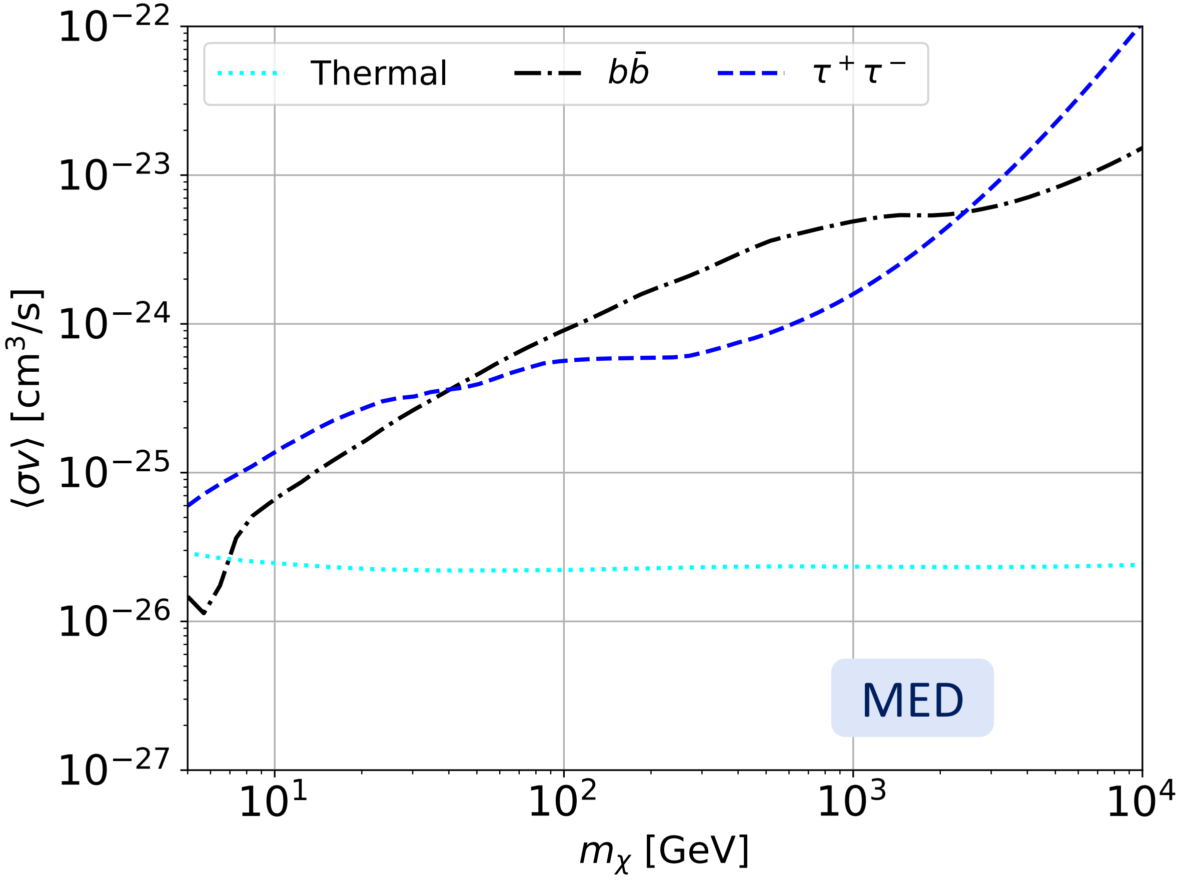

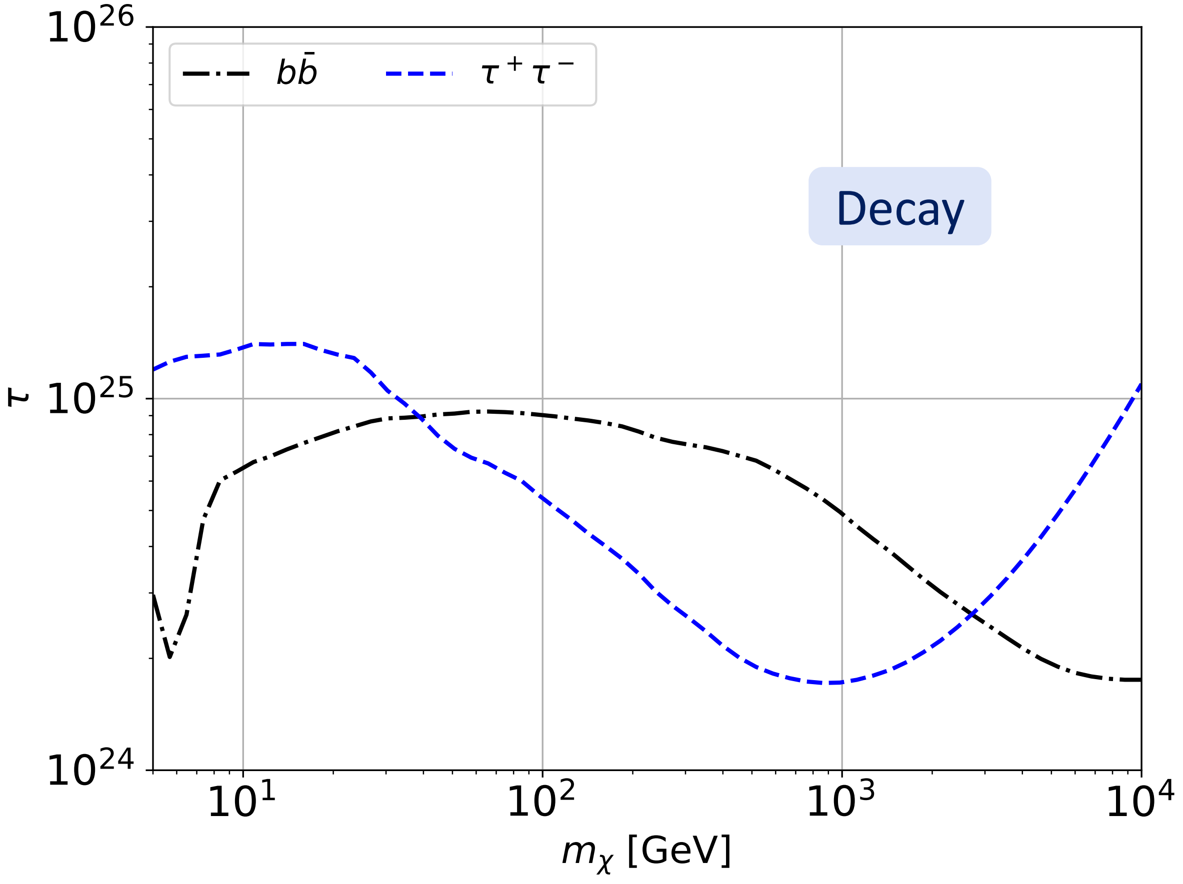

INSIGHT RESULTS: OTHER CHANNELS & MODELS

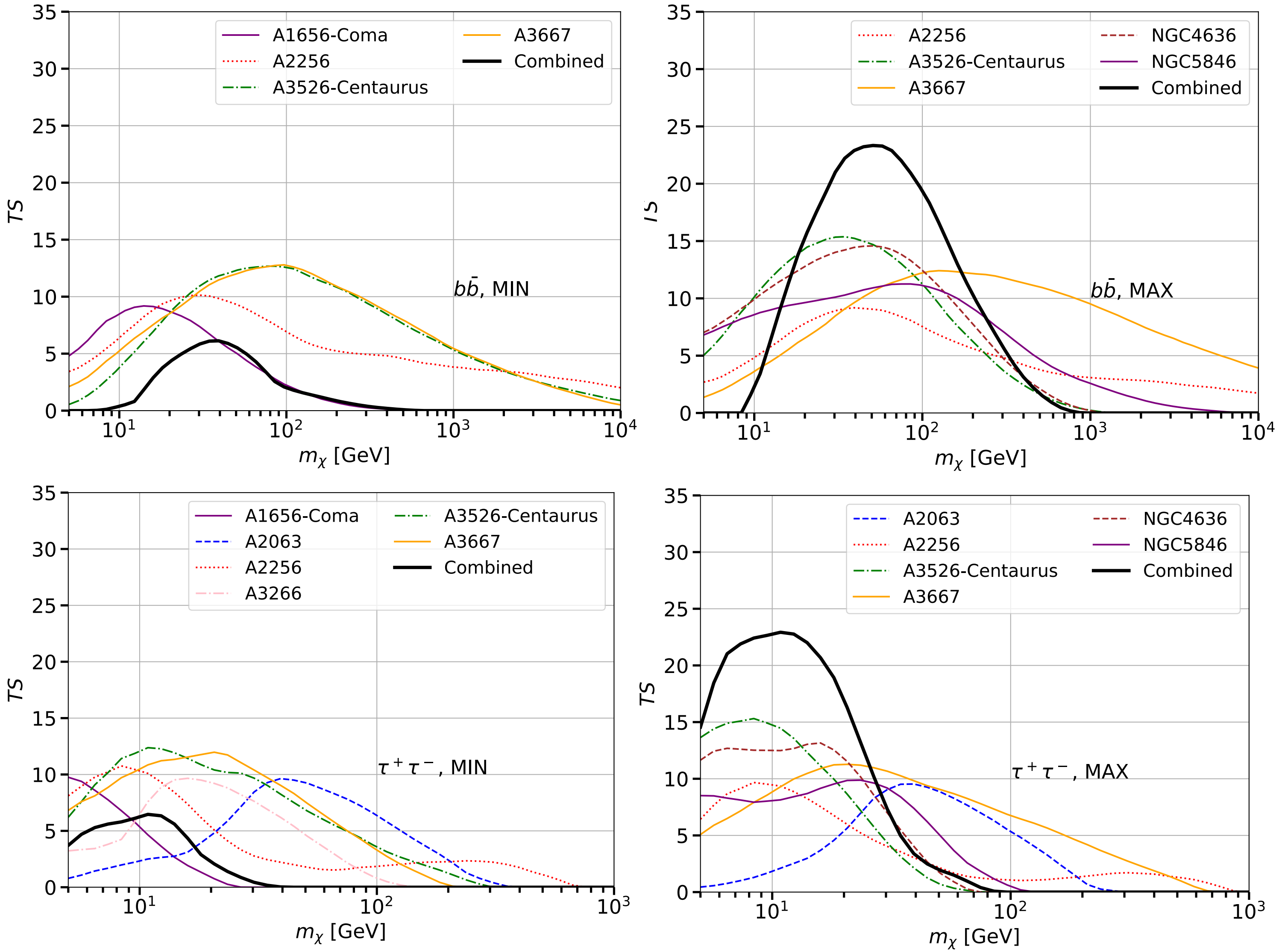

INSIGHT RESULTS: OTHER CHANNELS & MODELS

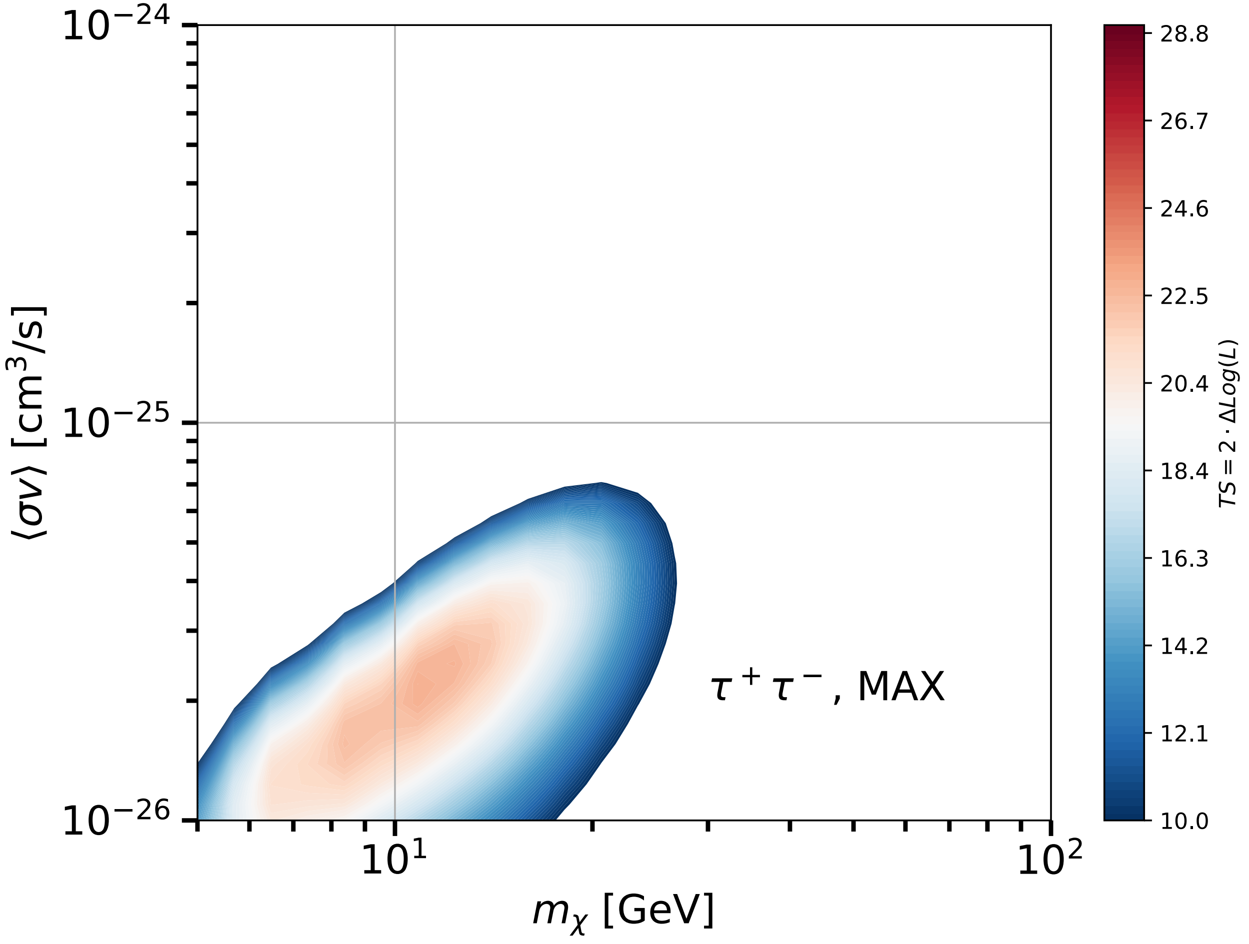

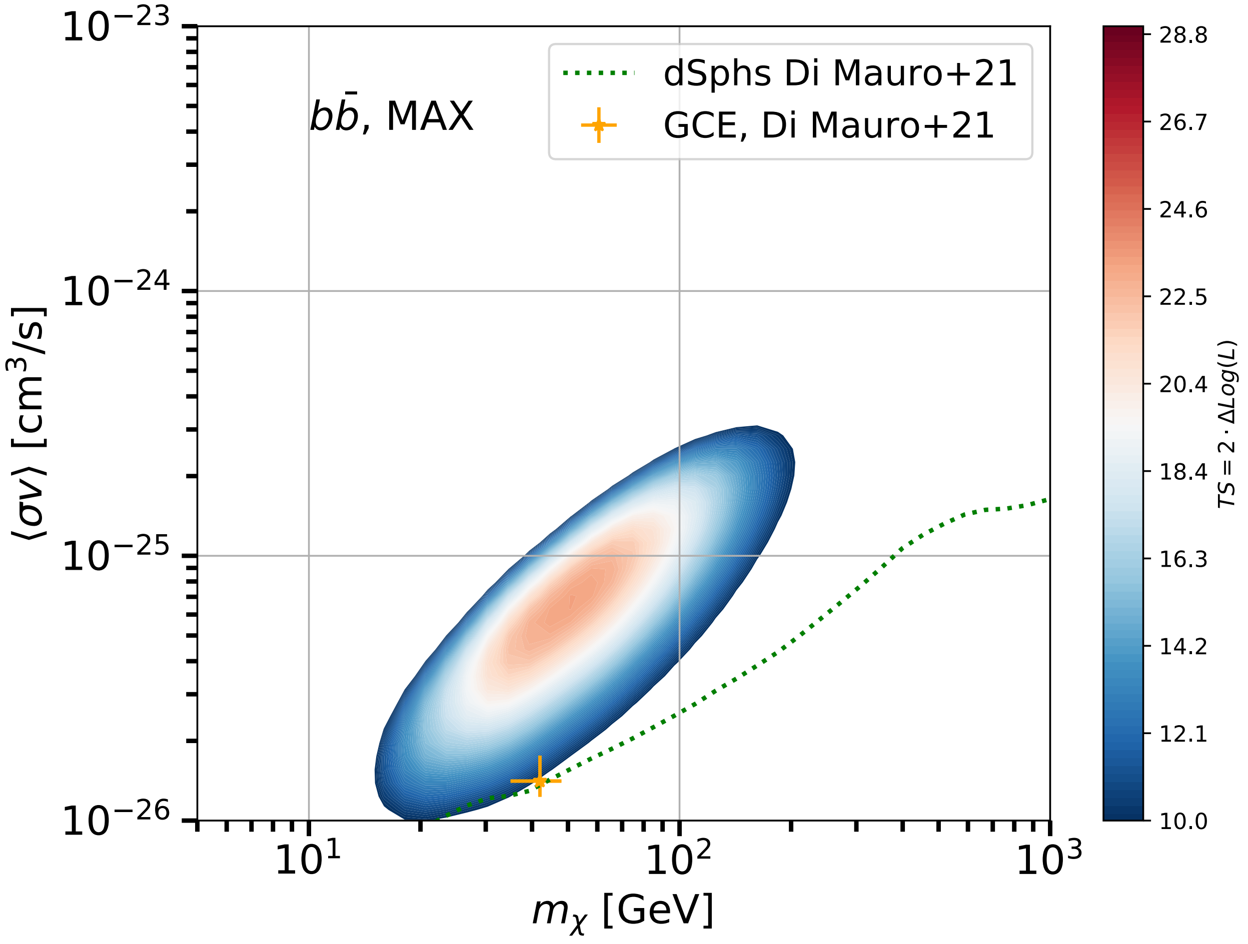

INSIGHT RESULTS: OTHER CHANNELS & MODELS

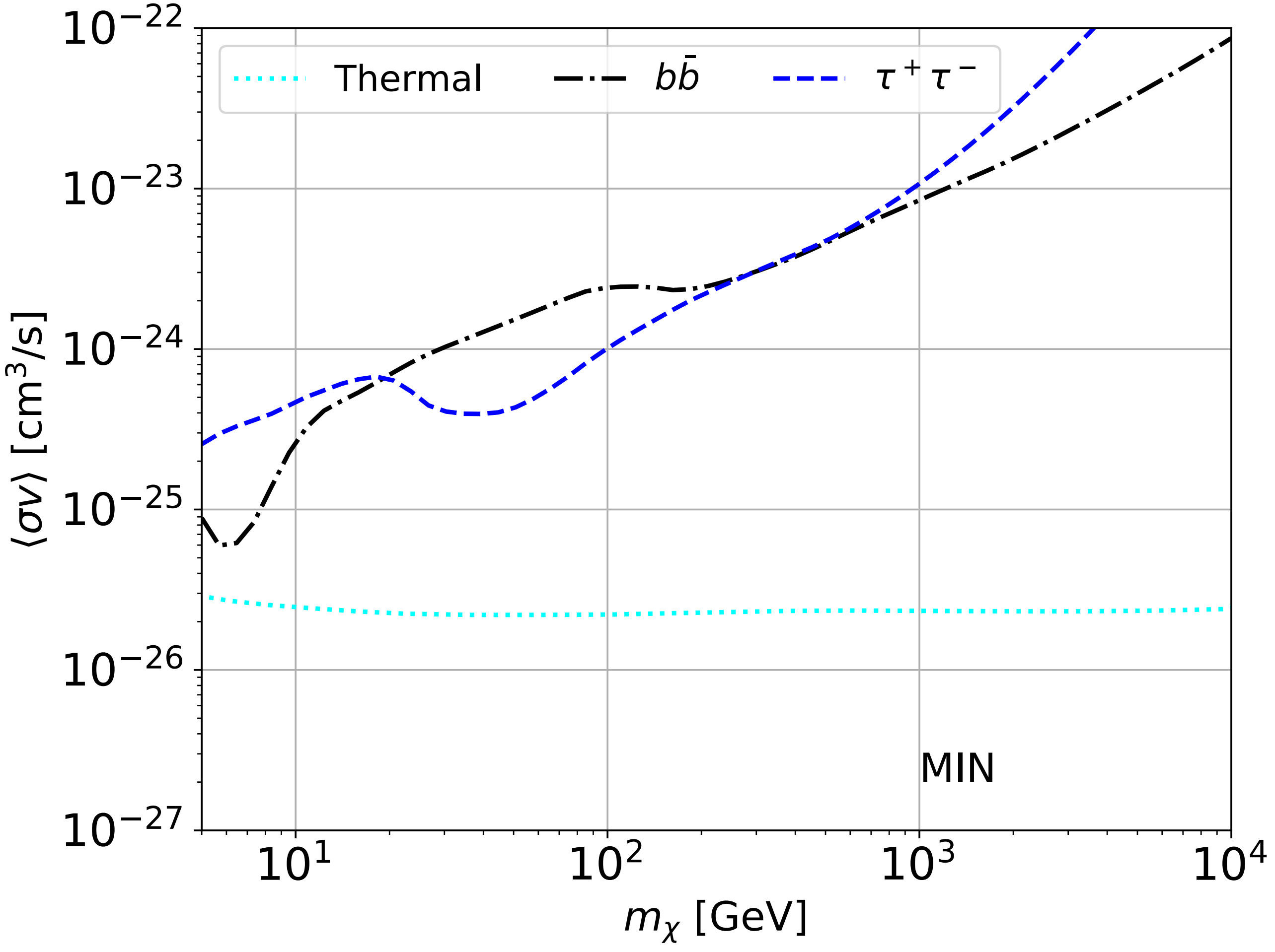

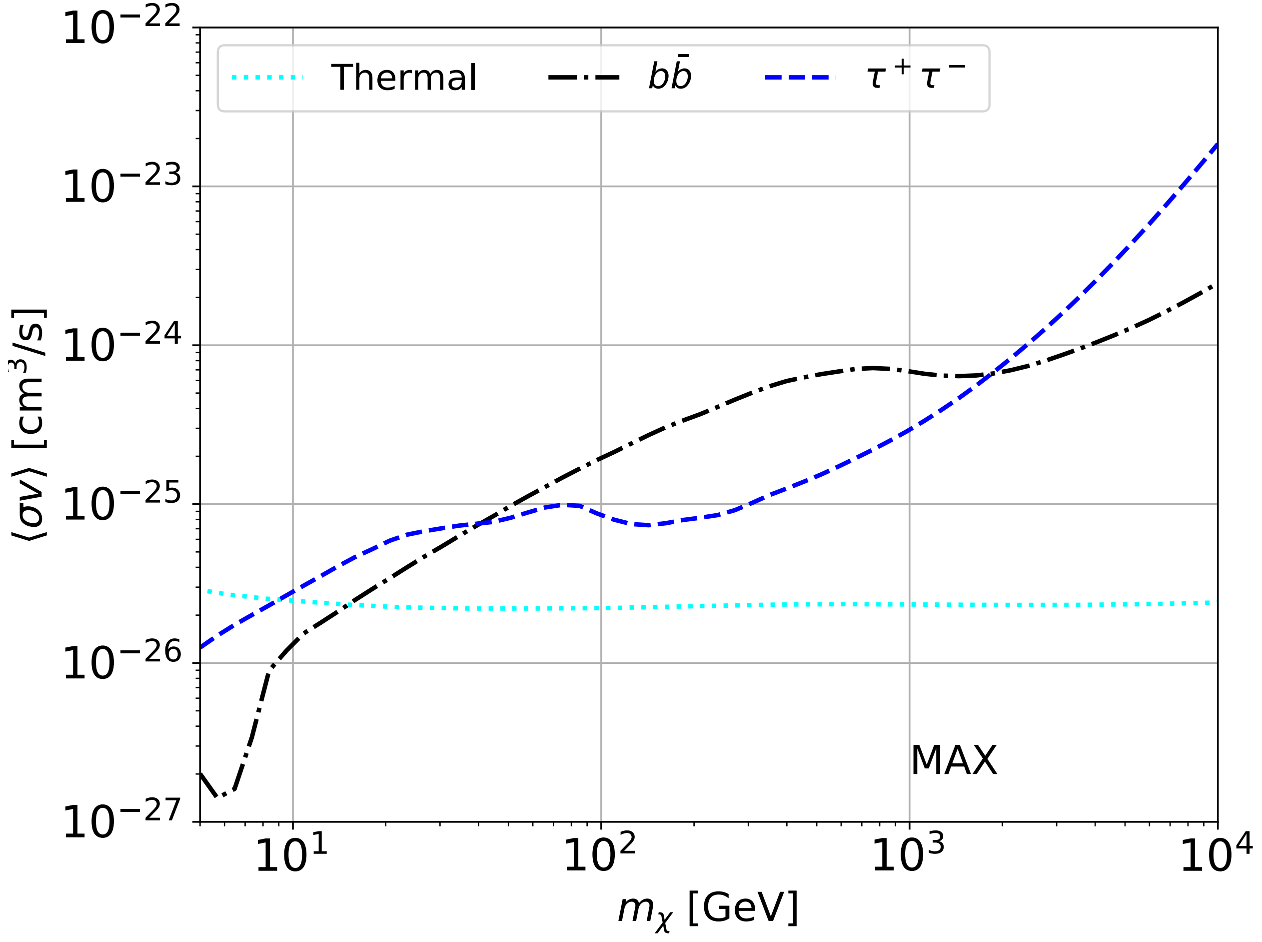

INSIGHT RESULTS: OTHER ANALYSIS SET-UPS

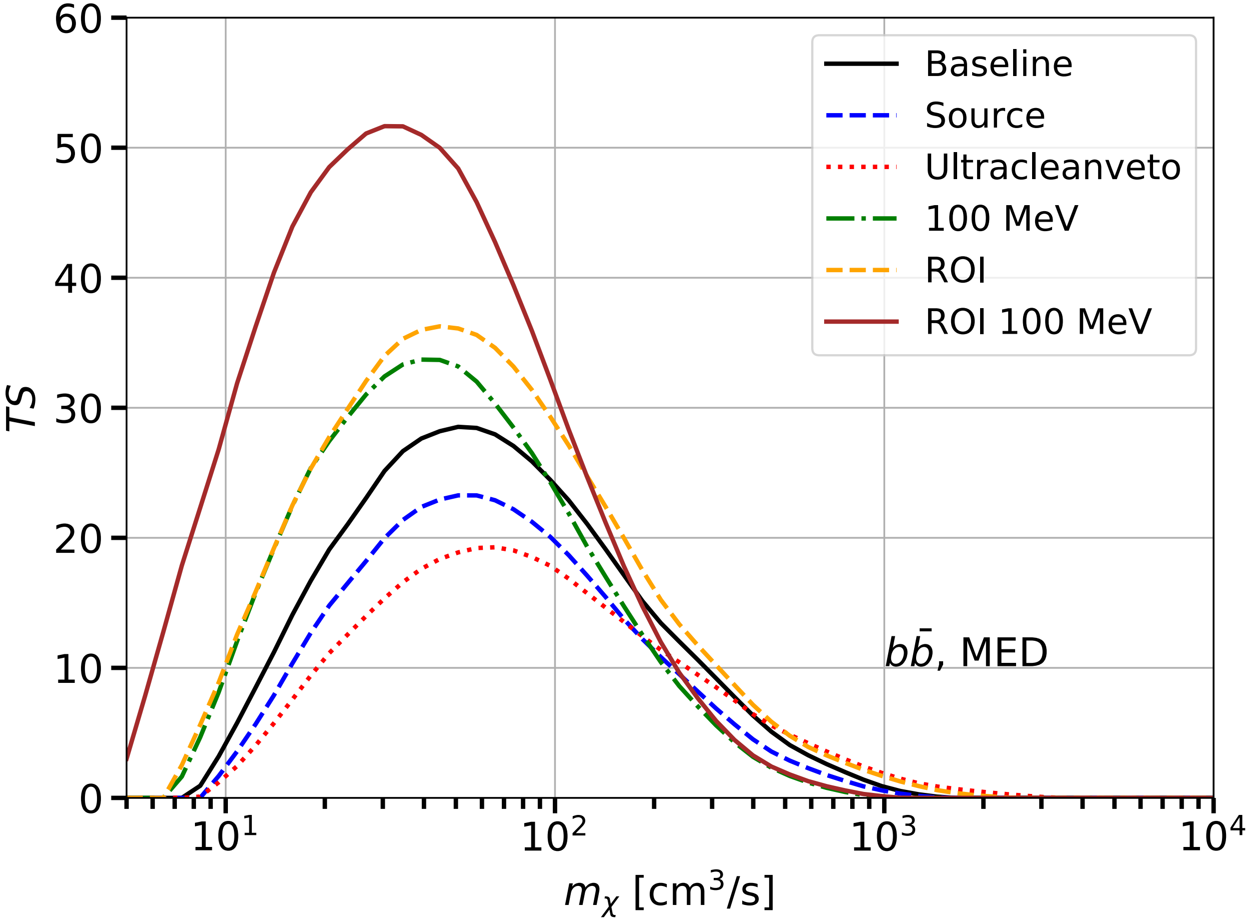

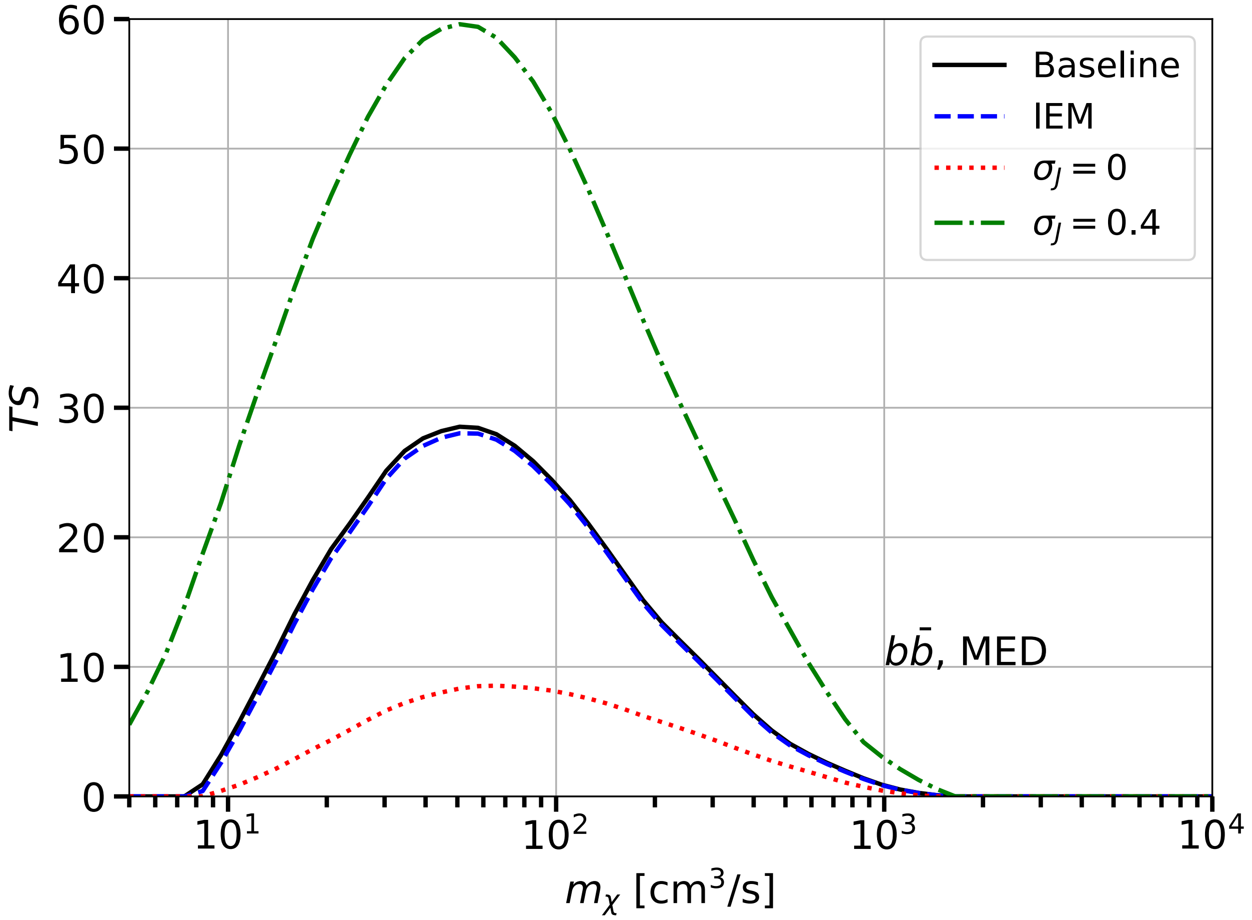

CAN WE CLASSIFY THE STUDIED TARGETS?

- Several astrophysical objects studied, with pros and cons

Clusters of galaxies

- Most massive - 10^{14}-10^{15} $M_\odot$
- Further – $z < 0.1$
- Higher substructure boost – B~9
- Best targets for decay
- Astrophysical γ–ray emission
- Up to $\log_{10} J_{MED}$ ~18.40

dIrrs

- Less massive - $10^8 - 10^{10}$ $M_\odot$
- Closer – $d_L < 1$ Mpc
- Lower substructure boost – B~4
- Not studied for decay
- Negligible astrophysical γ–ray emission
- Several at $\log_{10} J_{MED}$ ~ 18.50

\+ **dSphs**

- Classical
- Ultra-faint

CAN WE CLASSIFY THE STUDIED TARGETS?

- Build intra- and inter-family ranking of targets for γ-ray DM searches
- The absence of firm detection of vanilla-WIMP DM

Let us broaden the theoretical particle framework…

Velocity dependence of <σv>	Canonical *s*-wave partial wave may be naturally suppressed	Mediator is a scalar
Modification of the short-range <σv>	Exchange of light mediator induces a long-range interaction between DM particles	Complex dark sectors
Contribution of DM subhalos	Dependent on host halo mass and their structural properties	ΛCDM structure formation paradigm

→ *p*-wave dominates $\sigma v_{\rm rel} \propto v_{\rm rel}^2$

→ Sommerfeld enhacement

→ Boost computation for velocity-dependent annihilations

RESULTS ON CLASSIFICATION OF TARGETS

Classification of gamma-ray targets for velocity-dependent and subhalo-boosted dark-matter annihilation
T. Lacroix, G. Facchinetti, JPR, M. Stref, J. Lavalle, D. Maurin and M. A. Sánchez-Conde
JCAP10(2022)021, [arXiv:2203.16440]

Main halos

$$\epsilon_\phi \equiv \frac{m_\phi}{\alpha_D \, m_\chi}$$

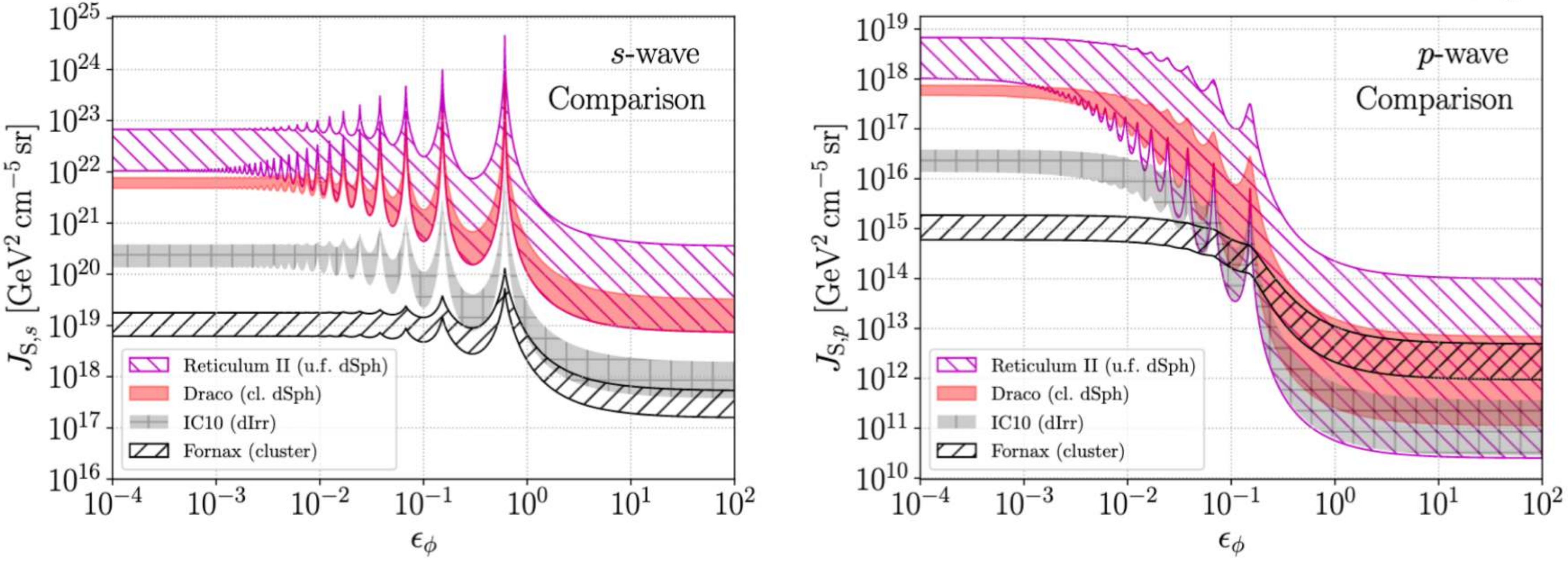

RESULTS ON CLASSIFICATION OF TARGETS

Main halos
+
substructures

$$\mathcal{B}_S = \frac{J_{S,tot}}{J_{S,host}}$$